Virginia Commonwealth University
VCU Scholars Compass

Theses and Dissertations | Graduate School

2016

SYSTEMATIC POSTSYNTHETIC MODIFICATION OF NANOPOROUS ORGANIC FRAMEWORKS AND THEIR PERFORMANCE EVALUATION FOR SELECTIVE CO2 CAPTURE

Timur Islamoglu

Follow this and additional works at: https://scholarscompass.vcu.edu/etd

Part of the Environmental Chemistry Commons, Materials Chemistry Commons, Oil, Gas, and Energy Commons, Physical Chemistry Commons, and the Polymer Chemistry Commons

© The Author

Downloaded from
https://scholarscompass.vcu.edu/etd/4264

This Dissertation is brought to you for free and open access by the Graduate School at VCU Scholars Compass. It has been accepted for inclusion in Theses and Dissertations by an authorized administrator of VCU Scholars Compass. For more information, please contact libcompass@vcu.edu.

www.manaraa.com

© COPYRIGHT BY

Timur İslamoğlu

2016

All Rights Reserved

المنارة للاستشارات

www.manaraa.com

SYSTEMATIC POSTSYNTHETIC MODIFICATION OF NANOPOROUS ORGANIC FRAMEWORKS AND THEIR PERFORMANCE EVALUATION FOR SELECTIVE CO_2 CAPTURE

A dissertation submitted in partial fulfillment of the requirements for the degree of Doctor of Philosophy at Virginia Commonwealth University.

by

Timur İslamoğlu

Bachelor of Science

Dumlupinar University, 2008

Master of Science

Virginia Commonwealth University, 2013

Director: Hani M. El-Kaderi,

Associate Professor, Department of Chemistry

Virginia Commonwealth University

Richmond, Virginia

May 2016

المنارة للاستشارات

www.manaraa.com

Acknowledgement

I would like to acknowledge the support and guidance of Dr. Hani M. El-Kaderi whose ideas and talents helped to make this work possible. I would also like to acknowledge my committee members Dr. Scott Gronert, Dr. Indika Arachchinge, Dr. Julio Alvarez and Dr. Purusottam Jena for their input in my pursuit of a degree. I am very thankful to the members of the El-Kaderi Group who have been a pleasure to work beside. I would also like to acknowledge the Ministry of National Education of Turkey for granting me a graduate fellowship to complete my PhD at Virginia Commonwealth University. I would also like to thank the Department of Chemistry at Virginia Commonwealth University for giving me the chance to pursue a doctorate degree. I also need to thank to Dr. Joseph Turner and Dr. Dmitry Pestov for their time training me on the instruments and giving their valuable time for discussing the results. I cannot thank enough to my parents, Ibrahim and Saniye Islamoglu for everything they have done for me. Last but not least, my wife Ulku Islamoglu. She is my other half and my better half and she gave me two wonderful daughter during my graduate study and took care of them mostly by herself to allow me to work more.

المنارة للاستشارات

www.manaraa.com

Table of Contents

List of Tables……vii

List of Schemes……...……...viii

List of Figures……..……..…ix

List of Abbreviations……..……xii

Chapter 1 Introduction 1

1.1 Global CO_2 Concerns 1

1.2 CO_2 Capture Technologies 3

1.3 Porous Solid Adsorbents for CO_2 Capture 6

1.4 Synthesis of Porous Organic Polymers 9

1.5 Pre- and Postsynthetic Modification of POPs 14

1.6 Sorbent Evaluation Criteria 17

1.7 Dissertation Problem 19

Chapter 2 Impact of Post-Synthesis Modification of Nanoporous Organic Frameworks On Small Gas Uptake And Selective CO_2 Capture 21

2.1 Introduction 21

2.2 Experimental Section 24

2.2.1 Materials and Methods 24

2.2.2 Synthetic Aspects 27

المنارة للاستشارات

www.manaraa.com

2.3 Results and Discussion 29

2.3.1 Synthesis and Characterization of NPOFs 29

2.3.2 Porosity Measurements and Gas Storage Studies 35

2.3.3 Gas Selectivity Studies 43

2.4 Conclusions 47

Chapter 3 Systematic Postsynthetic Modification of Nanoporous Organic Frameworks for Enhanced CO_2 Capture from Flue Gas and Landfill Gas 49

3.1 Introduction 49

3.2 Experimental Section 52

3.2.1 General Techniques, Materials and Methods 52

3.3 Results and Discussion 57

3.3.1 Synthesis and Characterization 57

3.3.2 Textural Properties 61

3.3.3 Gas uptake and selectivity studies 65

3.3.4 Working Capacity Study 71

3.4 Conclusions 74

Chapter 4 Enhanced Carbon Dioxide Capture from Landfill Gas using Bifunctinalized Benzimidazole-Linked Polymers 75

4.1 Introduction 75

4.2 Experimental Section 77

المنارة للاستشارات

www.manaraa.com

4.2.1 General Techniques, Materials and Methods 77

4.3 Results and Discussion 81

4.3.1 Synthesis and Characterization 81

4.3.2 Textural Properties 86

4.3.3 Gas uptake and selectivity studies 88

4.3.4 DFT Study 91

4.3.5 Sorbent Evaluation Criteria 94

4.4 Conclusions 96

Chapter 5 Concluding Remarks 97

List of References 100

Vita 113

المنارة للاستشارات

www.manaraa.com

List of Tables

Table 1.1 Physical parameters of selected gases. (Ref. 24) 7

Table 1.2 Adsorbent evaluation criteria suggested by Bae and Snurr. 17

Table 2.1 Gas uptakes, binding affinities and selectivities of NPOFs. 40

Table 2.2 CO_2 and N_2 uptakes for CO_2/N_2 selectivity studies via Equation S. 44

Table 2.3 CO_2 and CH_4 uptakes for CO_2/N_4 selectivity studies via Equation S. 44

Table 3.1 CO_2 uptakes at 298 K, *Qst* and IAST selectivity results 63

Table 3.2 CH_4 and N_2 uptakes of polymers at 273 and 298 K. 67

Table 3.3 Adsorbents for VSA in flue gas (CO_2/N_2: 10/90) separation at 298 K, P_{ads} = 1 bar and P_{des} = 0.1 bar 70

Table 3.4 Adsorbents for VSA in landfill gas (CO_2/CH_4: 50/50) separation at 298 K, P_{ads} = 1 bar and P_{des} = 0.1 bar 70

Table 4.1 Surface areas, CO_2 uptakes at 298 K, *Qst* and IAST selectivity results of polymers 86

Table 4.2 VSA Evaluation Criteria for CO_2 Separation from Landfill Gas[a] 95

المنارة للاستشارات

www.manaraa.com

List of Schemes

Scheme 1.1 Formation of carbamate and bicarbonate from reaction of CO_2 and amines.carbamate and bicarbonate from reaction of CO_2 and amines. 4

Scheme 1.2 Yamamoto Coupling Formation of PAF-1 10

Scheme 1.3 Synthesis routes of some hetero atom containing POPs. 11

Scheme 1.4 A schematic representation of the syntheis of BILPs. 13

Scheme 1.5 Post-synthesis modification of Porous Polymer Networks. 16

Scheme 2.1 Synthesis of 1,3,5,7-tetrakis(4-acetylphenyl)adamantane. 25

Scheme 2.2 Schematic representation of NPOF-4 synthesis and its post-synthesis modification. 28

Scheme 3.1 Schematic representation of NPOF-1 synthesis and its post-synthesis modification. 56

Scheme 4.1 Schematic representation of synthesis of BILP-6 and BILP-6-NH_2. 80

المنارة للاستشارات

www.manaraa.com

List of Figures

Figure 1.1 Different technologies and associated materials for CO_2 separation and capture. 2

Figure 1.2 Schematic representation of pre- and post-synthetic modification synthesis 14

Figure 1.3. Basicity of some nitrogen rich functional groups. 18

Figure 2.1 Selective CO_2 capture with NPOFs. 22

Figure 2.2 ^{1}H NMR for 1,3,5,7-tetrakis(4-acetylphenyl)adamantane in $CDCl_3$..... 26

Figure 2.3 ^{13}C NMR for 1,3,5,7-tetrakis(4-acetylphenyl)adamantane in CDCl3..... 26

Figure 2.4. TGA traces of NPOF-4, NPOF-4-NO_2 and NPOF-4-NH_2..... 30

Figure 2.5 Solid state ^{13}C NMR of NPOF-4 (A), NPOF-4-NO_2 (B), NPOF-4-NH_2 (C)... 31

Figure 2.6 SEM images of NPOF-4 (A) and its modified frameworks NPOF-4-NO_2 (B) and NPOF-4-NH_2 (C). 32

Figure 2.7 FTIR spectra of TAPA, and NPOFs..... 34

Figure 2.8 Gas uptake isotherms Ar (A), PSD from NLDFT (B), CO_2 (C), Q_{st} for CO_2 (D), CH_4 (E), Q_{st} for CH_4 (F) and H_2 (G), Q_{st} for H_2 (H).Adsorption (filled) and desorption (empty). PSD is offset by 0.02 for NPOF-4-NO_2 and 0.04 for NPOF-4 for clarity..... 36

Figure 2.9 Gas uptake isotherms for NPOF-4 (green triangles), NPOF-4-NO_2 (blue squares) and NPOF-4-NH_2 (red circles) at 273 and 298 K. 38

Figure 2.10 Gas sorption capacities of NPOF-4 (A), NPOF-4-NO_2 (B), and NPOF-4-NH_2 (C) at 273 K. CO_2 (red circle), CH_4 (olive square), and N_2 (blue triangle). 42

Figure 2.11 IAST selectivities of CO_2 over N_2 (A) and CO_2 over CH_4 (B) for binary gas mixtures of 15/85 and 5/95 molar compositions, respectively, in NPOFs at 298 K. 46

Figure 3.1 Schematic representation of post functionalized POPs. 50

المنارة للاستشارات

www.manaraa.com

Figure 3.2 FT-IR spectra of NPOF-1 and its derivative**s.**..... 57

Figure 3.3 TGA traces of polymers..... 58

Figure 3.4 PXRD pattern of polymers..... 58

Figure 3.5 SEM images of polymers..... 60

Figure 3.6 Nitrogen isotherms at 77 K (A) and pore size distribution from NLDFT using N_2 at 77 K (B). 61

Figure 3.7 Pore size distribution of polymers from CO_2 isotherm at 273 K using NLDFT. 62

Figure 3.8 CO_2 uptakes at 273 (A) and 298 K (B), and corresponding *Qst* plot (C) of NPOFs. 64

Figure 3.9 CH_4 uptakes at 273 K (A) and 298 K (B), N_2 uptakes at 273 K (C) and 298 K (D) of polymers..... 66

Figure 3.10 Selectivity calculated by IAST for CO_2/N_2 (A) and CO_2/CH_4 (B) at 298 K.. 69

Figure 4.1 Interactions of CO_2 and BILP-6-NH_2..... 76

Figure 4.2 ^{1}H NMR spectra of TPAL-NO_2 in $CDCl_3$. 78

Figure 4.3 FT-IR spectra of TPAL-NO_2 and polymers. 82

Figure 4.4 TGA traces of polymers..... 83

Figure 4.5 SEM images of BILP-6 and BILP-6-NH_2..... 84

Figure 4.6 Nitrogen isotherms at 77 K (A) and pore size distribution from NLDFT using N_2 at 77 K (B). 85

Figure 4.7 CO_2 (A) and CH_4 (B) uptakes of BILP-6 and BILP-6-NH_2 at 273 and 298 K. 87

Figure 4.8 Isosteric heat of adsorption of CO_2 for BILP-6 and BILP-6-NH_2. 89

المنارة للاستشارات

www.manaraa.com

Figure 4.9 CO_2/CH_4 selectivity calculated by IAST for BILPs at 298 K. 90

Figure 4.10 Fully optimized geometries of BILPs–CO_2 interactions calculated at the M06/6-311+G* level of theory. (a) BILP-6@CO_2 top view; (b) and (c) BILP-6-NH_2@CO_2 top and side view, respectively; (d) BILP-6@2CO_2 top view; (e) and (f) BILP-6-NH_2@2CO_2 top and side view, respectively; The bond lengths are in Å. The blue, grey, white and red colours stand for N, C, H and O atoms, respectively. 92

Figure 4.11 Electrostatic potential map for BILP-6- and BILP-6-NH2. 93

المنارة للاستشارات

www.manaraa.com

List of Abbreviations

NPOF ..... Nanoporous Organic Framework

BILP ..... Benzimidazole-Linked Polymer

PAF……Porous Aromatic Framework

POP.....Porous Organic Framework

PSM .....Postsynthetic Modification

MOF ..... Metal Organic Framework

COF.....Covalent Organic Framework

DFT .....Density Functional Theory

IAST ..... Ideal Adsorbed Solution Theory

IR..... Infrared Spectroscopy

LDA .....Local Density Approximation

NLDFT..... Non-Local Density Functional Theory

NMR .....Nuclear Magnetic Resonance Spectroscopy

SEM .....Scanning Electron Microscopy (Microscope)

XRD..... X-Ray Diffraction

المنارة للاستشارات
www.manaraa.com

Abstract

SYSTEMATIC POSTSYNTHETIC MODIFICATION OF NANOPOROUS ORGANIC FRAMEWORKS AND THEIR PERFORMANCE EVALUATION FOR SELECTIVE CO_2 CAPTURE

By Timur Islamoglu, Ph.D.

A dissertation submitted in partial fulfillment of the requirements for the degree of Doctor of Philosophy at Virginia Commonwealth University.

Virginia Commonwealth University, 2016

Director: Hani M. El-Kaderi, Associate Professor, Department of Chemistry

Porous organic polymers (POPs) with high physicochemical stability have attracted significant attention from the scientific community as promising platforms for small gas separation adsorbents. Although POPs have amorphous morphology in general, with the help of organic chemistry toolbox, ultrahigh surface area materials can be synthesized. In particular, nitrogen-rich POPs have been studied intensively due to their enhanced framework-CO_2 interactions. Postsynthetic modification (PSM) of POPs has been instrumental for incorporating different functional groups into the pores of POPs which would increase the CO_2 capture properties. We have shown that functionalizing the surface of POPs with nitro and amine groups increases the CO/N_2 and CO_2/CH_4 selectivity significantly due to selective polarization of CO_2 molecule. In addition, controlled postsynthetic nitration of NPOF-1, a nanoporous organic framework constructed by nickel(0)-catalyzed Yamamoto coupling of 1,3,5-tris(4-

المنارة للاستشارات
www.manaraa.com

bromophenyl)benzene, has been performed and is proven to be a promising route to introduce nitro groups and to convert mesopores to micropores without compromising surface area. Reduction of the nitro groups yields aniline-like amine-functionalized NPOF-1-NH_2. Adequate basicity of the amine functionalities leads to modest isosteric heats of adsorption for CO_2, which allow for high regenerability. The unique combination of high surface area, microporous structure, and amine-functionalized pore walls enables NPOF-1-NH_2 to have remarkable CO_2 working capacity values for removal from landfill gas and flue gas. Benzimidazole-linked polymers have also been shown to have promising CO_2 capture properties. Here, an amine functionalized benzimidazole-linked polymer (BILP-6-NH_2) was synthesized via a combination of pre- and postsynthetic modification techniques in two steps. Experimental studies confirm enhanced CO_2 uptake in BILP-6-NH_2 compared to BILP-6, and DFT calculations were used to understand the interaction modes of CO_2 with BILP-6-NH_2. Using BILP-6-NH_2, higher CO_2 uptake and CO_2/CH_4 selectivity was achieved compared to BILP-6 showing that this material has a very promising working capacity and sorbent selection parameter for landfill gas separation under VSA settings. Additionally, the sorbent evaluation criteria of different classes of organic polymers have been compared in order to reveal structure-property relationships in those materials as solid CO_2 adsorbents.

المنارة للاستشارات
www.manaraa.com

Chapter 1

Introduction

1.1 Global CO_2 Concerns

Globally, the main greenhouse gases (GHGs) produced by human activities are carbon dioxide, methane, nitrous oxide, and fluorinated gases. In 2013, carbon dioxide (CO_2) accounted for 82% of all greenhouse gas emissions from human activities in U.S.[1] The industrial revolution has caused a dramatic rise in CO_2 emission reaching 401.62 ppm as of December 2015.[1] The increase in CO_2 concentration in the atmosphere is an urgent global problem that needs to be addressed immediately because of its effect on global climate, ocean pH levels and chemistry of plants. In 2013, electricity production was responsible for 31% of GHGs while transportation accounted for 27%.[1] In 2012, as high as ~87% of the world's energy has harvested from fossil fuel sources and realistically, this situation will not change until sustainable and cleaner energy sources and technologies become widely available at a reasonable cost which can take a significant amount of time.[2] Switching from coal-fired power plants to natural gas-fired power plants has been consider an alternative way to mitigate CO_2 emission since the latter has lower carbon footprint.[3] In addition, replacing the oil based gas with natural gas in automotive industry is also highly desirable for the abovementioned reasons; however, natural gas is found in reservoirs and has tangible amounts of CO_2, N_2, and H_2S that need to be minimized before transport and use to prevent pipeline corrosion and to increase

المنارة للاستشارات
www.manaraa.com

the energy density.[4] Another renewable energy source of methane is landfill-gas which is endorsed by the Environmental Protection Agency (EPA) as an alternative to fossil fuels.[5] Landfill gas, a by-product of the decomposition of municipal solid waste (MSW), is mainly composed of ~50% CH4 and ~50% CO2 where CO_2 needs to be separated prior to usage.[5] Therefore, CO_2 capture and sequestration (CCS) efforts have attained great attention over the past decades.[6] In particular, the selective separation of CO_2 from N_2, CH_4, and H_2 has gained interest since carbon dioxide is the main impurity in flue gases (gases that exit to the atmosphere via an exhaust port such as smoke stacks from power plants) as well as natural gas.[3]

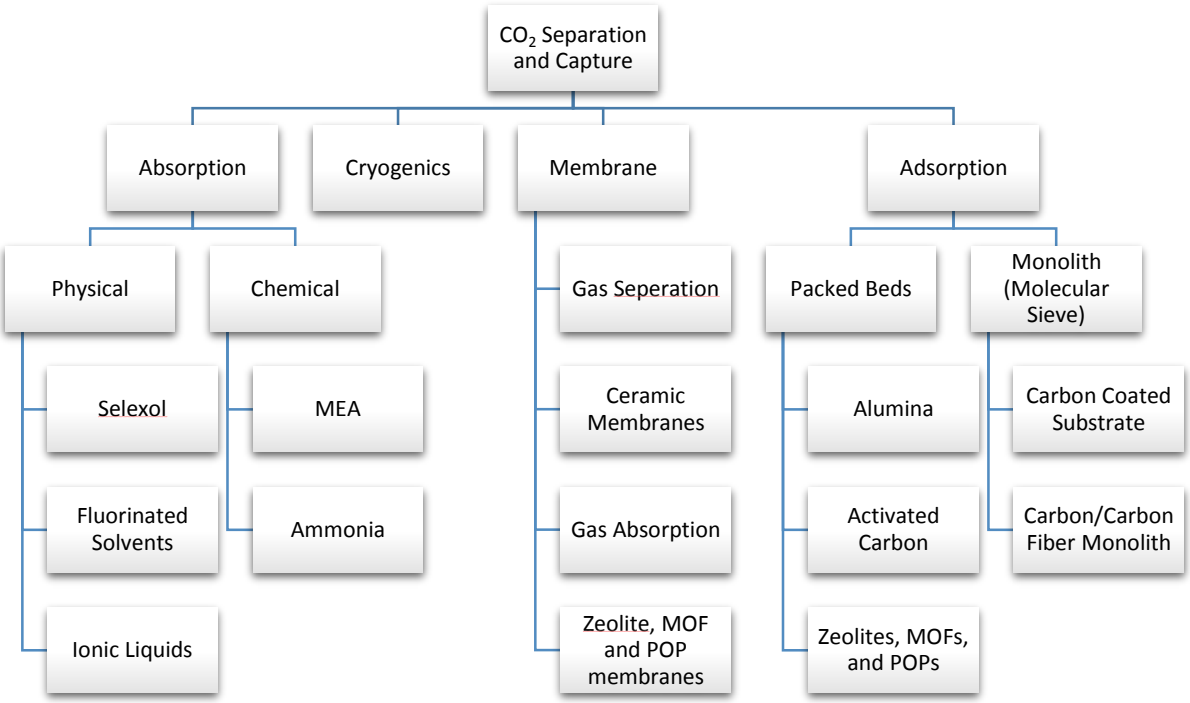

Figure 1.1. Different technologies and associated materials for CO_2 separation and capture.

المنارة للاستشارات
www.manaraa.com

1.2 CO_2 Capture Technologies

There are several methods that have been proposed for CO_2 capture from a power plant gas stream, where in some cases multiple techniques can be combined to achieve more efficient separation.[7] (1) Post-combustion capture where CO_2 is separated from the gas mixtures at the end of the process. (2) Pre-combustion (Syngas/Hydrogen) capture where fossil fuel or biomass is first converted to a mixture of H_2, CO, and CO_2 then CO_2 removed prior to use of hydrogen as a fuel. (3) Oxy-fuel combustion where high purity O_2 is used to replace the air by separating N_2 from air so the flue gas from this process is rendered CO_2 rich compared to post-combustion gas mixture. Different technologies have been suggested to yield high purity of gas stream with each of them possesing advantages and disadvantages (**Figure 1.1**). Among those the most promising techniques can be summarized as membrane based separation, chemical absorption by amine solutions and adsorption based separation by porous solids.

Membranes are semipermeable thin layers of different materials that can selectively separate gas molecules. Membranes can be either organic (polymeric) or inorganic (carbon, zeolite, ceramic or metallic) and can be either porous or non-porous. In general, the performances of membranes decrease for selective CO_2 capture from low CO_2 concentration in feed stream (<20%).[7]

With the current technology, alkonolamine solutions (typically 30 wt% in water) are widely employed to capture CO_2 from flue gas by chemisorption where CO_2 is chemically absorbed. This process is also known as amine scrubbing, here a chemical reaction occurs between CO_2 and amine solution to form carbamate or bicarbonate anion depending on the amine type (**Scheme 1.1**) and therefore up to 98% of CO_2 can be

المنارة للاستشارات
www.manaraa.com

captured.[8] The CO_2-laden solvent is then transferred to a regeneration vessel where heat is applied to regenerate the amine solution for further use. Due to high heat capacity of water and the strong binding of CO_2 and alkonolamine, high temperatures (>120 ^oC) are needed to regenerate the amine.[9] Therefore, there is a ~30% energy penalty in coal-fired power plants in amine scrubbing step. In addition, low boiling point of amines and their decomposition during regeneration makes them less attractive. The expected properties of an ideal liquid absorbent can be summarized as high capture capacity and selectivity towards the targeted gas, regeneration with a minimal amount of input energy, thermal and chemical stability, and a straightforward synthetic route from accessible precursors.[10] Today's inventories of absorbents for carbon dioxide capture application, unfortunately, are far from combining two or more of these properties together.

The idea of the use of porous solid materials as CO_2 adsorbent to purify flue gas/landfill gas has been intensively investigated. The biggest advantage of the proposed

Scheme 1.1. Formation of carbamate and bicarbonate from reaction of CO_2 and amines.carbamate and bicarbonate from reaction of CO_2 and amines.

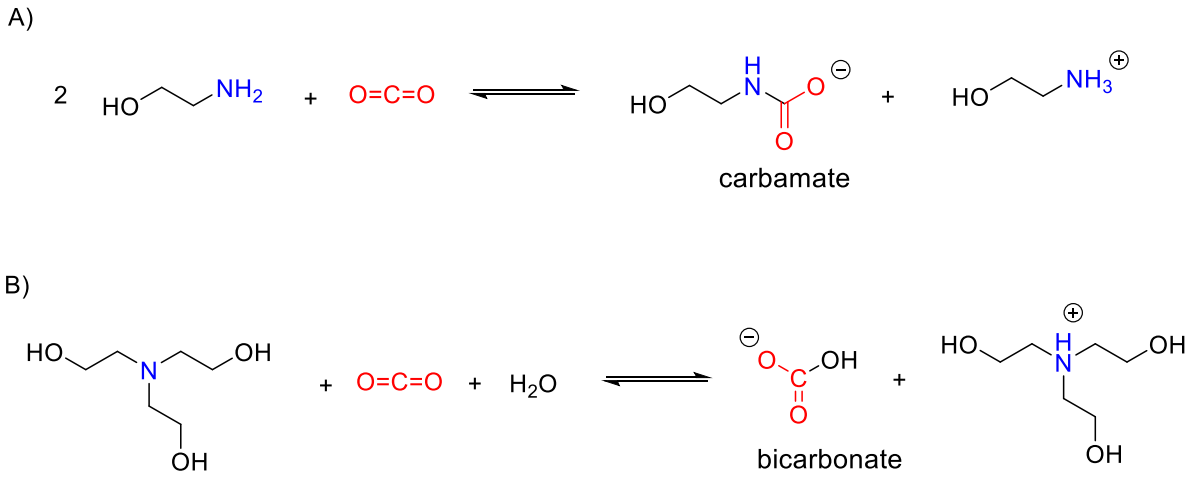

المنارة للاستشارات
www.manaraa.com

method is that the separation takes place in the gas phase and so the regeneration energy penalty is greatly reduced compare to MEA solution process because water is not involved. The heat capacities of porous sorbents are reported to be much lower compared to water.[11] There are numerous porous materials that have been tested for selective CO_2 capture. Zeolites are more effective compared to MEA solutions, however, they suffer from low CO_2 uptake capacity and structure tunability.[12] Activated carbons are also intensively studied as CO_2 adsorbents and their low selectivity of CO_2/N_2 and CO_2/CH_4 limits their usage. The development of efficient solid adsorbents depends on the design of new materials with high chemical and physical stability, reversible adsorption, high adsorption capacity of CO_2, and high selectivity under industrial conditions. One of the emerging porous materials that can address the aforementioned problems are Metal-organic frameworks (MOFs) which are crystalline hybrid materials that are composed of organic ligands (struts) and metal ions (nodes).[13] MOFs are the most studied porous materials in the areas including but not limited to gas separation,[14] heterogeneous catalysis[15-17] and sensing[18] due their tunable chemical and physical properties. Their ultra-high surface area, permanent porosity, thermal stability, well-defined structures, and tunable pore functionality have made them promising candidates for CO_2 capture. Although there are MOFs that survive harsh conditions, in general, due to the reversible nature of coordination bonding, MOFs are subject to hydrolysis which limits their usage as flue gas contains significant amounts of water.[19] Porous organic polymers (POPs) have been suggested to tackle the abovementioned problems since POPs are superior to MOFs in terms of chemical stability due to their covalently bonded highly cross-linked porous structure.[20] Due to their stable covalent nature, POPs are not subject to hydrolysis

المنارة للاستشارات
www.manaraa.com

in the presence of water and remain intact under acidic or basic conditions.[21] POPs can also be designed to form crystalline networks known as covalent-organic frameworks (COFs) i.e. B-O, C-N, and B-N bonds, if the linkage forming the framework allows for correction under thermodynamic conditions.[22] The crystalline structure of COFs, however, comes with the price of low chemical stability under aqueous conditions. On the other hand, physicochemical stability of POPs allows researchers to modify the pore surface with polar functional groups to attract CO_2 molecules.[23]

1.3 Porous Solid Adsorbents for CO_2 Capture

Recently, a great amount of effort has spent on reducing the parasitic energy, the minimum energy required to release captured CO_2, for carbon capture processes because of the energy intensive regeneration of amine solvents. Lower heat capacity of solid adsorbents makes them a better candidate as low cost CO_2 adsorbent materials. However, the similar physical properties of the gases in the mixtures (CO_2, N_2, CH_4, H_2O) is one of the greatest challenge towards selective CO_2 capture (**Table 1.1**).[24] Therefore, researchers are required to develop materials that can differentiate those small differences in gas molecules. Thus, synthetic porous materials (MOFs, POPs, etc) have attracted considerable attention which can be modified to have targeted properties such as surface area, pore size and pore functionality.[10] Although the structure of other porous materials such as zeolites, porous silica, and activated carbon can also be tuned, it is

المنارة للاستشارات
www.manaraa.com

Table 1.1 Physical parameters of selected gases. (Ref. 24)

Gas	Kinetic Diameter (Angstrom)	Polarizability ($\times 10^{-25}$ cm^3)	Quadrupole Moment ($\times 10^{-26}$ esu cm^2)	Dipole Moment ($\times 10^{-18}$ esu cm)
He	2.55	2.0	0.0	0
Ar	3.54	16.4	0.0	0
N_2	3.64	17.4	1.5	0
CH_4	3.82	25.9	0.0	0
CO_2	3.30	29.1	4.3	0
H_2O	2.65	14.5	-	1.85

very limited compared to POPs and MOFs. As mentioned above, the relatively low chemical stability of MOFs towards moisture limits their usage as solid sorbents for CO_2 capture.

According to IUPAC classification, microporous solids have pore width not exceeding 2 nm; mesoporous materials are materials that exhibit pore width ranging from 2 - 50 nm, and macroporous materials having pores larger than 50 nm.[25] It is well known that microporous materials show better performance for CO_2 capture and separation processes while materials possessing mesopores are more promising as CO_2 storage adsorbents. Although the kinetic diameters of the targeted gases are close, the much higher quadrupole moment of CO_2 enables for the selective CO_2 capture by adsorption.[24] Due to lower polarizability of N_2 compared to CH_4, the much higher selectivity for CO_2 over N_2 compared to CO_2 over CH_4 can be achieved. It is worth noting that the vast majority of the studied POPs and MOFs in the literature have pore diameters much bigger

المنارة للاستشارات
www.manaraa.com

than the targeted gases, and therefore the separation mechanism relies on selective adsorption rather than a size exclusion mechanism.

Porous Organic Polymers (POPs), a class of highly cross-linked, amorphous microporous polymers, have recently emerged as a promising adsorbent for small gas capture and separation.[26] POPs, in general, exhibit exceptional physicochemical stability towards acid, base and moisture. This is in a part a result of the covalently linked backbone used to form the frameworks. Although, POPs are amorphous because of irreversible reactions, exceptionally high surface areas can be achieved with only a small percentage comprise from their calculated geometric surface areas.[27] Qiu *et al* reported a new class of POPs referred to as PAFs (Porous Aromatic Framework).[28] PAF-1 was synthesized by Yamamoto coupling using tetra(bromo phenyl)methane (**Scheme 1.2**) as a building block with an exceptionally high BET surface area of 5600 m^2 g^{-1}.This suggests that the lack of long-range order in POPs does not necessarily translates into low surface area materials. In addition, surface area, average pore size and pore functionality can be tuned for targeted applications.

In order for a porous organic polymer to be employed as solid adsorbent for carbon capture from flue gas as well as natural gas stock, the following criteria must be met.[24]

- The adsorbent needs to have high CO_2 adsorption capacity under industrial settings in order to make separation column smaller.
- The adsorbent needs to have high selectivity toward CO_2 to increase the purity of captured gas CO_2 which is crucial as CO_2 is not the main component in the gas mixtures.

المنارة للاستشارات
www.manaraa.com

- The adsorbent needs to be chemically stable towards moisture, SOx and NOx as they are present in the gas stream as contaminants.
- The adsorbent needs to be mechanically stable in order to allow for dense packing for maximum volumetric capacity.
- The adsorbent itself and building blocks should be readily synthesized from abundant and accessible chemicals to make the process cost-effective.
- The regeneration of adsorbent should be achieved with minimal additional energy input to decrease the energy penalty of the total system.
- The mass and heat transfer of the adsorbents should be good. Densely packed adsorbents should allow the adsorption and desorption of the guest molecules. In addition, heat conductivity is needed since temperature can be used to regenerate the adsorbents.

1.4 Synthesis of Porous Organic Polymers

Since organic chemistry is the tool box of porous organic polymer design, numerous different routes have been explored to synthesize new functional materials. Although some methods employ expensive metals to catalyze the reaction, there are metal-free condensation reactions which present an economically viable route for the mass production of porous adsorbents. Some of the most common reactions used to synthesize POPs are Yamomoto coupling, Suzuki coupling, Friedel-Crafts alkylation, imidazole ring formation, dibenzo-dioxane formation, imidization, amidation, Sonagashira cross-coupling, homocoupling of aromatic amines, nitrile cyclotrimerization and acetyl cyclotrimerization.[28-34] It is worth noting that the same (considering their amorphous

المنارة للاستشارات
www.manaraa.com

Scheme 1.2. Yamamoto Coupling Formation of PAF-1

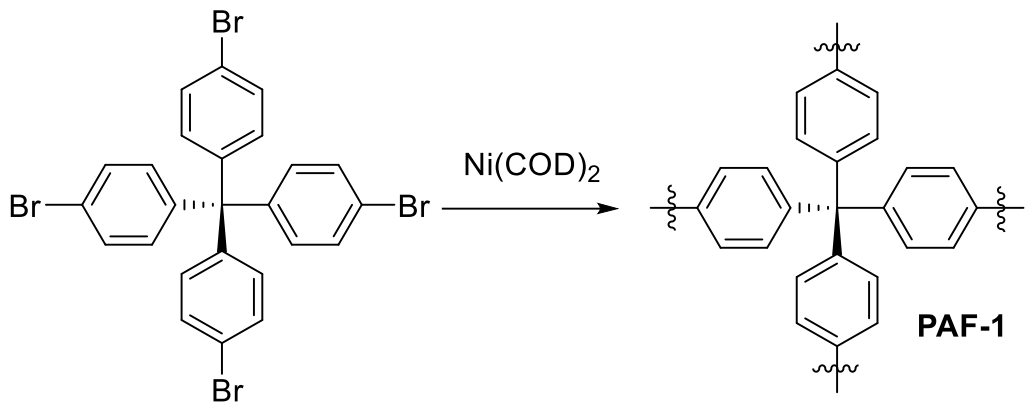

morphology) POP can be synthesized from different synthetic routes as long the functional groups survives the synthesis and work up steps. Almost all synthetic strategies to obtain porous materials employ either ditopic or polytopic functional organic linkers in order to attain extended frameworks. It has been shown that targeted textural properties such as extremely high surface area, permanent porosity, and narrow pore size distribution, hierarchical pore structure and chemical functionality can be achieved by varying the molecular building units and/or modifying the synthesis condition.[29] Combined together, these parameters dictate the structure-function relationship in POPs and determine their effectiveness in CO_2 capture applications. Metal catalyzed cross-coupling reactions are perhaps the most extensively used synthetic routes for POPs preparation.

As mentioned above PAF-1 presents remarkably high surface area which uptakes significant amounts of gas (H_2, CH_4, CO_2) under high pressure settings. The very high surface area of PAF-1 and PPN-4 was attributed to diamond-like framework topology which provides accessible pores with highly cross-linked structures.[35] Due to its robust

المنارة للاستشارات
www.manaraa.com

Scheme 1.3 Synthesis routes of some hetero atom containing POPs.

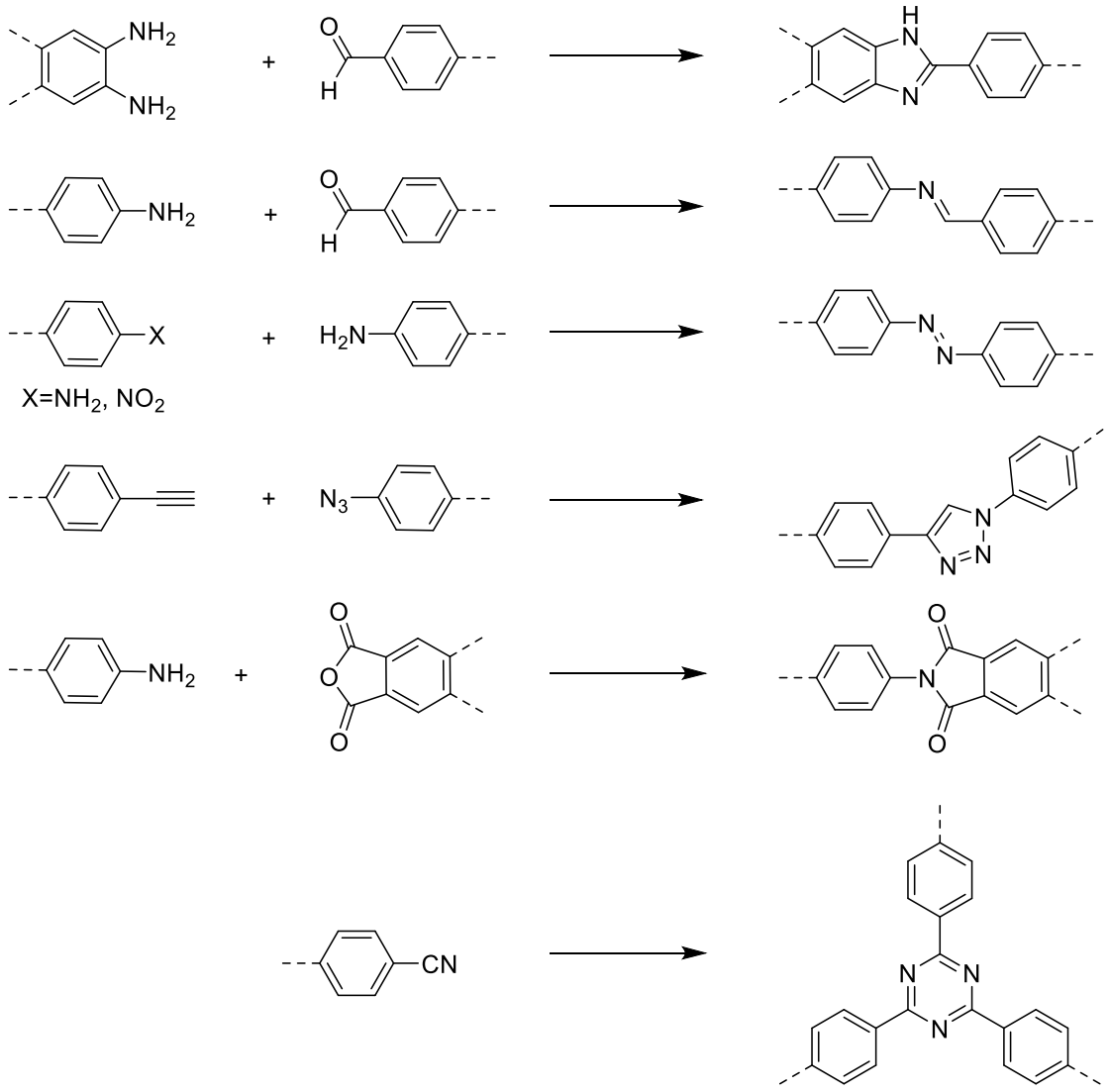

aromatic structure, PAF-1 showed high thermal and chemical stability. However, carbon-based PAFs do not perform well in gas storage applications at low pressure (1 bar) due to their uniform and non-functionalized pore walls that lead to low isosteric heats of adsorption for CO_2 (~17 kJ mol^{-1}).[36]

المنارة للاستشارات
www.manaraa.com

Theoretical screening of MOFs and POPs have shown that incorporation of hetero atoms (N, S, O, F) into the pores of POPs results in enhanced CO_2 binding affinities and therefore higher CO_2 uptake capacity at low pressures.[37, 38] This is due to dipole-quadrupole interactions between hetero atoms on POPs and CO_2 molecules. Since CO_2 has a greater quarupole moment and polarizability compared to CH_4 and N_2, the materials possessing those functional sites allow for selective CO_2 capture.[3] Therefore, a great amount of effort has been devoted to developing POPs that features Lewis basic sites which capture CO_2 selectively from gas mixtures by polarizing CO_2 molecules. Some selected hetero atom decorated POPs are shown in **Scheme 1.3**. The list for hetero atom containing POPs includes those developed by El-Kaderi such as Benzaimidazole-Linked Polymers (BILP),[39, 40] Borazine-Linked Polymers (BLPs),[41] and Azo-Linked Polymers (ALP)[32] and many other systems: Polymer Intrinsic Microporosity (PIM),[42] Covalent Triazine Frameworks (CTZ)[33] and Conjugated Microporous Polymers(CMP),[43] Covalent Organic Polymers (COPs),[44] and imine,[45] and imide[46] linked porous polymers.

El-Kaderi and coworkers introduced a new class of porous organic materials called Benzaimidazole-Linked Polymers (BILPs), prepared by metal-free catalyzed condensation of aryl-o-diamine and arylaldehyde that resulted in imidazole-ring formation **Scheme 1.4**.[30] BILPs show CO_2 uptake as high as 5.4 mmol g^{-1} at 273 K and 1 bar and very good selectivity as high as 113 for CO_2 over N_2 and 17 for CO_2 over CH_4 at 273 K. In addition, the sorbent selection criteria also showed BILPs outperform most of the best performing materials in the literature which will be discussed in detail in Chapter 4.[39] Benzimidazole is one of many functionalities that can be incorporated in the POPs to achieve selective CO_2 capture. Decorating the pores of POPs with strongly polar groups

المنارة للاستشارات
www.manaraa.com

Scheme 1.4. A schematic representation of the syntheis of BILPs.

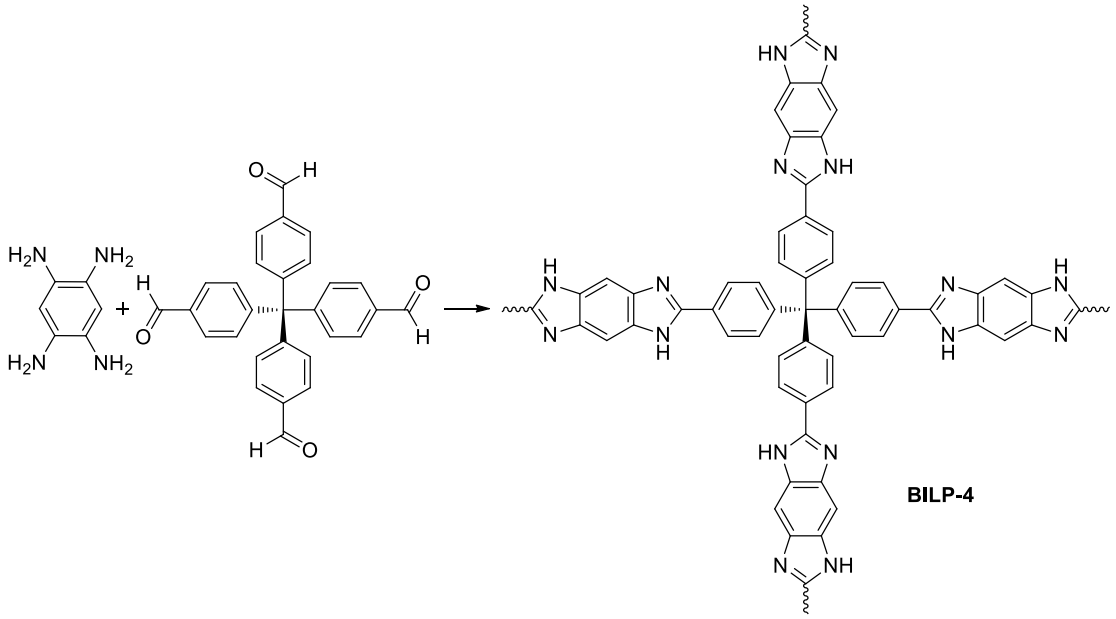

such as –OH, -NH_2, -SO_3, has been instrumental for achieving selective CO_2 capture and high uptake capacity.[21, 47] In the case of BILP, benzimidazole functional groups are formed as the framework grows via a self-assembly method. There are mainly two other methods to have targeted functionality in POPs: (1) pre-synthesis modification (PEM) of building blocks wherein CO_2-philic moieties are attached to building blocks before framework formation, (2) post-synthesis modification (PSM) processes in which functional groups are tethered to the pore walls after framework assembly as depicted in **Figure 1.2** As mentioned above, selective CO_2 capture and capacity are the most important features for CO_2 adsorbents. High surface area materials do not necessarily lead to high CO_2 uptake since gas uptake capacity depends on the favorable interactions between pore walls and guest gas molecules.[21]

المنارة للاستشارات
www.manaraa.com

1.5 Pre- and Postsynthetic Modification of POPs

Decorating the pore walls of POPs with functional groups via the self-assembly network process provides access to only limited functional groups. On the other hand presynthetic and postsynthetic modification of POPs has been instrumental for incorporating many different functional groups into POPs.[48] Even though PEM and PSM of POPs have been studied more recently and in far less depth compared to MOFs,[49] there are very few successful studies reported. Each method has its own merits and demerits. Presynthetic modification allows us to install functional groups on specified

A. Pre-synthetic Modification

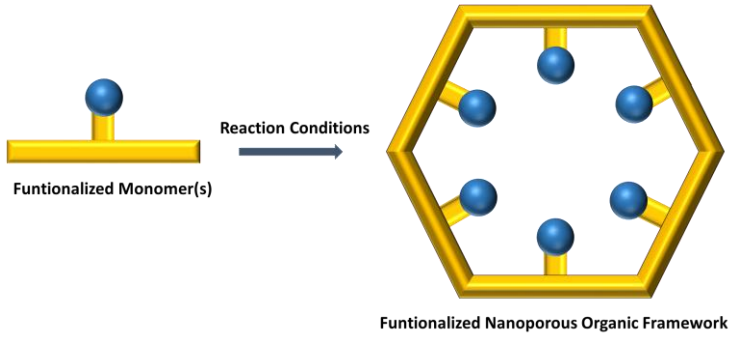

B. Post-synthetic Modification

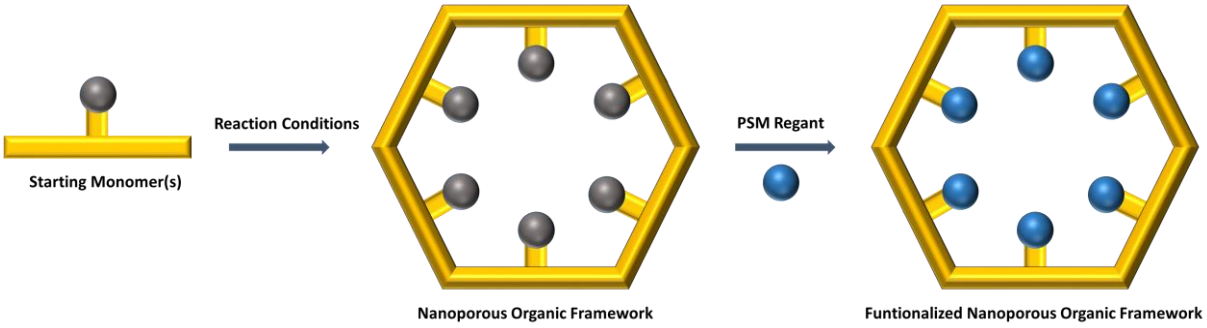

Figure 1.2. Schematic representation of pre- and post-synthetic modification synthesis.

المنارة للاستشارات
www.manaraa.com

positions in a more controlled manner compared to postsynthetic modification since the monomer(s) that are used in synthesis can be purified prior to framework formation. However, there are some problems associated with this method. First, functionalization of building blocks often necessitates alternate reaction conditions (i.e. protection of some functional groups) due to possible side reactions , and these reactions are often time consuming and non-trivial. In addition, synthesis of POPs requires harsh conditions such as high temperature, acidic or basic media where the functional groups on the building blocks may Undergo side reactions or decompose. Therefore, it has been found convenient to introduce targeted functionalities within the pores after framework formation via PSM where almost countless of functional groups can be incorporated with the help of organic chemistry. Chemical and thermal stability of POPs have allowed researchers to introduce heterogeneity to the surface even at harsh reaction conditions such as low/high pH and high temperature.[50] On the other hand, PSM of POPs often leads to much lower surface areas due to uncontrolled loading of functional groups which block the ultramicropores making them inaccessible to gas molecules.[51] In addition, functional group loading per linker is always much lower compared to presynthetic modification even under controlled conditions also the sites that are being functionalized in POPs may be difficult to control if there is more than one site which can undergo the same reaction. Nevertheless, PSM of POPs to incorporate amine functionality has been reported recently for many systems.[21, 50, 52, 53]

Zhou and coworkers have shown the successful incorporation of polyamine groups in PPN-6 which resulted in excellent CO_2 uptake as high as 4.3 mmol g^{-1} and selectivity of 442 (calculated by Ideal Adsorbed Solution Theory) CO_2 over N_2 at 1 bar and 295 K.[50]

المنارة للاستشارات
www.manaraa.com

Scheme 1.5. Post-synthesis modification of Porous Polymer Networks.

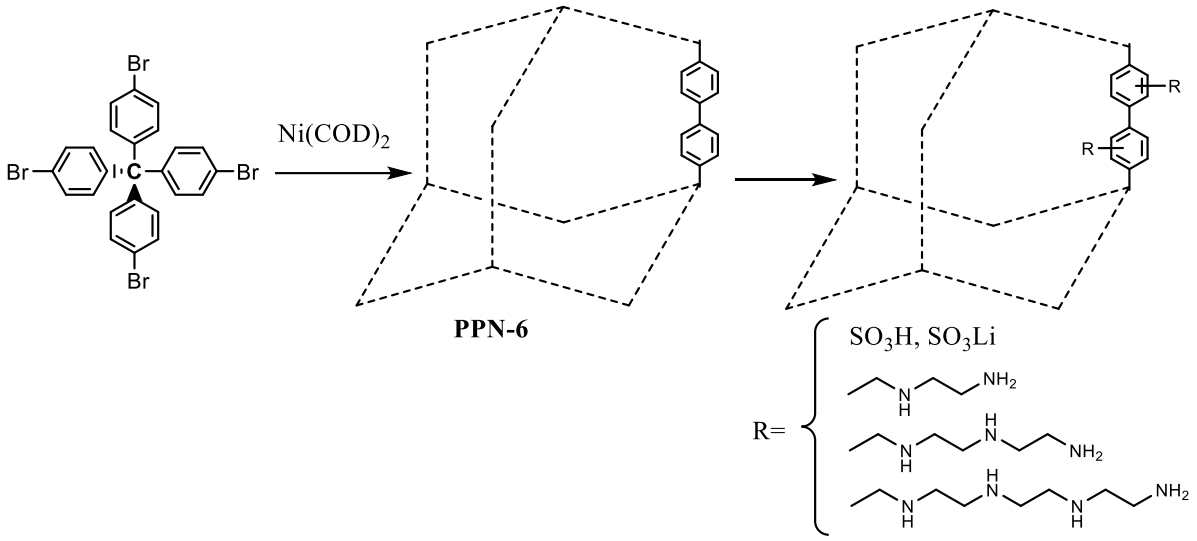

They have observed significant increase in the heat of adsorption, correspondingly, CO_2 uptake capacity which is attributed to strong electrostatic interaction between basic amine functionality and CO_2 molecule. They have also previously reported on incorporation of sulfonic acid and its lithium salt within the pores of PPN-6 (**Scheme 1.5**) via PSM and an increase in binding affinity of CO_2 and corresponding CO_2 uptakes has been observed.[47] Alkyl amine tethering to POPs also reported by Garibay et.al where *de novo* synthesis of methyl-, hydroxymethyl-, and phthalimidomethyl functionalized POPs were achieved and treatment of phtalimide functionalized POP with hydrazine has resulted in alkyl amine functionalized POP.[53] This method presents amine loading in a more controlled manner due to presynthetic functionalization of the framework. Similar observations have been reported by the authors where more basic amines resulted in significant enhancement in CO_2 uptake and binding affinity. However, both studies resulted in low loading of

المنارة للاستشارات
www.manaraa.com

functional group (~0.25–0.3 N rich linker / phenyl) yet dramatic decrease in surface areas.[53]

1.6 Sorbent Evaluation Criteria

Although numerous porous organic and organic–inorganic hybrid materials have been evaluated for CO_2 capture and separation, a careful analysis of the tradeoff between selectivity and uptake capacity was not evaluated until the recent work of Bae and Snurr.[54] The general observation made by Bae and Snurr was that the high surface area property favors CO_2 separation from landfill gas in pressure swing adsorption (PSA) where adsorption takes place at high pressure (>5 bar) and desorption takes place at atmospheric pressure (1 bar), whereas the narrow pore size and high enthalpies of adsorption lead to optimal CO_2 removal from flue gas using vacuum swing adsorption (VSA) where adsorption takes place at atmospheric pressure (1 bar) and desorption is done at reduced pressure (0.1 bar). In both cases an ideal adsorbent shows high

Table 1.2. Adsorbent evaluation criteria suggested by Bae and Snurr.

CO_2 uptake under adsorption conditions *(mol kg^{-1})*	N_1^{ads}
Working CO_2 capacity (mol kg^{-1}), $N_1^{ads} - N_1^{des}$	ΔN_1
Regenerability (%), $(\Delta N_1/N_1^{ads})x100$	R
Selectivity under adsorption conditions, $(N_1^{ads}/N_2^{ads})x(y_2/y_1)$	α_{12}^{ads}
Sorbent selection parameter, $(\alpha_{12}^{ads})^2/(\alpha_{12}^{des})x\ (\Delta N_1/\Delta N_2)$	S

N: adsorbed amount, y: molar fraction in the bulk phase. Subscripts 1 and 2 correspond to the strongly adsorbed component (CO_2) and the weakly adsorbed component (CH_4 or N_2), respectively. α_{12} : Selectivity of gas component 1 over 2. ads and des correspond to adsorption and desorption conditions, respectively. Reproduced from Ref. 54 with permission from The Royal Society of Chemistry.

المنارة للاستشارات
www.manaraa.com

selectivity and gas uptake at adsorption pressure and minimum uptake at desorption pressure which yields high working capacity as well as high regenerability levels.[37]

Five evaluation criteria (**Table 1.2**) were adopted from the chemical engineering field to investigate the effectiveness of porous adsorbents: CO_2 uptake, working capacity for CO_2, adsorbent regenerability, selectivity under adsorption conditions, and sorbent selection parameter. At this point the strength of the POP-CO_2 interaction becomes very important. As depicted in **Figure 1.3** the basicity of N-rich functional groups shows variation depending on the conjugation, hybridization etc. Although sorbents that are functionalized with very basic functional groups result in higher binding affinity and initial

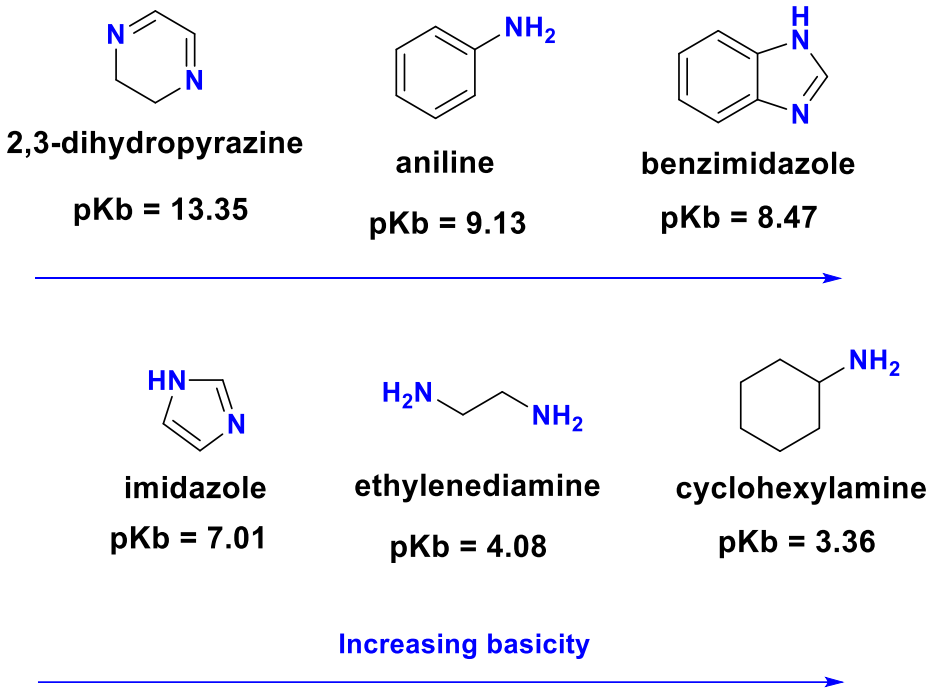

Figure 1.3. Basicity of some nitrogen rich functional groups.

المنارة للاستشارات
www.manaraa.com

CO_2 uptake, their regenerability levels are much lower compared to ones that are mildly basic such as aniline and benzimidazole.[37] These criteria, although not perfect, provide a more comprehensive approach for assessing the suitability of porous adsorbents in CCS processes.

1.7 Dissertation Problem

Considerable effort has been made to develop efficient solid sorbent materials for CO_2 capture from flue gas and landfill gas via adsorption-based separation to mitigate CO_2 level in the atmosphere. Among the solid adsorbents investigated, POPs have received considerable attention because of their physical and chemical stability in addition to structural tunability. However, POPs that do not possess hetero atoms i.e N, O, S, F do not show high selective adsorption of CO_2 under ambient temperature and pressure Incorporation of those hetero atom containing functional groups can be done via different routes. The main objectives of this dissertation are to functionalize POPs with amino groups which are capable of increasing binding affinity of CO_2. PSM has been instrumental for incorporating many different functional groups including amino groups. However, excess amount of reagent and longer reaction times yields materials with much lower surface area due to blocking of micropores. With these considerations in mind, we set out to design, synthesize, and characterize POPs with high physicochemical stability which allows us to decorate the pore walls with functional groups without destroying the backbone even in concentrated acidic media. This was achieved by nitration of aromatic rings and subsequent reduction to amine in order to compare the effect of different functionalities. Optimizing the reaction conditions for functional group loading, it is possible to obtain POPs with high surface area which shows higher uptake of CO_2 even

المنارة للاستشارات
www.manaraa.com

at low pressures compared to POPs with higher degree of functionalization. Gas sorption capabilities and textural properties were investigated through gas sorption experiments at different temperatures.

Functionalization of BILPs with amine groups was also among the goals of this dissertation. Functionalization of POPs with dual functional groups has been shown to be useful in order to have a synergetic effect of each functional group on CO_2 uptake and selectivity. Our group has recently reported that triazine functionalized BILPs show enhanced selectivity as well as thermal stability compared to traditional BILPs. However due to lower basicity of triazine groups compared benzimidazole, the effect on CO_2 uptake is less pronounced. Here, we have designed an amino functionalized BILP which showed enhanced CO_2 capture capacity due to comparable basicity of aniline like amine and benzimidazole. In addition, amine and benzimidazole groups involved in intramolecular hydrogen bonding lead to different binding modes with CO_2 compared to traditional BILP. To have a better understanding of the effect of amine groups on CO_2 binding capabilities we have also performed DFT calculations. Advancements in understanding the effect of different functional groups on CO_2 adsorption properties could guide the scientific community on designing materials with better performance. In our opinion, the research presented here provides an important step for the development of advanced materials for CO_2 capture and separation

المنارة للاستشارات
www.manaraa.com

Chapter 2

Impact of Post-Synthesis Modification of Nanoporous Organic Frameworks On Small Gas Uptake And Selective CO_2 Capture[1]

2.1 Introduction

Porous organic polymers (POPs) have received considerable attention due to their potential in important fields such as catalysis, sensing, optoelectronics, as well as gas storage and separation.[26, 55-61] Among the attractive features of POPs are their exceptionally high surface area, remarkable physicochemical stability, adjustable pore size, and chemical nature tunability, which collectively dictate the structure–function relationship in POPs. In general, chemical heterogeneity of the pores in porous architectures plays a significant role especially in selective gas binding and separation (**Figure 2.1**) In this regard, post-synthesis modification (PSM) of organic polymers[23, 53, 62, 63] and their inorganic counterparts metal–organic frameworks (MOFs)[49, 64] have emerged as an invaluable synthetic tool that allows for pore surface modification. This approach can overcome some of the synthetic challenges that can be encountered when pre-

[1] Islamoglu, T.; Gulam Rabbani, M.; El-Kaderi, H. M., *J. Mat. Chem. A* **2013**, *1*, 10259-10266. Reproduced by permission of The Royal Society of Chemistry.

المنارة للاستشارات
www.manaraa.com

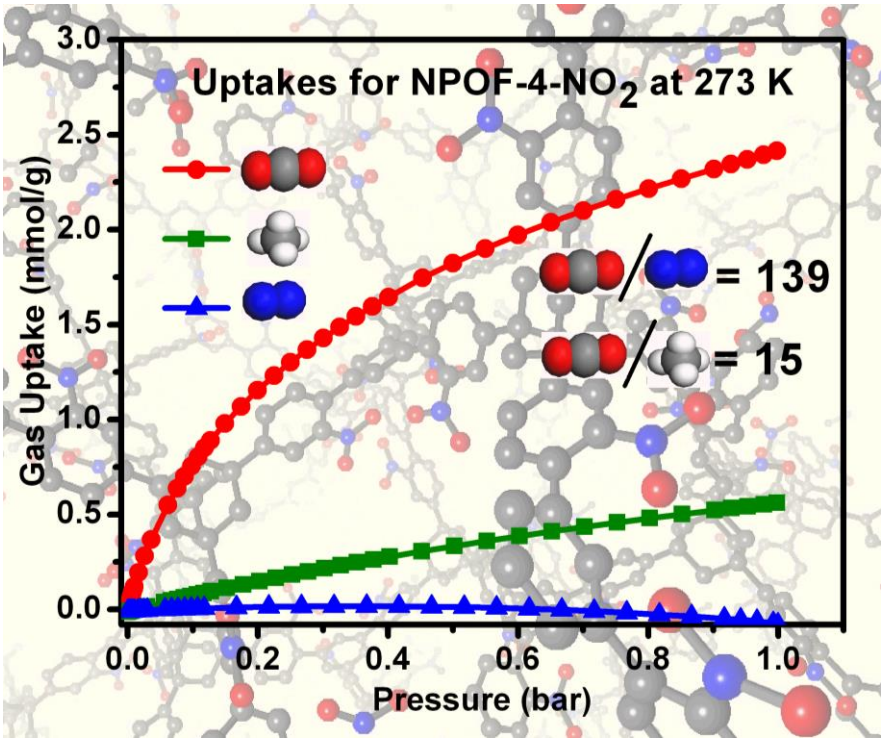

Figure 2.1 Selective CO_2 capture with NPOFs.

functionalized building units cannot be employed to construct porous materials due to chemical or physical incompatibility. Although PSM has been well documented for MOFs, the metal-linker interactions in some MOFs can limit their use in PSM processes which, in some cases, require harsh reaction conditions such as those encountered in the nitration of aryl linkers by a mixture of concentrated HNO_3–H_2SO_4.[49] In contrast, the covalent nature of POPs makes them chemically robust and enables pore chemical modification under the aforementioned conditions without compromising porosity.

It is now well established that tailoring accessible nitrogen[40] or amine[50] functionalities into the framework of porous materials can significantly enhance CO_2 binding and

المنارة للاستشارات
www.manaraa.com

uptake. CO_2 capture and sequestration (CCS) has received considerable attention due to the greenhouse nature of CO_2 and the fact that it is one of the major contaminants of methane-rich gases (shale, natural, landfill) and hydrogen fuels.[65] It has been recognized that a high surface area property is very relevant to gas storage under high pressure conditions while it plays a less significant role in CO_2 separation.[31] For example, in flue gas the CO_2 composition is only ~15% and its removal by porous materials is mainly driven by the chemical nature of the pores that can selectively bind CO_2 over other gases present in flue gas such as N_2, SO_2, NO_2, *etc.* Moreover, a very recent report by Wilmer *et al.* indicates that the pore functionalization with alkylamines is less favourable for CO_2 separation from flue gas by vacuum swing adsorption (VSA) that operates in the pressure range of 0.1–1.0 bar because of the high charge density on the nitrogen sites that react with CO_2 and lead to very high heats of adsorption.[37] On the contrary, direct amination of aryl linkers leads to pore functionalization wherein the less negative charge on the amine affords moderate binding affinities that are advantageous for CO_2 removal from flue gas and natural gas thereby facilitating adsorbents regeneration.

With these considerations in mind, we report in this study on post-synthesis modification of NPOFs through direct nitration of aryl linkers followed by reduction and we illustrate the consequence of pore modification on small gas uptake and storage. The resulting functionalized frameworks have moderate isosteric heats of adsorption that are optimal for post-combustion CO_2 capture from flue gas and separation from methane-rich gases as evidenced by the presented CO_2/N_2 and CO_2/CH_4 selectivity studies.

2.2 Experimental Section

2.2.1 Materials and Methods

المنارة للاستشارات
www.manaraa.com

All starting materials and solvents, unless otherwise noted, were obtained from Acros Organics and used without further purification. 1,3,5,7-Tetraphenyladamantane was synthesized according to a published method.[66] (**Scheme 2.1**) $SiCl_4$ was purchased from Sigma-Aldrich. $SnCl_2$ was purchased from MP Biomedicals, LLC. Absolute ethanol was purchased from Pharmaco Products. Solvents were dried by distillation. Air-sensitive samples and reactions were handled under an inert atmosphere of nitrogen using either glovebox or Schlenk line techniques. Elemental microanalyses were performed at the Midwest Microlab, LLC. Liquid ^{1}H and ^{13}C NMR spectra were obtained on a Varian Mercury-300 MHz NMR spectrometer (75 MHz carbon frequency). Solid-state ^{13}C cross-polarization magic angle spinning (CP-MAS) NMR spectra for solid samples were taken at Spectral Data Services, Inc. Spectra were obtained using a Tecmag-based NMR spectrometer operating at a H-1 frequency of 363 MHz, using a contact time of 1 ms and a delay of three seconds for CP-MAS experiments. All samples were spun at 7.0 kHz.Thermogravimetric analysis (TGA) was carried out using a TA Instruments Q-5000IR series thermal gravimetric analyser with samples held in 50 μL platinum pans under an atmosphere of air (heating rate 5 °C min^{-1}). For scanning electron microscopy imaging (SEM), samples were prepared by dispersing the material onto a sticky carbon surface attached to a flat aluminium sample holder. The samples were then coated with platinum at a pressure of 1×10^{-5} mbar under a nitrogen atmosphere for 90 seconds before imaging. Images were taken on a Hitachi SU-70Scanning Electron Microscope. Powder

المنارة للاستشارات
www.manaraa.com

Scheme 2.1 Synthesis of 1,3,5,7-tetrakis(4-acetylphenyl)adamantane.

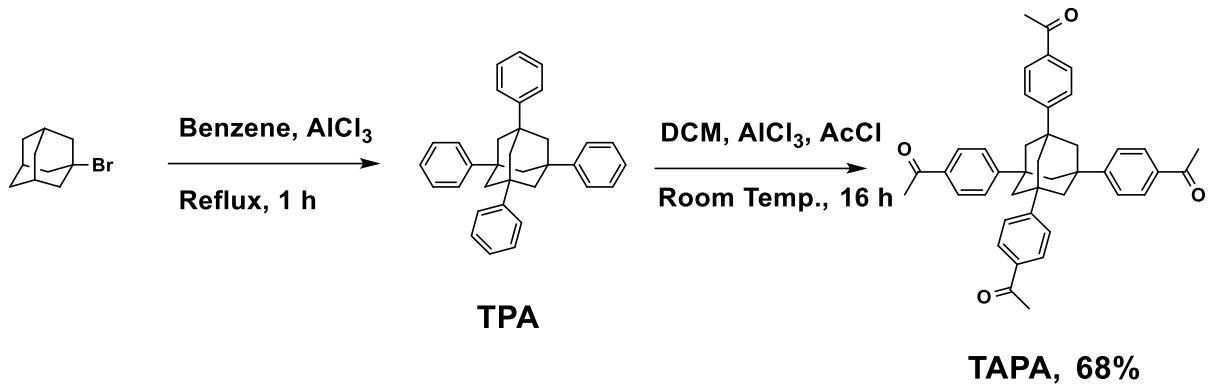

X-ray diffraction data were collected on a Panalytical X'pert pro multipurpose diffractometer. Samples were mounted on a sample holder and measured using Cu Kα radiation with a 2θ range of 1.5–35. FT-IR spectra were obtained on a Nicolet-Nexus 670 spectrometer furnished with an attenuated total reflectance accessory. Porosity and gas sorption experiments were collected using a Quantachrome Autosorb 1-C volumetric analyser using adsorbates of UHP grade. In a typical experiment, a sample of polymer (~60 mg) was loaded into a 9 mm large bulb cell (Quantachrome) of known weight which is then hooked up to the Autosorb 1-C and degassed at 120 °C/1.0 × 10^{-5} bar for 12 hours. The degassed sample was refilled with helium, weighed precisely then transferred back to the analyser. The temperatures for adsorption measurements were controlled by using a refrigerated bath of liquid nitrogen (77 K), liquid argon (87 K), or temperature controlled water bath (273 K and 298 K).

المنارة للاستشارات
www.manaraa.com

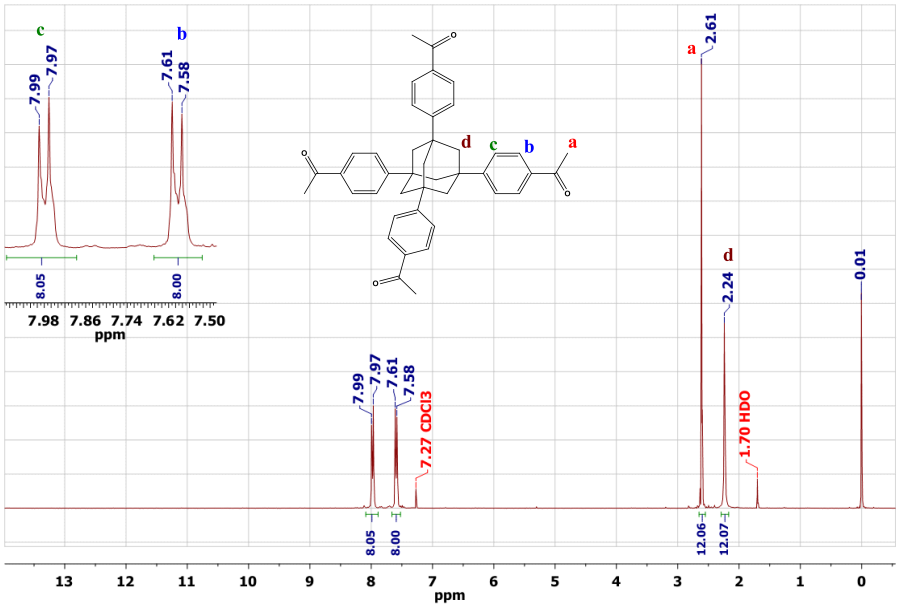

Figure 2.2 ^{1}H NMR for 1,3,5,7-tetrakis(4-acetylphenyl)adamantane in $CDCl_3$.

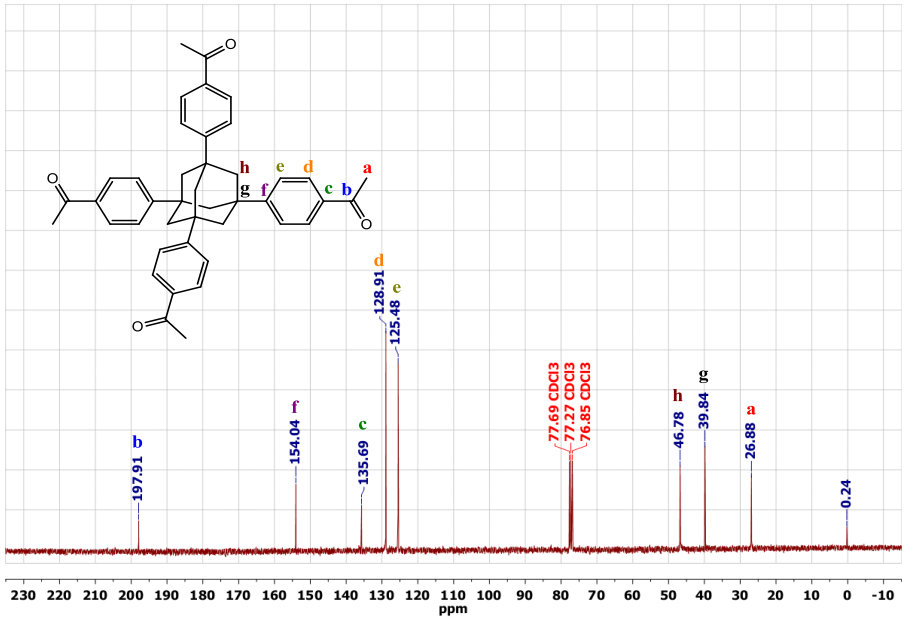

Figure 2.3 ^{13}C NMR for 1,3,5,7-tetrakis(4-acetylphenyl)adamantane in $CDCl_3$.

المنارة للاستشارات
www.manaraa.com

2.2.2 Synthetic Aspects

Synthesis of 1,3,5,7-tetrakis(4-acetylphenyl)adamantane (TAPA). A 250 mL reaction flask was charged with $AlCl_3$ (16.4 g, 123 mmol), placed in an ice bath and 90 mL of acetyl chloride was added under N_2 to afford a colourless solution. A mixture of tetraphenyladamantane(TPA) (2.50 g, 5.67 mmol) and freshly distilled dichloromethane, DCM, (100 mL) was added to this solution at 0 °C and stirred for 10 minutes, and then it was allowed to warm to room temperature and stirred for 16 h. The reaction mixture was carefully poured into ice (200 mL) then stirred for 30 minutes at room temperature. The organic layer was extracted with DCM and washed with 10% $NaHCO_3$ solution. The resulting yellow solution was dried over $MgSO_4$ and filtered over a medium glass frit. Excess DCM was removed by evaporation under reduced pressure. The resulting product was crystallized from DCM–EtOH mixture to afford TAPA as off-white crystals (2.35 g, 68% yield). ^{1}H NMR ($CDCl_3$, 300 MHz) δ (ppm) 7.98 (d, J_{HH} = 6.0, 8H), 7.595 (d, J_{HH} = 9.0, 8H), 2.61 (s, 12H), 2.24 (s, 12H). ^{13}C NMR ($CDCl_3$, 75 MHz) δ(ppm) 197.9, 154.0, 135.7, 128.9, 125.5, 46.8, 39.8, 26.9. TOF MS ES+ *m/z* for $C_{42}H_{40}O_4$ calcd 609.3005, $[M + H]^+$ 609.353.

Synthesis of NPOF-4. A 200 mL reaction flask was charged with TAPA (300 mg, 0.493 mmol), 60 mL absolute ethanol and 60 mL xylenes (dried over Na). The colourless solution was cooled to 0 °C and $SiCl_4$ (18.3 mL, 157.8 mmol) was added dropwise under N_2. The solution was allowed to stir for 30 minutes at 0 °C, and then 1 hour at room temperature to give a black colored solution which was further refluxed at 80 °C for 16 h. The solution was allowed to cool down to room temperature then was filtered over a glass

المنارة للاستشارات
www.manaraa.com

Scheme 2.2 Schematic representation of NPOF-4 synthesis and its post-synthesis modification.

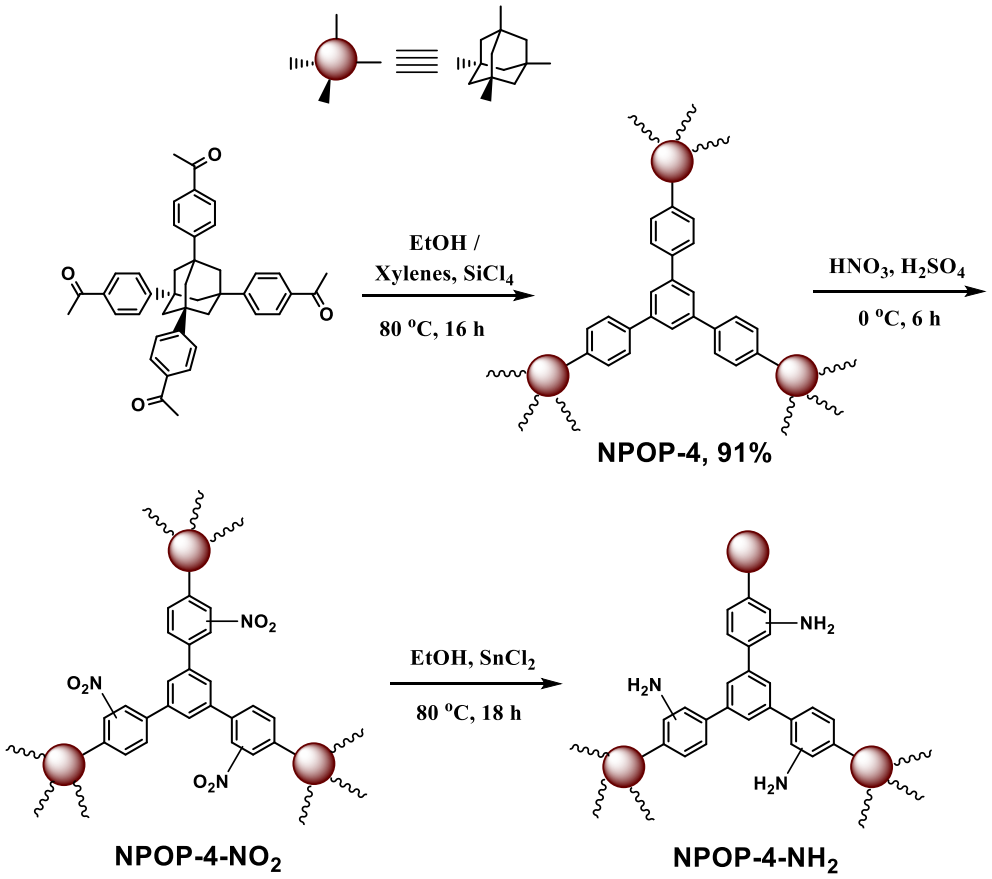

frit. The yellow powder was washed with ethanol, 2.0 M HCl, 2.0 M NaOH, water, DCM, and then dried to afford NPOF-4 (240 mg, 91% yield) as a yellow powder. Anal. calcd for $C_{126}H_{96}$: C, 93.99%; H, 6.01%. Found: C, 83.09%; H, 6.11%.

Synthesis of NPOF-4-NO_2. A 50 mL round bottom flask was charged with 12.5 mL of concentrated H_2SO_4then cooled to 0 °C. To this solution, 180 mg NPOF-4 was added in small portions followed by dropwise addition of 9 mL 70% HNO_3 and stirred for 6 h at 0 °C. The mixture was poured into 100 mL of ice and stirred for 30 minutes at room

المنارة للاستشارات
www.manaraa.com

temperature. The resulting powder was isolated by filtration through a glass frit and washed with water and ethanol. The obtained powder was soaked in ethanol–water mixture for 16 h, filtered and dried to give NPOF-4-NO_2 (225 mg) as a brown powder. Anal. calcd for $C_{126}H_{84}N_{12}O_{24}$: C, 70.39%; H, 3.94%; N, 7.82%. Found: C, 67.52%; H, 4.61%; N, 4.84%.

Synthesis of NPOF-4-NH_2. A 100 mL reaction flask was charged with 50 mg NPOF-4-NO_2, 30 mL EtOH, and 350 mg of $SnCl_2$. The mixture was refluxed at 80 °C for 18 h. The resulting green suspension was filtered, then suspended in 20 mL of concentrated HCl and stirred for 16 h at room temperature. The HCl was replenished and stirring continued for 5 h at room temperature. The mixture was filtered and washed with copious amounts of water and with 0.25 M NaOH in order to neutralize it. The resulting polymer was purified by Soxhlet extraction in a water–EtOH mixture. The polymer was finally washed with EtOH and dried to give NPOF-4-NH_2 (42 mg) as a dark brown powder. Anal. calcd for $C_{126}H_{108}N_{12}$: C, 84.53%; H, 6.08%; N, 9.39%. Found: C, 65.49%; H, 4.77%; N, 7.42%.

2.3 Results and Discussion

2.3.1 Synthesis and Characterization of NPOFs

Cyclotrimerization of acetyl functional groups which is frequently used to construct macromolecules through benzene ring formation has been employed here for synthesizing the adamantane-based nanoporous organic polymers. This acid catalyzed cyclotrimerization of three acetyl groups results in the formation of a 1,3,5-substituted benzene ring with the elimination of three water molecules. NPOF-4 was synthesized in

المنارة للاستشارات
www.manaraa.com

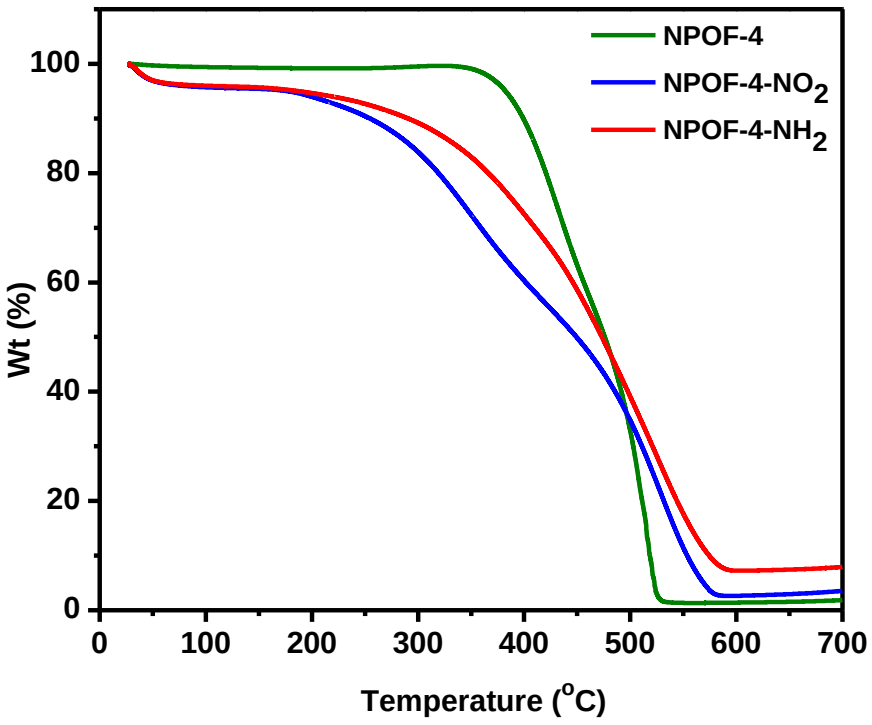

Figure 2.4. TGA traces of NPOF-4, NPOF-4-NO_2 and NPOF-4-NH_2.

good yields following a slightly modified procedure that was reported recently by Kaskel as depicted in **Scheme 2.2**[34] We have noticed that the controlled addition of $SiCl_4$ at 0 °C prevents rapid premature oligomers formation and leads to a more controlled pore formation and enhanced porosity. Although there are reports describing the room temperature cyclotrimerization of acetylated aromatic molecules to generate isolated molecules, high temperatures are frequently used to either accelerate the rate of reactions or to overcome the steric and electronic effects of substituents. NPOF-4 is insoluble in common organic solvents such as DMF, THF, toluene, ethanol, *etc.*, and remains intact upon washing with aqueous HCl and NaOH (6 M) as evidenced by spectral and physical studies. The high chemical stability of NPOF-4 enables post-synthesis

المنارة للاستشارات
www.manaraa.com

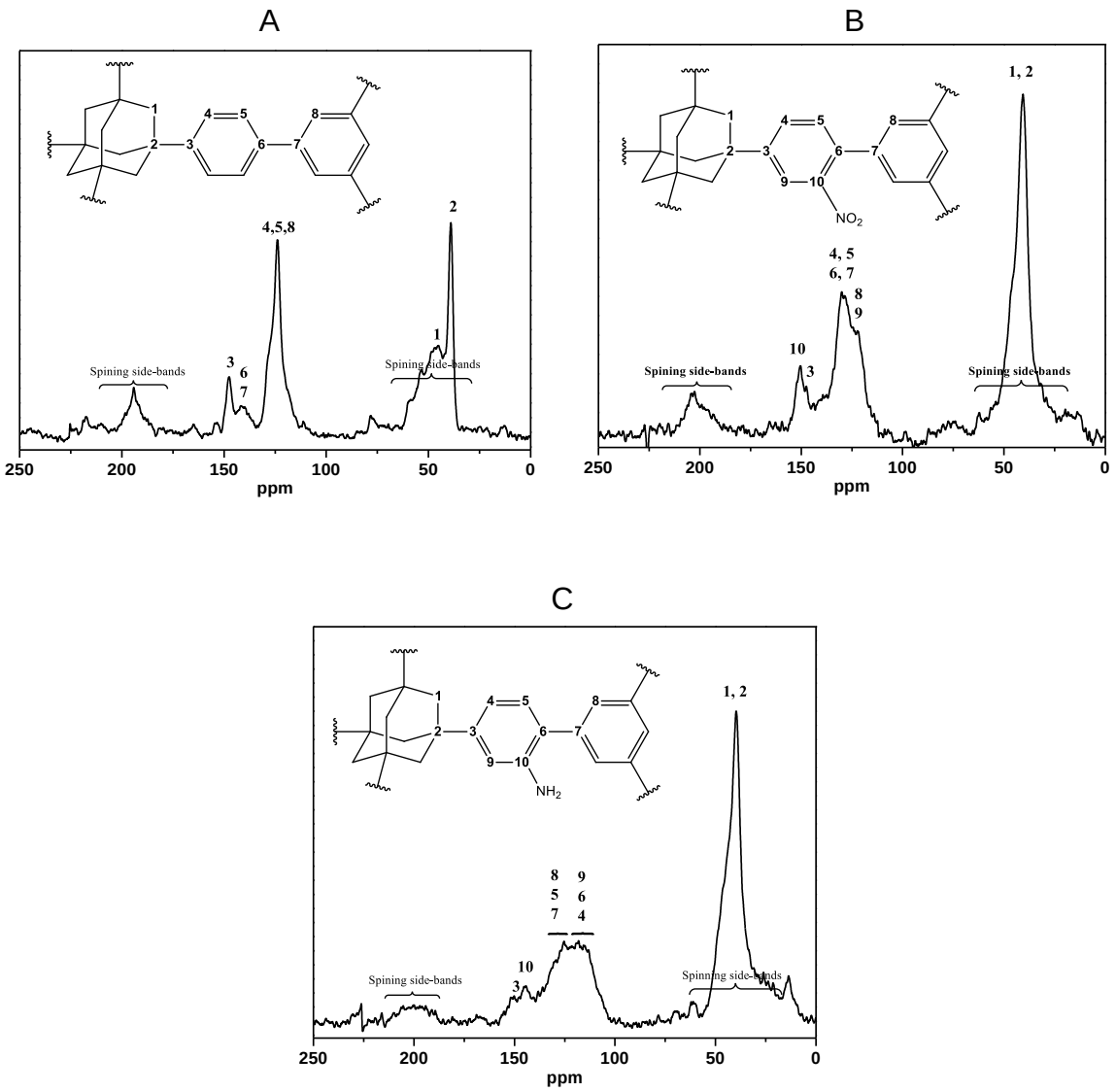

Figure 2.5 Solid state ^{13}C NMR of NPOF-4 (A), NPOF-4-NO_2 (B), NPOF-4-NH_2 (C).

modification of the framework particularly to introduce polar functional groups that are known to enhance gas storage or separation properties. For example, pore surface chemical modification of organic frameworks with amino groups has significantly enhanced CO_2 binding in porous polymer networks (PPNs)[50] and PAFs.[53] In addition to

المنارة للاستشارات
www.manaraa.com

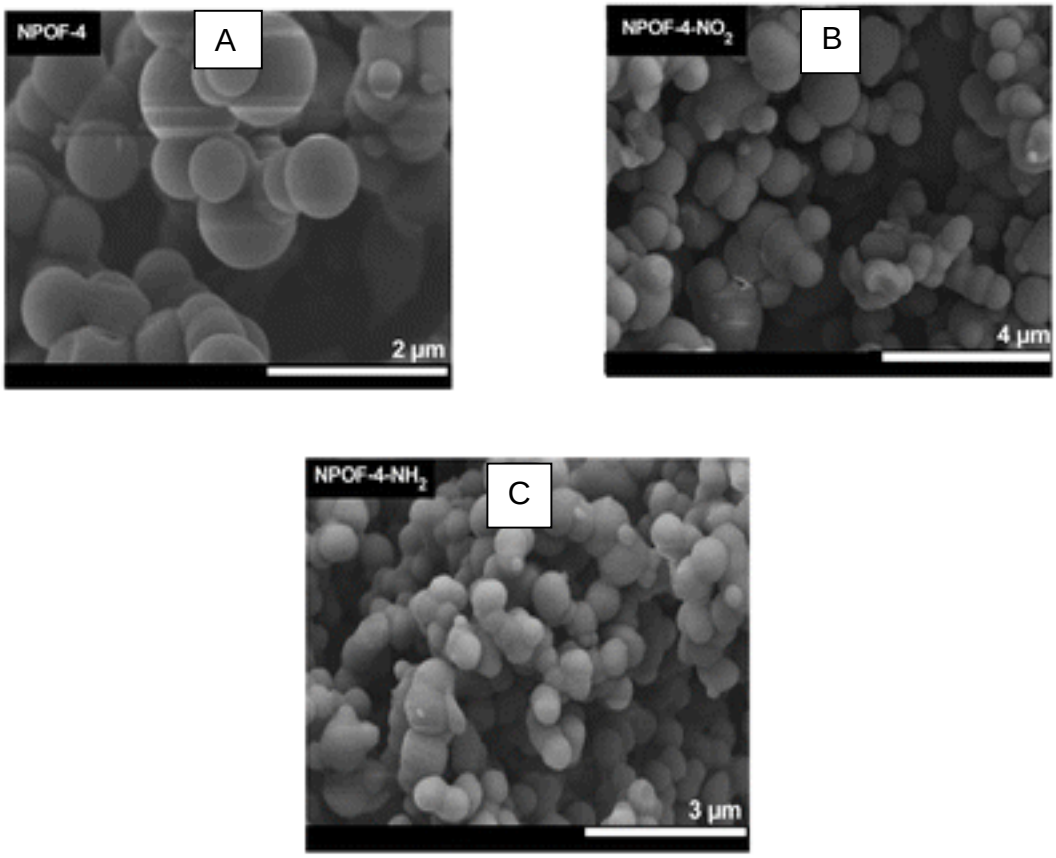

Figure 2.6 SEM images of NPOF-4 (A) and its modified frameworks NPOF-4-NO_2 (B) and NPOF-4-NH_2 (C).

the amine functionality, pore decoration with nitro (NO_2) groups is also important for separating polar gases as predicted by theoretical calculations and supported by experimental studies. Integrating these functionalities into the pore of MOFs and ZIFs led to noticeable enhancement in the selective binding of CO_2 over CH_4 and N_2. Consequently, we have first modified NPOF-4 by nitration (NPOF-4-NO_2) then reduced the resulting network to the corresponding amino-functionalized framework (NPOF-4-NH_2) and evaluated their gas uptake and selective binding. Nitration of NPOF-4 was

المنارة للاستشارات
www.manaraa.com

carried out by treatment with a mixture of concentrated HNO_3–H_2SO_4 to yield NPOF-4-NO_2 as a brown powder in a quantitative yield. The nitrated framework was then reduced to NPOF-4-NH_2 by using $SnCl_2$ in ethanol under refluxing conditions at 80 °C for 18 h which resulted in a dark brown powder. While the synthesis of NPOP-4-NO_2 and NPOP-4-NH_2 under harsh acidic conditions attests to the chemical robustness of the resultant polymers, their thermal stability was examined by TGA (**Figure 2.4**). The parent NPOP-4 remains stable up to 400 °C, while the functionalized networks; NPOF-4-NO_2 and NPOF-4-NH_2, are less stable and start to decompose at about 200 °C. SEM imaging of the polymers revealed aggregated spherical particles of variable size in the range of ~0.4 to 1.1 μm (**Figure 2.6**). As expected, NPOF-4 and its modified networks are amorphous as evidenced by powder X-ray diffraction study. The chemical functionalization of the polymers was investigated by FT-IR and solid-state ^{13}C NMR spectroscopic methods. Error! Reference source not found. shows the FT-IR spectra of the building block, TAPA, and the synthesized polymers. Upon polymerization, the intensity of the band at 1680 cm^{-1} (C=O) of TAPA is substantially decreased in the spectrum of NPOF-4 as a result of acetyl groups cyclotrimerization. This was further supported by the disappearance of the signal at 26.0 ppm in the ^{13}C NMR spectrum of NPOF-4 which corresponds to the methyl carbon in acetyl groups **(Figure 2.5).** Successful incorporation of nitro groups were confirmed by the appearance of new FT-IR bands at 1532 and 1350 cm^{-1} (**Figure 2.7**) which can be ascribed to the asymmetrical and symmetrical stretching of NO_2, respectively, in NPOF-4-NO_2.[67] Upon reduction, these bands disappear and the new bands at 3350 and 3230 cm^{-1} confirm the conversion of the nitro groups into the amine functionality. Solid-state ^{13}C NMR spectra reveal the

المنارة للاستشارات
www.manaraa.com

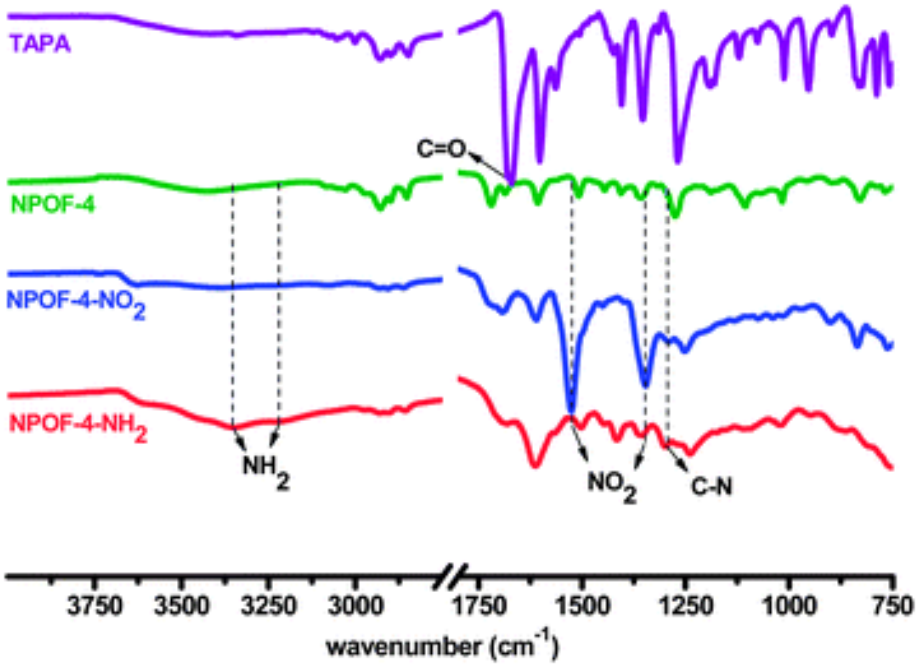

Figure 2.7 FTIR spectra of TAPA, and NPOFs.

broadening of the peaks at around 150 ppm upon nitration and reduction most probably due to the overlap between the signals of substituted carbons (**Figure 2.5**). The chemical composition of the functionalized networks was investigated by elemental analysis that indicated the content of nitrogen by mass to be 4.84% for NPOF-4-NO_2 (~0.54 N per phenyl directly attached to adamantane) as illustrated in **Scheme 2.2** (The functional group loading calculation is based on 100% cyclotrimerization of TAPA to afford NPOF-4). The nitrogen content, as expected, increased to 7.42% upon reduction. Notably, this method seems to be more effective than the previous methods reported for porous aromatic frameworks (PAFs) which resulted in only 0.25–0.3 N per phenyl rings.[53] It should be noted that attaining acceptable microelemental values for modified covalent networks and their post-synthesis modified material has been very problematic perhaps

المنارة للاستشارات
www.manaraa.com

because of uncontrolled functionalization reactions and incomplete reduction of the nitro groups. Other factors may include trapping of metal and/or byproducts inside the pores.

2.3.2 Porosity Measurements and Gas Storage Studies

The porosity of polymers was investigated by argon uptake measurements. **Figure 2.8A** shows the argon adsorption–desorption isotherms for NPOF-4, NPOF-4-NO_2, and NPOF-NH_2 at 87 K. All isotherms are fully reversible and exhibit hysteresis that is well pronounced for NPOF-4 most likely due to the flexible nature of the framework as documented for numerous porous organic materials. The rapid argon uptakes at very low pressure (below 0.1×10^{-3} bar) are indicative of microporosity and applying the Brunauer–Emmett–Teller (BET) model within the pressure range of P/P_o = 0.01–0.15 resulted in apparent surface areas SA_{BET} of 1249 $m^2\ g^{-1}$ (NPOF-4), 337 $m^2\ g^{-1}$ (NPOF-4-NO_2), and 554 $m^2\ g^{-1}$ (NPOF-4-NH_2). The surface area decreased significantly upon pore functionalization with nitro groups which can restrict pore accessibility by argon. Further modification by nitro group reduction resulted in a surface area value that is intermediate between those of NPOF-4 and NPOF-4-NO_2. Pore size distribution (PSD) was estimated by fitting the argon uptake branch of the isotherms with NLDFT (cylindrical/spherical pore geometry with zeolites/silica model) and found to have two major pore size distributions, 8.05 and 16.8 Å for NPOF-4, 7.73 and 10.8 Å for NPOF-4-NO_2, and 7.73 and 15.4 Å for NPOF-4-NH_2 (**Figure 2.8B**). Pore volumes were calculated from single-point measurements (P/P_o = 0.95) and found to be 0.78, 0.21, and 0.28 $cm^3\ g^{-1}$ for NPOF-4, NPOF-4-NO_2, and NPOF-NH_2, respectively. The porous properties of NPOF-4 and its functionalized networks are comparable to those of porous organic networks and the

المنارة للاستشارات
www.manaraa.com

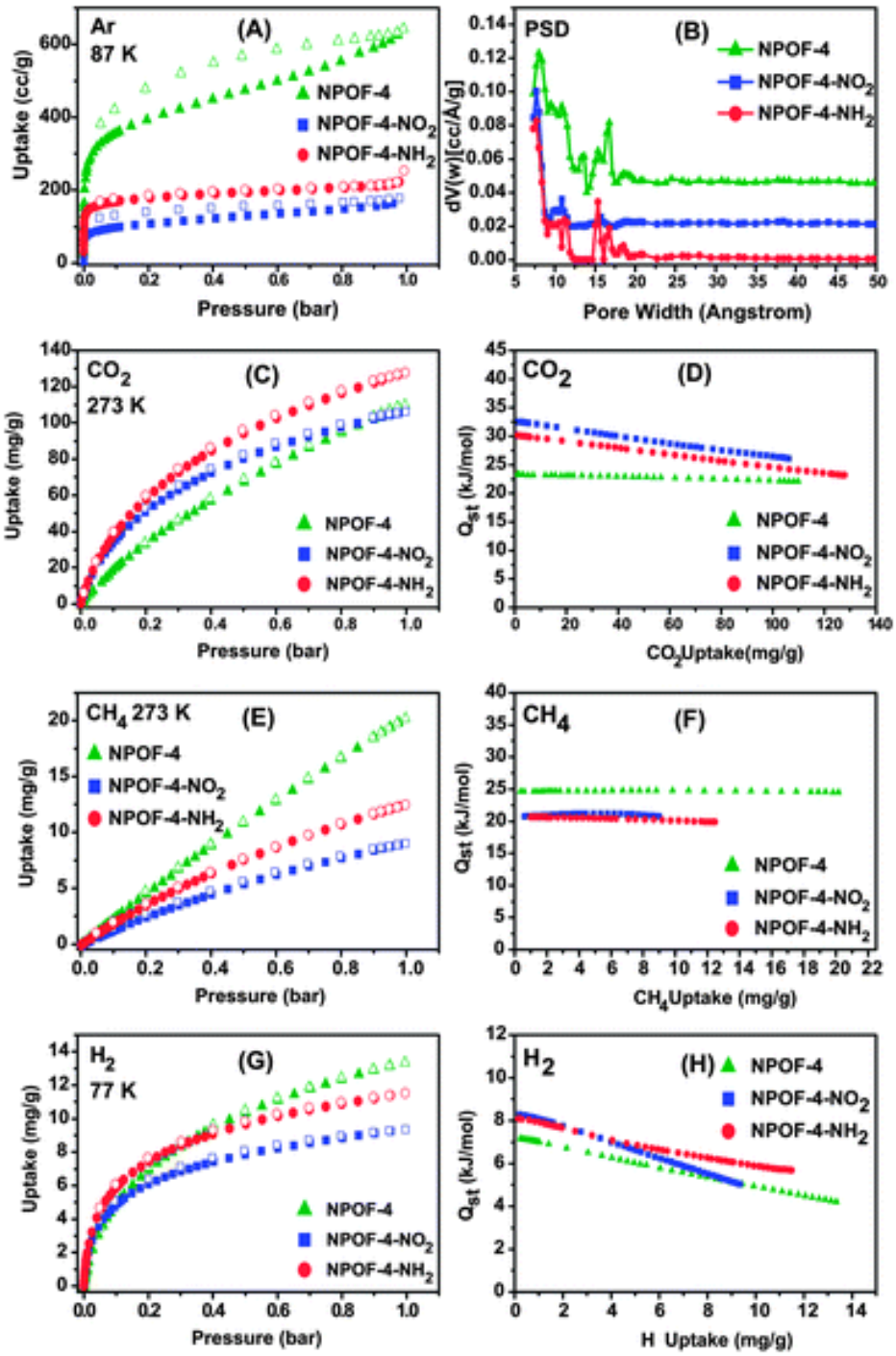

Figure 2.8 Gas uptake isotherms Ar (A), PSD from NLDFT (B), CO_2 (C), Q_{st} for CO_2 (D), CH_4 (E), Q_{st} for CH_4 (F) and H_2 (G), Q_{st} for H_2 (H).Adsorption (filled) and desorption (empty). PSD is offset by 0.02 for NPOF-4-NO_2 and 0.04 for NPOF-4 for clarity.

المنارة للاستشارات
www.manaraa.com

chemical nature of the latter can be advantageous for small gas storage and separation applications as described below.[23]

Low-pressure gas sorption measurements for CO_2, H_2, CH_4, and N_2 were collected (**Figure 2.8**) in order to investigate the impact of pore functionalization on gas storage and the preferential binding of CO_2 over CH_4 and N_2. The impact of pore functionalization on CO_2 uptake at 273 K and 298 K is depicted in **Figure 2.9** which indicate that NPOF-4-NH_2 has the highest uptake (2.90 mmol g^{-1}) at 1 bar and 273 K. This uptake is about 20% higher than the uptakes of NPOF-4-NO_2 (2.41 mmol g^{-1}) and 16% higher than that of NPOF-4 (2.50 mmol g^{-1}) despite of the much higher surface area of the latter. Moreover, the resulting isotherms were used to estimate the enthalpies of adsorption (Q_{st}) by employing the virial method as summarized in **Table 2.1** Pore modification increases the CO_2 binding affinity from 23.2 kJ mol^{-1} (NPOF-4) to 32.2 kJ mol^{-1} (NPOF-4-NO_2) and 30.1 kJ mol^{-1} (NPOF-4-NH_2). These observations originate from the polarizable nature of the CO_2 molecule and its large quadrupole moment which enhance CO_2 interactions with the –NO_2 and –NH_2 functional sites of the modified frameworks. In addition to these favourable interactions, the narrower pores generated upon modification can also increase the adsorption potential of CO_2 by multiple wall interactions. The Q_{st} drops with increased CO_2 loading for functionalized NPOFs and this clearly indicates the significant interactions between the CO_2 molecules and the functionalized pore surface. In contrast to this observation, the chemically homogeneous and non-functionalized pore surface of NPOF-4 leads to a uniform Q_{st} upon increased CO_2 loading. The Q_{st} values for functionalized NPOFs exceeds most of organic polymers including benzimidazole-linked polymers (BILPs),[30, 40] functionalized conjugated

المنارة للاستشارات
www.manaraa.com

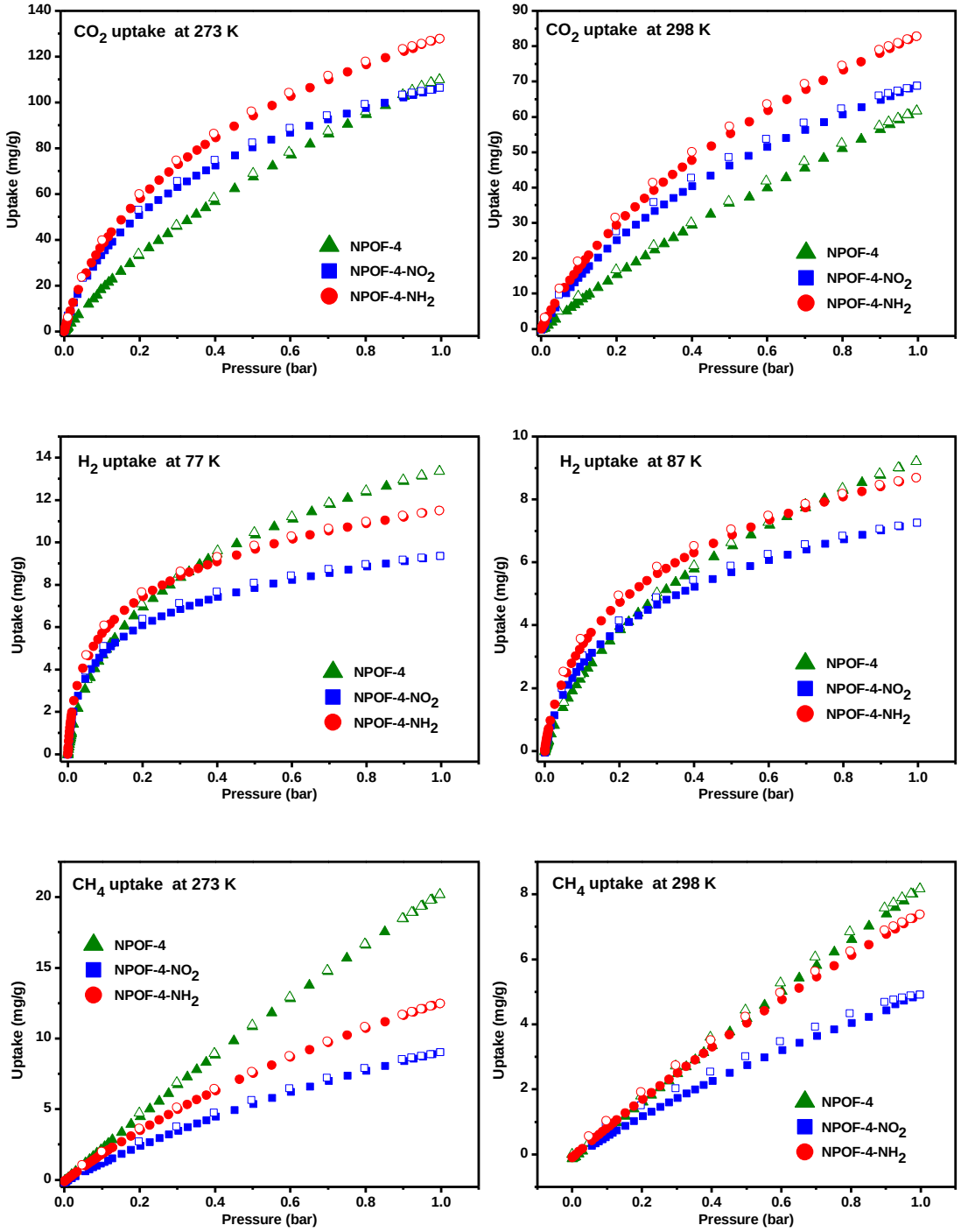

Figure 2.9 Gas uptake isotherms for NPOF-4 (green triangles), NPOF-4-NO_2 (blue squares) and NPOF-4-NH_2 (red circles) at 273 and 298 K.

المنارة للاستشارات
www.manaraa.com

microporous polymers (CMPs)[68] but are much lower than alkyl amine-tethered porous polymer networks (PPNs),[50] PAFs,[53] and alkylamine appended MOF[64] which feature short-chain aliphatic amines having CO_2 binding affinities similar to those of amine solutions being employed in CO_2 scrubbing technologies (50–100 kJ mol^{-1}).[50] It should be noted that PSM of highly porous aromatic frameworks such as PAF-1 with methylamine(PAF-1–CH_2NH_2) enhanced CO_2 uptake from 2.47 mmol g^{-1} (PAF-1) to 4.40 mmol g^{-1} (PAF-1–CH_2NH_2) at 273 K/1 bar; however, the amine functionality also gave rise to a much higher binding affinity (15.6 *vs.* 57.6 kJ mol^{-1})[53] that is similar to the values reported for polyamine-tethered PPN-6.[50] The higher CO_2 binding affinities are due to the reactive nature of the alkylamine employed for the functionalization of PAF-1 and PPN-6 as evidenced by the large initial Q_{st} values at very low CO_2 pressure. The reactivity of alkylamines toward CO_2 is prompted by the high charge density on the nitrogen sites. On the contrary, the nitrogen sites of arylamines are less reactive; nevertheless, they still have high affinity for CO_2. Tailoring the binding affinity for selective CO_2 capture and separation is essential because high heats of adsorption can lead to a major drawback wherein regeneration processes of adsorbents are associated with considerable energy penalties. While pore functionalization with –NO_2 and –NH_2 has drastic impact on the binding affinity of CO_2, its impact on the final CO_2 uptake at 1.0 bar was less significant (**Figure 2.9**). It seems that the microporous nature of NPOF-4 and its high surface area allow for significant CO_2 uptake at ambient pressure and 273 K.

For gas separation purposes, designing adsorbents that have high CO_2 uptake at low pressure (0.15 bar) is very desirable for low-pressure post-combustion CO_2 capture applications as flue gas usually consists of ~15% CO_2, ~75% N_2 and ~10% other gases.

المنارة للاستشارات
www.manaraa.com

Table 2.1 Gas uptakes, binding affinities and selectivities of NPOFs.

Network	SA_{BET}[a]	CO_2 at 1[b] bar			CH_4 at 1[b] bar			Selectivity[c] (*initial slope*)		Selectivity[d] (eqn (1))		Selectivity[e] (IAST)	
		273 K	298 K	Q_{st}	273 K	298 K	Q_{st}	CO_2/N_2	CO_2/CH_4	CO_2/N_2	CO_2/CH_4	CO_2/N_2	CO_2/CH_4
NPOF-4	1249	109.9	61.6	23.2	20.2	8.2	24.6	27(16)	3(3)	49 (14)	3(3)	12	3(3)
NPOF-4-NO_2	337	106.3	68.8	32.5	9.0	5.4	20.8	139(66)	15(10)	133 (62)	16(11)	59	12(11)
NPOF-4-NH_2	554	127.8	82.8	30.1	12.5	7.4	20.7	101(40)	11(8)	81 (29)	13(9)	38	9(9)

[a] Surface area ($m^2\ g^{-1}$) was calculated from Ar isotherm at 87 K. [b] Gas uptake in mg g^{-1} and the isosteric enthalpies of adsorption (Q_{st}) in kJ mol^{-1}. [c] Selectivity (mol mol^{-1}) was calculated from initial slope calculations at 273 K and (298 K). [d] Selectivity was calculated from the formula of $(q_1/q_2)/(p_1/p_2)$ at 273 K and (298 K). [e] Selectivity was calculated from IAST for 15/85 gas mixtures for CO_2/N_2 and 5/95 (50/50) gas mixtures for CO_2/CH_4 at 298 K.

In addition to the impact of pore miniaturization of functionalized NPOF-4 on CO_2 separation from N_2 and CH_4, integrating chemical heterogeneity into the pore walls to polarize the CO_2 molecule can have a significant effect on CO_2 uptake at low pressures. At 0.2 bar and 273 K, NPOF-4-NO_2 adsorbs 1.15 mmol g^{-1} (5.08 wt%) of CO_2 whereas NPOF-4-NH_2 adsorbs 1.32 mmol g^{-1} (5.80 wt%) which respectively correspond to 54% and 76% increase in the gravimetric capacity of CO_2 relative to that of the non-functionalized NPOF-4 (0.75 mmol g^{-1}, 3.30 wt%). The relatively large dipole moments of –NO_2 and –NH_2 result in dipole–quadrupole interactions with CO_2, and remarkably increase the initial CO_2 uptake in the low pressure range.

As stated earlier, recent findings by Wilmer *et al.* have suggested that very high binding affinities for CO_2 are less desirable when porous adsorbents such as MOFs were screened for CO_2 capture from flue gas or natural gas, and that only moderate surface areas (1000 to 1500 $m^2\ g^{-1}$) would be needed.[37] Ironically, the Q_{st} of NPOF-4-NO_2 (32.2 kJ mol^{-1}) and NPOF-4-NH_2 (30.1 kJ mol^{-1}) are within the desirable range and suggest that both materials can have novel properties for use in selective CO_2 separation from natural gas or flue gas. Additionally, the fully reversible nature of the CO_2 isotherms of both samples at ambient conditions (**Figure 2.9**) also indicate that CO_2–adsorbent interactions are weak enough to allow for adsorbent regeneration without applying heat.

المنارة للاستشارات
www.manaraa.com

We have also studied the H_2 and CH_4 uptake in order to evaluate the impact of –NO_2 and –NH_2 functionalities on the binding affinity of H_2 and CH_4. Both gases are being considered as alternative fuels for automotive applications because of their abundance and clean nature. The H_2 uptake by NPOF-4 (1.33 wt%) and its functionalized frameworks were modest (NPOF-NO_2, 0.93 wt% and NPOF-NH_2, 1.15 wt%) at 77 K/1 bar although the functionalized materials have higher binding affinities towards H_2 as depicted in **Figure 2.8G**. The Q_{st} values for H_2 were calculated from adsorption data collected at 77 K and 87 K by the virial method. At zero-coverage, the Q_{st} values are 7.17, 8.30 and 8.09 kJ mol^{-1} for NPOF-4, NPOF-4-NO_2 and NPOF-NH_2, respectively. These values are higher than the values reported for organic polymers in general and similar to those having functionalized pores.[69] In a similar fashion, the CH_4 uptake at 273 K, 298 K and 1 bar were collected for all materials and the corresponding heats of adsorption were again calculated by using the virial method, and the results are presented in **Figure 2.8H**. A comparison of the methane uptake capacities for NPOF-4 and its functionalized derivatives suggests that surface area is the dominant factor in attaining high H_2 and CH_4 storage capacities at low pressure (1.0 bar), while surface functionality plays a more important role for CO_2 capture. Additionally, the methane Q_{st} values suggest that pore functionalization with polar functionalities reduces the interaction with methane as a result of the non-polar nature of the CH_4 molecule which is consistent with recent reports on methane storage by non-functionalized PAFs.[70]

المنارة للاستشارات
www.manaraa.com

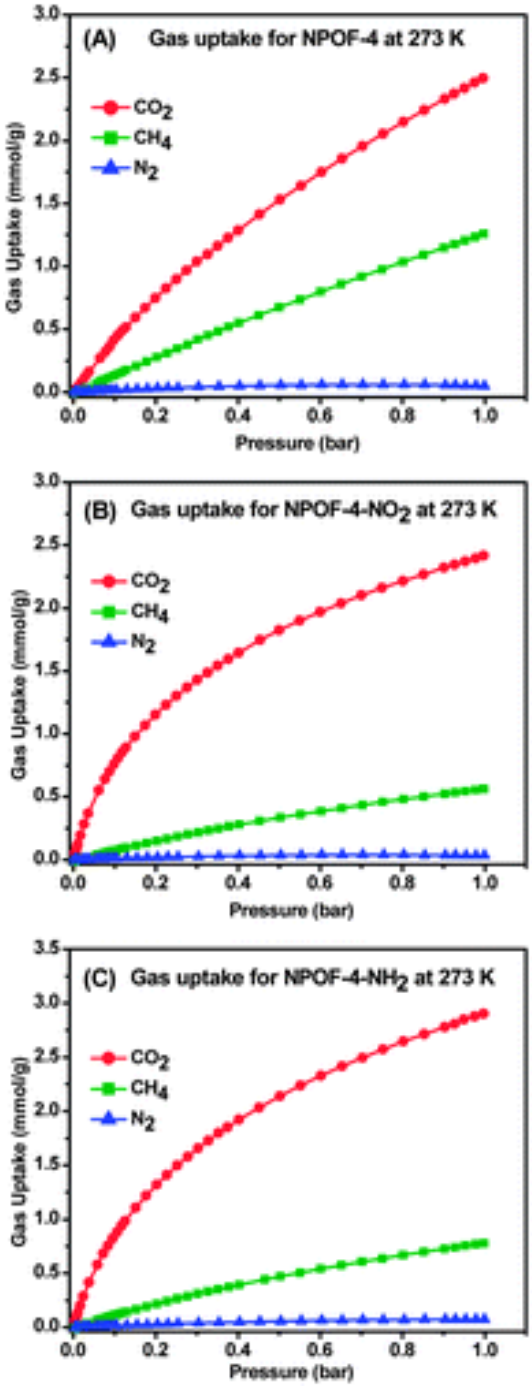

Figure 2.10 Gas sorption capacities of NPOF-4 (A), NPOF-4-NO_2 (B), and NPOF-4-NH_2 (C) at 273 K. CO_2 (red circle), CH_4 (olive square), and N_2 (blue triangle).

المنارة للاستشارات
www.manaraa.com

2.3.3 Gas Selectivity Studies

Effective CO_2 adsorbents are expected to have high selectivity for CO_2 over other gases such as N_2 (~75% in flue gas) and CH_4 (~95% in natural gas) along with high CO_2 capacity for gas separation application. Therefore, we carried out CO_2/N_2 and CO_2/CH_4 selectivity studies for NPOF-4 before and after framework functionalization to evaluate the preferential CO_2 adsorption at 273 K and 298 K. The general observation was that all materials show very low N_2 uptake but tangible CO_2 amounts at 0.15 bar (CO_2 partial pressure in flue gas) especially for the functionalized NPOFs. The same trend was also noticed for the CH_4 isotherms which show markedly lower uptakes for the modified frameworks (**Figure 2.8E**). Selectivity studies were first calculated according to Equation (1) where S is the selectivity factor, q_i represents the quantity adsorbed of component i, and p_i represents the partial pressure of component i.[8]

$$S = [q_1/q_2]/[p_1/p_2] \qquad \textbf{Equation 1}$$

The uptake values given partial pressures are tabulated in **Table 2.2**. For post-combustion CO_2 capture, the partial pressure of CO_2 and N_2 are 0.15 bar and 0.75 bar, respectively. The CO_2/N_2 selectivity studies resulted in a very high value for NPOF-4-NO_2 (133) and a lower value for NPOF-NH_2 (81) at 273 K. Furthermore, CO_2/N_2 selectivity studies were determined by using the ratios of Henry's law constants which can be calculated from the initial slopes of pure gas isotherms. The initial slope calculations for CO_2/N_2 selectivity resulted in higher values than those calculated according to **Equation (1)**; for example NPOF-4-NO_2 and NPOF-NH_2 have selectivities of 139 and 101 at 273 K, respectively. This simple and convenient method has been widely employed to

المنارة للاستشارات
www.manaraa.com

Table 2.2 CO_2 and N_2 uptakes for CO_2/N_2 selectivity studies via Equation S.

$$S = \frac{q_1/q_2}{p_1/p_2}$$

where q_i is the uptake of component i
and p_i is the partial pressure of component i

CO_2 / N_2	273 K				298 K			
	CO_2		N_2		CO_2		N_2	
Material	Pressure (bar)	Uptake (mmol)	Pressure (bar)	Uptake (mmol)	Pressure (bar)	Uptake (mmol)	Pressure (bar)	Uptake (mmol)
NPOF-4	0.15	0.593242	0.75	0.060413	0.15	0.260413	0.75	0.095581
NPOF-4-NO_2	0.15	0.967683	0.75	0.036526	0.15	0.447488	0.75	0.036100
NPOF-4-NH_2	0.15	1.088845	0.75	0.067599	0.15	0.531006	0.75	0.092921

Table 2.3 CO_2 and CH_4 uptakes for CO_2/N_4 selectivity studies via Equation S.

CO_2 / CH_4	273 K				298 K			
	CO_2		CH_4		CO_2		CH_4	
Material	Pressure (bar)	Uptake (mmol)	Pressure (bar)	Uptake (mmol)	Pressure (bar)	Uptake (mmol)	Pressure (bar)	Uptake (mmol)
NPOF-4	0.05	0.213302	0.95	1.203798	0.05	0.088479	0.95	0.484092
NPOF-4-NO_2	0.05	0.465319	0.95	0.540989	0.05	0.179618	0.95	0.310813
NPOF-4-NH_2	0.05	0.511641	0.95	0.750696	0.05	0.217542	0.95	0.440293

investigate the selective gas uptake nature of a wide range of porous adsorbents including porous organic materials as we have reported recently for BILPs.[30, 71] According to initial slope calculations presented in **Table 2.1,** the CO_2/N_2 selectivity levels for functionalized NPOFs are again much higher than the value calculated for NPOF-4 and are somewhat higher than the values obtained from **Equation (1).** Nevertheless, both methods revealed the highly selective nature of NPOF-4-NO_2 and NPOF-4-NH_2 towards CO_2 over N_2. It is noteworthy that the selectivity levels are among the highest by porous materials.[23] For comparison, NPOF-4-NO_2 out performs other selective adsorbents at 273

المنارة للاستشارات
www.manaraa.com

K including BILPs (59–128),[30, 71] PECONF-2 (109),[72] BPL carbon (17.8), ZIFs (17–50),[73, 74] Bio-MOF-11 (81)[75] and noncovalent porous materials (NPMs) (74).[76] By following the same procedure described above, we calculated CO_2 selectivity over CH_4 at 273 K and 298 K (**Table 2.1**). In a typical natural gas purification process, the mole fractions of CO_2 and CH_4 are 0.05 and 0.95, respectively, resulting in CO_2 having a partial pressure of only 0.1 bar in a mixture having 2 bar total pressure.[77] The CO_2/CH_4 selectivity values obtained from both methods; initial slope calculations and Equation (1), provided consistent data for each framework. The selectivity trend is in line with those observed for CO_2/N_2 studies and reveal that the NPOF-4-NO_2 with selectivity levels of 15 again outperforms the parent framework NPOF-4 (3) and its amine-functionalized derivative NPOF-4-NH_2 (11) at 273 K. The CO_2/CH_4 selectivity values of the functionalized frameworks fall within the range of recently reported porous materials such as diimide-based organic polymers,[78] BPL carbon,[73] ZIFs,[73] and most MOFs.[7, 79] The outcome of selectivity studies surprisingly indicates that introducing the nitro functionality into the pore walls of microporous organic frameworks have significant effect on CO_2 separation from N_2 and CH_4 **(Figure 2.9**).

In addition to the selectivity studies described above, we used the ideal adsorbed solution theory (IAST)[80] wherein selectivities of binary gas mixtures are calculated as a function of pressure like we have reported for the amorphous organic polymers BILP-10[71] and halogendecorated borazine-linked polymer BLP-10(Cl).[81] To be consistent with the data presented earlier, we have selected gas mixture compositions relevant to flue gas (CO_2/N_2: 15/85) and natural gas (CO_2/CH_4: 5/95) at 298 K as depicted in **Figure 2.11** and summarized the results in **Table 2.1**

المنارة للاستشارات
www.manaraa.com

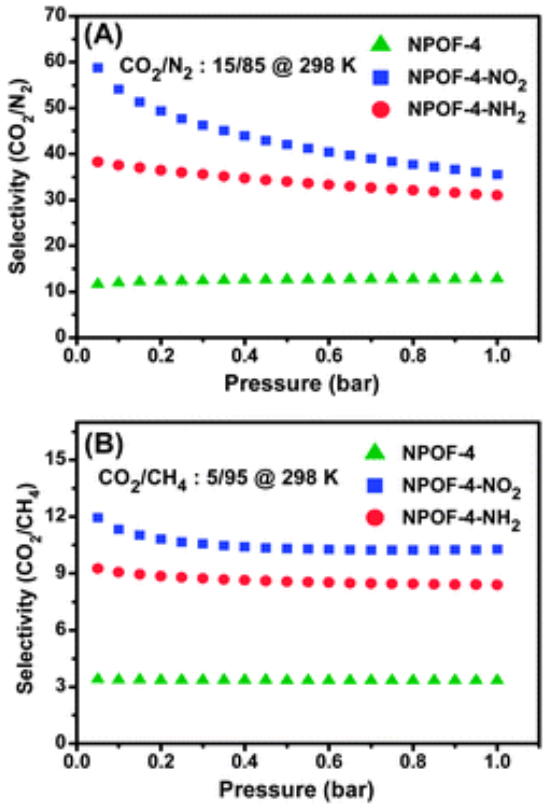

Figure 2.11 IAST selectivities of CO_2 over N_2 (A) and CO_2 over CH_4 (B) for binary gas mixtures of 15/85 and 5/95 molar compositions, respectively, in NPOFs at 298 K.

The results from IAST calculations agree with those obtained from **Equation (1)** and the initial slope calculation methods. The highest CO_2/N_2 selectivity was observed for NPOF-4-NO_2, which starts at 59 at low coverage and then drops gradually to ~40 as the pressure increases to 1.0 bar while the selectivity of NPOF-4-NH_2 is lower (38) and its change as a function of pressure is less steep. In contrast, the non-functionalized NPOF-4 has a much lower selectivity (12) that is independent of pressure. These clear differences in selectivity levels and trends can be ascribed to the favorable interactions between CO_2 and the chemically modified pore surface of NPOF-4-NO_2 and NPOF-4-NH_2, which become less accessible as the CO_2 pressure increases. The

المنارة للاستشارات
www.manaraa.com

CO_2/CH_4 selectivity for a binary gas mixture of 5/95 at low coverage is very similar for functionalized NPOFs (12–9) which is higher than that of NPOF-4 (3). Similarly, the same selectivity levels were also observed for CO_2/CH_4: 50/50 (bio-gas composition). The CO_2/CH_4 selectivity of all NPOFs as a function of pressure (0 to 1 bar) or composition does not change considerably when compared to the CO_2/N_2 selectivity because CH_4 has much higher adsorption potential than N_2 due to its more polarizable nature CH_4 (26×10^{-25} cm^3) *vs.* N_2 (17.6×10^{-25} cm^3).[82] It is worth noting that our reported selectivity data was obtained from pure gas isotherms and such studies do not take into consideration the competing nature of gas molecules or moisture for binding sites that can render functionalized NPOFs less selective for CO_2.[83] The enhanced selectivity upon pore functionalization originates from a combination of pore size reduction and the polar nature of the functional groups ($–NH_2$ and $–NO_2$), the latter is the most significant factor, however, recent studies have documented that variability in pore size and shape can alter CO_2 uptake and hence selectivity.[84, 85]

2.4 Conclusions

We have synthesized a new NPOF and successfully used post-synthesis modification processes to functionalize the framework with $–NO_2$ and $–NH_2$ functionalities and investigated their effect on CO_2 uptake and the potential use of functionalized NPOFs in small gas separation and storage applications. The metal-free synthesis of NPOF-4 and its convenient pore surface modification resulted in a significant enhancement in CO_2 binding affinity and selective binding over nitrogen and methane: CO_2/N_2 (139) and CO_2/CH_4 (15) at 273 K. We have confirmed that the high surface area does not

المنارة للاستشارات
www.manaraa.com

necessarily lead to high CO_2 uptake and selectivity. These results feature the potential of functionalized NPOFs in post-combustion CO_2 separation and its removal from natural gas. The functionalized NPOFs are also capable of storing up to 1.15 wt% H_2 at 77 K and 1.0 bar with a high isosteric heat of adsorption (8.1 and 8.3 kJ mol^{-1}).

المنارة للاستشارات
www.manaraa.com

Chapter 3

Systematic Postsynthetic Modification of Nanoporous Organic Frameworks for Enhanced CO_2 Capture from Flue Gas and Landfill Gas[2]

3.1 Introduction

Porous organic polymers (POPs), constructed from the assembly of organic building units, have gained significant attention as promising candidates for gas storage, separation, catalysis and sensing due to their tunable functionality.[29, 86] The use of POPs for selective CO_2 capture from flue gas and landfill gas is very promising due to the stable covalent nature which keeps POPs intact under acidic and basic conditions in addition to the tolerance of these materials towards water.[50, 87] Exceptionally high surface area POPs like PAFs (porous aromatic frameworks) and PPNs (porous polymer networks) can be synthesized by performing homocoupling reactions of aryl building blocks and the surface area of these materials can be further enhanced by controlling the reaction conditions.[28, 88] However, POPs composed of only carbon and hydrogen atoms do not perform well under gas separation settings at low pressure (1 bar) due to their lack of CO_2-philic sites

---

[2]Islamoglu, T; Kim, T.; Kahveci, Z.; El-Kadri, O.M.; El-Kaderi, H.M., *J. Phys. Chem. C 2016, 120, 2592−2599.* Reproduced by permission of The American Chemical Society.

المنارة للاستشارات
www.manaraa.com

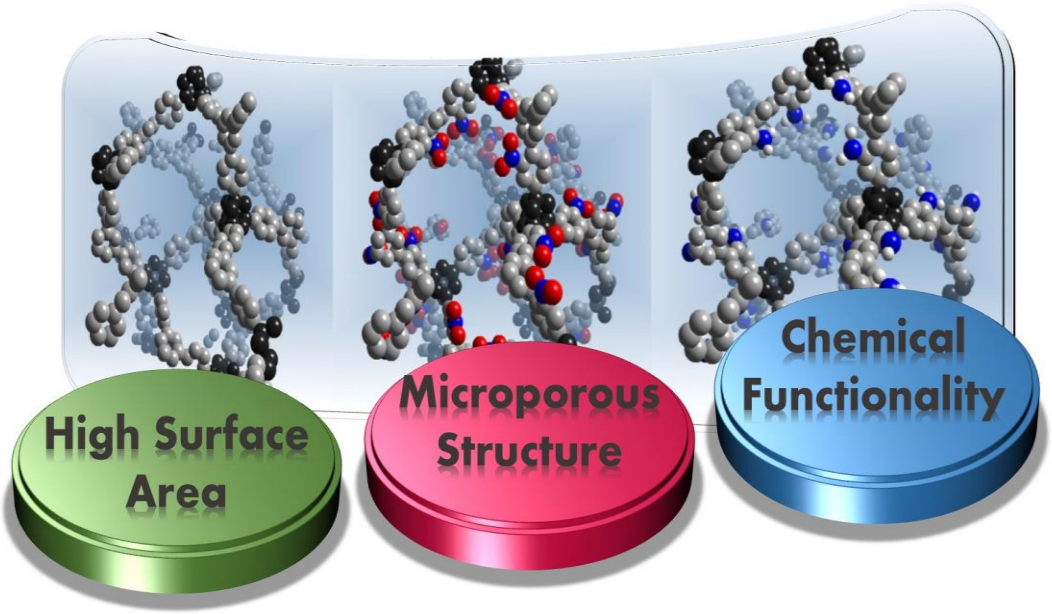

Figure 3.1 Schematic representation of post functionalized POPs.

which leads to low isosteric heats of adsorption for CO_2.[21] It is well documented that high surface area materials do not necessarily lead to high CO_2 uptake since gas uptake capacity depends on the favorable interactions between pore walls and guest gas molecules.[23] The physical and chemical stability of POPs allows for chemical modification, a process that can be used to impart desirable properties such as pore hydrophilicity which is central for gas separation and storage applications.[53]

Among the new directions that have been explored to enhance sorbent-CO_2 interactions is pore functionalization using polar groups such as hydroxy, nitro, amine, sulfonate, azo, imidazole, triazine, imine, etc. **(Figure 3.1)**[21, 38, 47, 63, 89-94] Incorporation of these functionalities in the framework can be achieved by pre-synthesis modification of building blocks wherein CO_2-philic moieties are attached to building blocks before framework formation, self-functionalization where functional groups are formed as

المنارة للاستشارات
www.manaraa.com

polymer networks grows i.e. imidazole, azo, triazine or through post-synthesis modification (PSM) processes in which functional groups are tethered to the pore walls after the framework assembly. Although pre-synthesis modification generally permits more controlled loading of functional groups, there are major drawbacks associated with the method. First, functionalization of building blocks often necessitates alternate reaction conditions (i.e. protection of functional groups), and these reactions are often time consuming and non-trivial. Second, some reaction conditions require harsh conditions such as high temperature and acidic or basic media where the functional groups on the building blocks may not survive or which may lead to side reactions due to competition with other functional groups in the reaction media.[95] Therefore, introducing targeted functionalities within the pores after framework formation (i.e. PSM) has been noted as an advantageous approach.[49]

Recently, post-nitration and subsequent reduction of porous networks has been demonstrated as a simple methodology for obtaining nitro and amine functionalized porous materials, respectively.[21] However, this method leads to much lower surface areas due to uncontrolled loading of functional groups which block the ultramicropores making them inaccessible to gas molecules. Partial framework collapse is also possible if the framework cannot tolerate prolonged exposure to harsh reaction conditions.[96] We recently used PSM to functionalize NPOF-4 with $–NO_2$ and $–NH_2$ and investigated the effect on CO_2 uptake and separation.[21] Significant enhancement in CO_2 binding affinity and selective binding over nitrogen and methane was observed. However, because of uncontrolled nitration the specific surface area of the $–NO_2$ and $–NH_2$ functionalized frameworks dropped dramatically and led to only modest CO_2 uptake at low pressure.

المنارة للاستشارات
www.manaraa.com

Thus, pore functionalization with CO_2-philic sites without compromising porosity remains a challenge for developing efficient CO_2 adsorbents. Uncontrolled functional group loading often leads to functionalization of the ultramicropores which then become inaccessible to gas molecules. Therefore new strategies for systematic functionalization of NPOFs are needed to retain the surface areas of these materials.

In this study we designed a set of experiments to combine both high surface area and chemical functionality in NPOFs and to demonstrate the remarkable performance of functionalized NPOFs in CO_2 separation from flue gas and landfill gas. PSM of NPOF-1 under controlled conditions afforded NPOF-1–NO_2 and NPOF-1–NH_2, which retain high surface area and accessible micropores. We also show that prolonged functionalization reaction time and the use of excess amounts of nitric acid have detrimental impact on the textural properties of the functionalized frameworks which diminish their use as CO_2 adsorbents. For simplicity, the nitrated NPOF-1, made by using 2 eq. of HNO_3 and the reduced amine functionalized derivative will be denoted as NPOF-1-NO_2 and NPOF-1-NH_2, respectively. While NPOFs nitrated using excess amounts of HNO_3 (125 eq./phenyl) and the reduced derivatives will be denoted as NPOF-1-NO_2(xs) and NPOF-1-NH_2(xs), respectively.

3.2 Experimental Section

3.2.1 General Techniques, Materials and Methods

All starting materials and solvents, unless otherwise noted, were obtained from Acros Organics and used without further purification. 1,3,5-tris(4-bromophenyl)benzene (TPBBr) was synthesized according to literature.[97] Solvents were dried by distillation. Air-

المنارة للاستشارات
www.manaraa.com

sensitive samples and reactions were handled under an inert atmosphere of nitrogen using either glovebox or Schlenk line techniques. Elemental microanalyses were performed at the Midwest Microlab, LLC. Liquid ^{1}H and ^{13}C NMR spectra were obtained on a Varian Mercury-300 MHz NMR spectrometer (75 MHz carbon frequency). Solid-state ^{13}C cross-polarization magic angle spinning (CP-MAS) NMR spectra for solid samples were taken at Spectral Data Services, Inc. Spectra were obtained using a Tecmag-based NMR spectrometer operating at a H-1 frequency of 363 MHz, using a contact time of 1 ms and a delay of three seconds for CP-MAS experiments. All samples were spun at 7.0 kHz. Thermogravimetric analysis (TGA) was carried out using a TA Instruments Q-5000IR series thermal gravimetric analyser with samples held in 50 µL platinum pans under an atmosphere of air (heating rate 5 °C /min). For scanning electron microscopy imaging (SEM), samples were prepared by dispersing the material onto a sticky carbon surface attached to a flat aluminium sample holder. The samples were then coated with platinum at a pressure of 1 x 10-5 mbar under a nitrogen atmosphere for 70 seconds before imaging. Images were taken on a Hitachi SU-70 Scanning Electron Microscope. Powder X-ray diffraction data were collected on a Panalytical X'pert pro multipurpose diffractometer. Samples were mounted on a sample holder and measured using Cu Kα radiation with a 2θ range of 1.5-35. FT-IR spectra were obtained on a Nicolet-Nexus 670 spectrometer furnished with an attenuated total reflectance accessory. Porosity and gas sorption experiments were collected using a Quantachrome Autosorb iQ volumetric analyser using adsorbates of UHP grade. In a typical experiment, a sample of polymer (~50 mg) was loaded into a 9 mm large bulb cell (Quantachrome) of known weight which is then hooked up to the gas analyser and degassed at 130 °C / 1.0 x 10^{-5} bar for 12

المنارة للاستشارات
www.manaraa.com

hours. The degassed sample was refilled with helium, weighed precisely then transferred back to the analyser. The temperatures for adsorption measurements were controlled by using a refrigerated bath of liquid nitrogen (77 K), and a temperature controlled water bath (273 K and 298 K).

Synthesis of NPOF-1: NPOF-1 was synthesized following a modified method from previous reports.[97] A 200 mL reaction flask equipped with a stir bar was charged with TPBBr (400 mg, 0.736 mmol) then filled with N_2 after evacuation under vacuum. Under inert conditions (glove box), $Ni(COD)_2$ (1.03 g, 3.75 mmol), COD (0.4 mL, 3.75 mmol), 2,2-bipyridyl (585 mg, 3.75 mmol), 60 mL anhydrous DMF, and 40 mL of freshly distilled THF were added. The resultant suspension was heated at 80 °C for 24 h. The mixture was cooled to room temperature and 40 mL of 6 M HCl was added and stirred for 3 h. The resultant white powder was filtered and washed with 2 M HCl, hot water, THF, ethanol and acetone, and dried under reduced pressure to afford NPOF-1 as a white powder (255 mg, 87% yield) Anal. Calcd. for $C_{24}H_{15}$: C, 95.02; H, 4.98. Found: C, 88.36; H, 4.93.

Synthesis of NPOF-1-NO_2: A 50 mL round bottom flask was charged with 10 mL of concentrated H_2SO_4 then cooled to 0 °C. To this solution, 100 mg NPOF-1 was added in small portions followed by dropwise addition of 93 µL fuming HNO_3 and stirred for 90 min at 0 °C. The mixture was poured into 75 mL of ice and stirred for 30 minutes at room temperature. The resulting powder was isolated by filtration through a medium glass frit and washed with copious amounts of water and ethanol, and dried under reduced pressure to afford NPOF-1-NO_2 (108 mg) as a brownish powder. Anal. Calcd. for $C_{24}H_{12}N_3O_6$: C, 65.76%; H, 2.76%; N, 9.59%. Found: C, 71.86 %; H, 3.70%; N, 4.70%.

المنارة للاستشارات
www.manaraa.com

Synthesis of NPOF-1-NH_2: A 50 mL round bottom flask equipped with a stir bar was charged with 80 mg NPOF-1-NO_2, 10 mL methanol, and 10 mL distilled water under nitrogen. The resultant suspension was degassed with N_2 for 20 min before adding sodium dithionite (1.2 g, 6.9 mmol) then was heated to 75 ºC for 18 hours. The resultant material was filtered and suspended in warm water (25 mL) for 30 min. The suspension was filtered and washed with warm water twice. The resultant polymer was suspended in 25 mL 4 M HCl in order to ensure complete reduction to amine then was washed with water followed by 2 M NaOH in order to neutralize the amine. The isolated product was suspended in warm water (30 mL) for 60 minutes. After filtration the polymer was suspended in warm ethanol and THF twice for 30 min cycles. The polymer lastly was filtered and washed with methanol and dried overnight under vacuum at 120 ºC to yield dark brownish NPOF-1-NH_2 (68 mg). Anal. Calcd. for $C_{24}H_{18}N_3$: C, 82.73%; H, 5.21%; N, 12.06%. Found: C, 75.47%; H, 4.22%; N, 5.01%.

Synthesis of NPOF-1-NO_2(xs): A published procedure was followed. A 50 mL round bottom flask was charged with 10 mL of concentrated H_2SO_4 then cooled to 0 °C. To this solution, 75 mg NPOF-1 was added in small portions followed by drop wise addition of cold HNO_3 (6 mL, 70%) and stirred for 6 h at 0 °C. The mixture was poured into 100 mL of ice and stirred for 30 minutes at room temperature. The resulting powder was isolated by filtration through a glass frit and washed with copious amount with water and ethanol, and dried under reduced pressure to afford NPOF-1-NO_2(xs) (89 mg) as a brownish powder. Anal. Calcd. for $C_{24}H_{12}N_3O_6$: C, 65.76%; H, 2.76%; N, 9.59%. Found: C, 60.44 %; H, 2.81%; N, 6.49%.

المنارة للاستشارات
www.manaraa.com

Synthesis of NPOF-1-NH_2(xs): A published procedure was followed. A 100 mL reaction flask was charged with 70 mg NPOF-1-NO_2(xs),, 30 mL EtOH, and 300 mg of $SnCl_2$. The mixture was refuxed at 80 °C for 18 h. The resulting green suspension was filtered, then suspended in 20 mL of concentrated HCl and stirred for 5 h at room temperature. The HCl was replenished twice and stirring continued for another 2 h at room temperature. The mixture was then filtered and washed with copious amounts of water and with 0.25 M NaOH in order to neutralize it. After washing with water again polymer was finally washed with EtOH and dried to yield dark brownish NPOF-1-NH_2(xs) (55 mg). Anal. Calcd. for $C_{24}H_{18}N_3$: C, 82.73%; H, 5.21%; N, 12.06%. Found: C, 64.71%; H, 4.76%; N, 9.58%.

Scheme 3.1 Schematic representation of NPOF-1 synthesis and its post-synthesis modification.

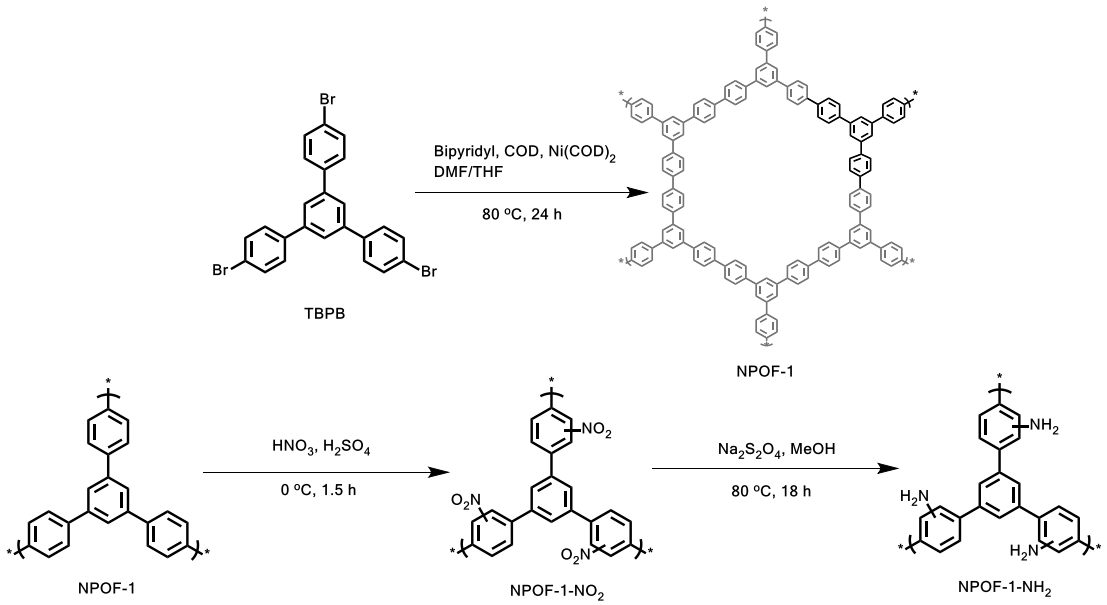

المنارة للاستشارات
www.manaraa.com

3.3 Results and Discussion

3.3.1 Synthesis and Characterization

The synthesis of NPOF-1 was carried out according to literature methods as presented in **Scheme 3.1.** We have noticed that room temperature polymerization procedure resulted in low surface area materials and therefore heating the reaction

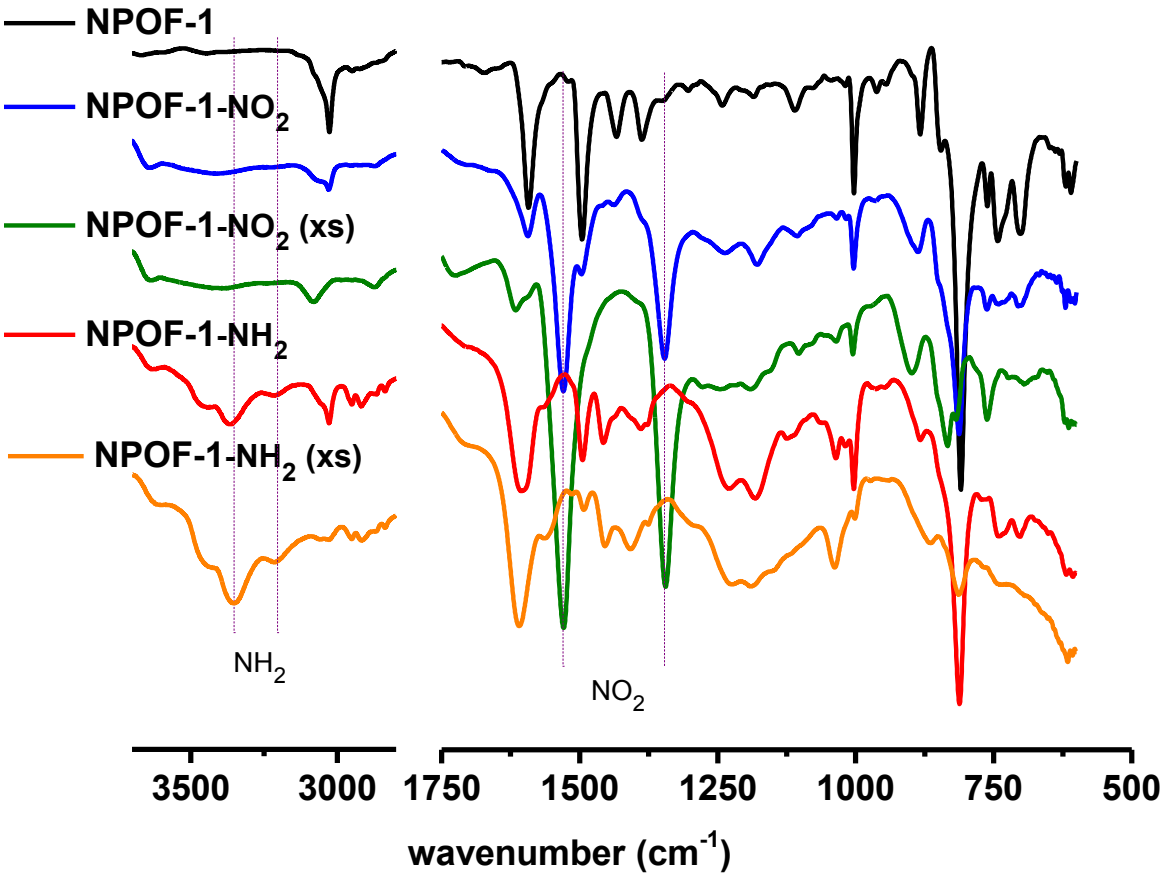

Figure 3.2 FT-IR spectra of NPOF-1 and its derivatives.

المنارة للاستشارات
www.manaraa.com

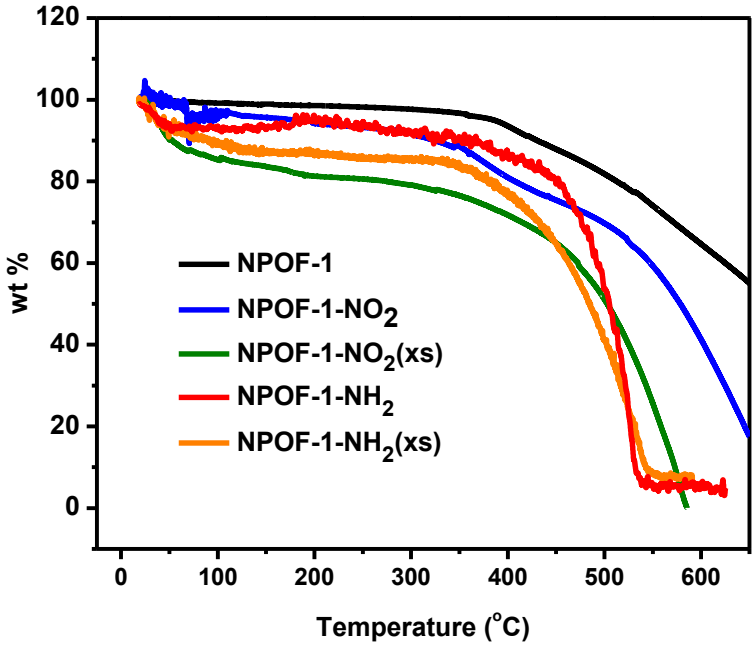

Figure 3.3. TGA traces of polymers.

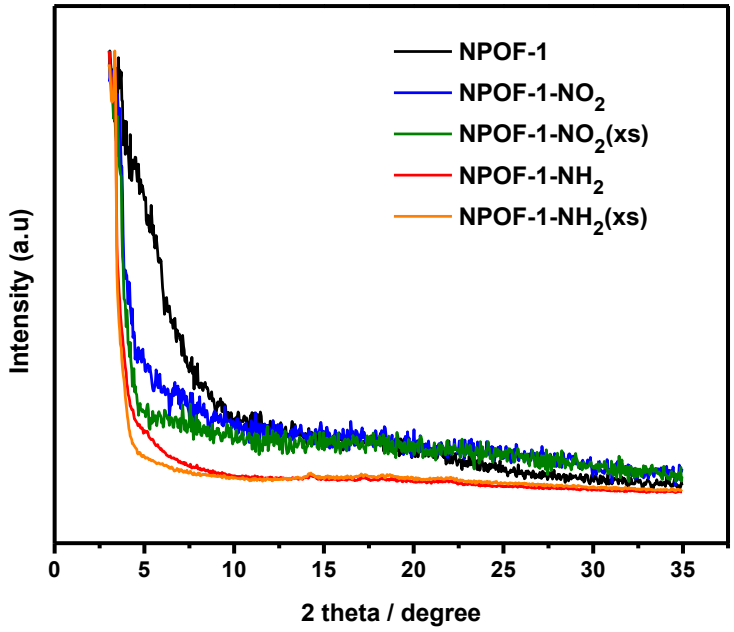

Figure 3.4. PXRD pattern of polymers.

المنارة للاستشارات
www.manaraa.com

NPOF-1

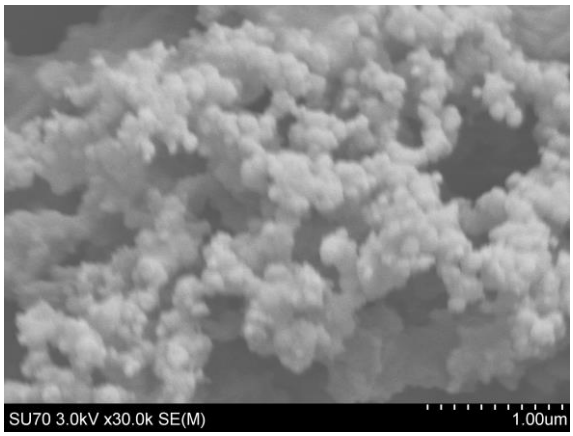

NPOF-1-NO_2

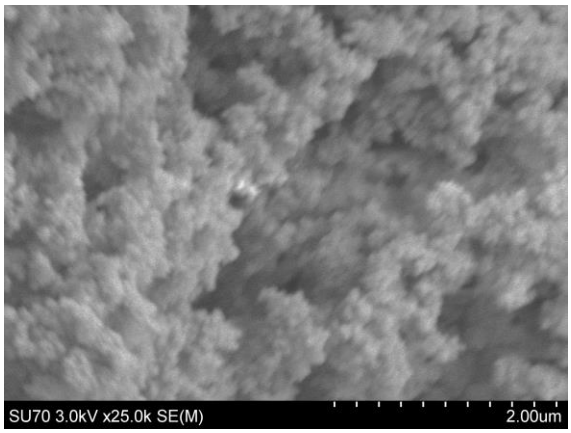

NPOF-1-NO_2(xs)

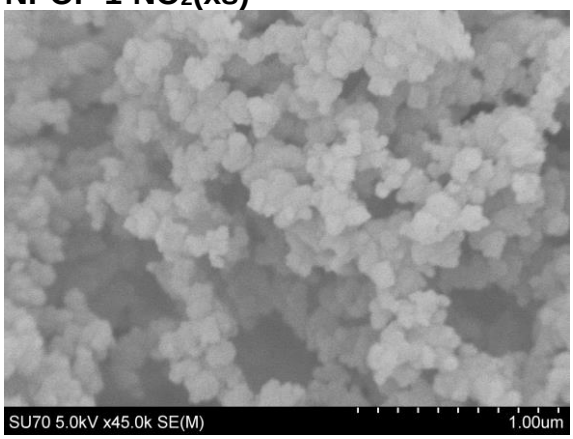

NPOF-1-NH_2

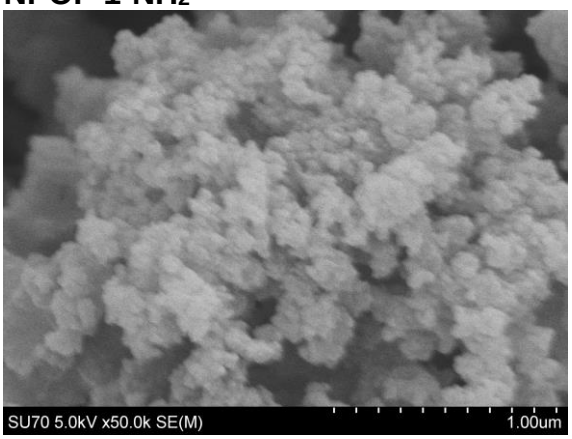

NPOF-1-NH_2(xs)

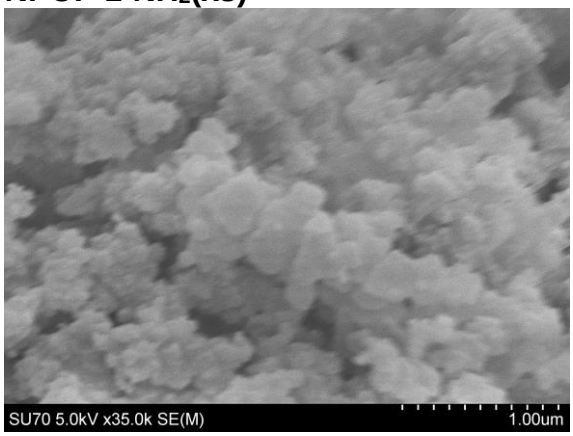

Figure 3.5. SEM images of polymers.

المنارة للاستشارات
www.manaraa.com

mixture to 80 °C was needed to optimize the porosity of NPOF-1.[35] Additionally, using a mixture of DMF/THF solvent system and heating all reactants and reagents together to 80 °C starting from room temperature resulted in a slight increase in the reported surface area (1950 vs 2060 m^2 g^{-1}).[97] The nitration of NPOF-1 was performed at 0 ºC in the presence of 2 equivalents of HNO_3 per phenyl ring for 90 min resulting in NPOF-1-NO_2. NPOF-1 was also nitrated with excess HNO_3 for 6 h at 0 ºC (previously published method) and named as NPOF-1-NO_2(xs).[21] However, the long nitration period and use of excess HNO_3 resultes in much lower surface area for NPOF-1-NO_2(xs) (749 m^2 g^{-1}) compared to NPOF-1-NO_2 (1295 m^2 g^{-1}). The sorption data was collected for both nitro-functionalized materials in order to reveal the effect of over-functionalization. Functionalized NPOFs were then reduced to afford corresponding amine-functionalized frameworks, namely NPOF-1-NH_2 and NPOF-1-NH_2(xs). **Figure 3.2** shows the FT-IR spectra of the pristine polymer NPOF-1 and its post-synthetic functionalized derivatives. Upon nitration, new FT-IR bands appeared at 1532 and 1350 cm^{-1} which can be ascribed to the asymmetrical and symmetrical stretching of NO_2, respectively.[67] Reduction of nitro groups to amino functionalities resulted in the disappearance of these bands and the presence of new bands at 3350 and 3230 cm^{-1} that correspond to asymmetrical and symmetrical N-H stretching, respectively. According to PXRD studies, all frameworks are amorphous and lack long-range ordering (**Figure 3.4).** SEM images revealed aggregated spherical particles of variable sizes as shown in **Figure 3.5**. TGA analysis (Figure 4.4) shows that the functionalized polymers lost only ~5 wt% up to 300 °C after subtracting the initial weight lost which is due to residual solvents and/or moisture. To gain more information about the chemical composition of the polymers, we performed elemental analysis which

المنارة للاستشارات
www.manaraa.com

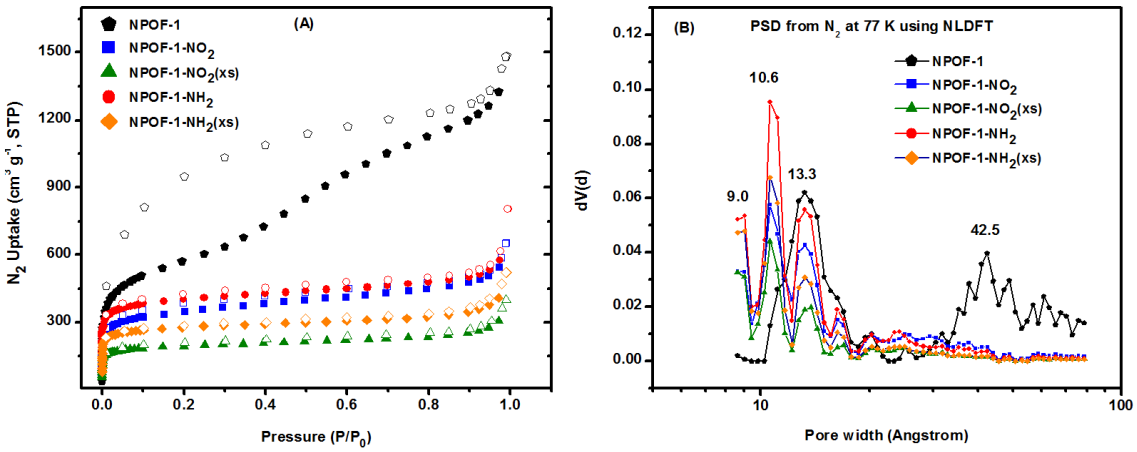

Figure 3.6. Nitrogen isotherms at 77 K (A) and pore size distribution from NLDFT using N_2 at 77 K (B).

can be used to estimate nitrogen loading. Interestingly, the use of excess HNO_3 resulted in a lower than expected nitration levels of 1,4 substituted phenyl rings (~0.59 nitro/phenyl ring) while controlled nitration yields ~0.4 nitro loading per phenyl ring which is still more efficient than previously reported method for POPs resulting in ~0.25-0.3 N/phenyl.[53] Presumably, the nitrogen content increase upon reduction (5.01%) due to replacement of oxygen with a much lighter atom, hydrogen. It is worth noting that the deviation in elemental analysis results is common with amorphous polymers, especially for post-functionalized POPs. This could be a result of one or a combination of several factors such as (1) frameworks are considered to be non-defective structure, (2) remaining/unreacted end groups, (3) inaccessible pores where functionalization does not take place, (4) trapped salts/reagents/catalysts inside the pores.[48, 98, 99]

3.3.2 Textural Properties

المنارة للاستشارات
www.manaraa.com

The specific surface area and pore size distribution of NPOF-1 and its derivatives were comparatively characterized by means of CO_2 (273 K) and N_2 (77 K) sorption-desorption measurements for ultramicro and micro/mesopores, respectively. The corresponding nitrogen adsorption isotherms and pore size distribution of NPOFs are depicted in **Figure 3.6.** All nitrogen isotherms of functionalized NPOFs show a sharp uptake at very low pressure region ($P/P_0 < 0.01$) and then form a plateau in most of the pressure range which is consistent with their expected microporous nature. In contrast, NPOF-1 displayed a gradual increase in N_2 uptake and pronounced hysteresis at $P/P_0 > 0.1$ as a result of mesopores and framework swelling. The textural properties of all frameworks are listed in Table 1. As stated earlier, NPOF-1 was synthesized according to a modified published

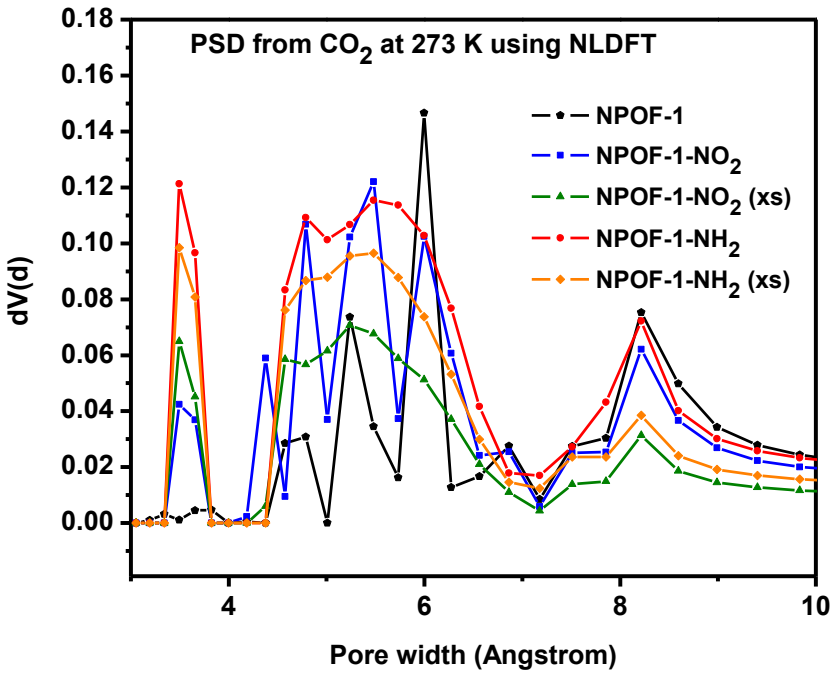

Figure 3.7. Pore size distribution of polymers from CO_2 isotherm at 273 K using NLDFT.

المنارة للاستشارات
www.manaraa.com

Table 3.1. CO_2 uptakes at 298 K, *Qst* and IAST selectivity results

			CO_2 at 298 K			IAST Selectivities	
Polymer	[a]**SA_{BET}**	[b]**$V_{Mic,DFT}$**	[c]*0.15 bar*	[c]*1 bar*	[d]Q_{st}	[e]CO_2/N_2	[e]CO_2/CH_4
NPOF-1	2062	0.28 (19)	11 (-)	67 (-)	21.7	8	3
NPOF-1-NO_2	1295	0.36 (58)	27 (2.5)	111 (1.7)	29.2	20	6
NPOF-1-NO_2(xs)	749	0.23 (70)	26 (2.4)	88 (1.3)	32.0	45	11
NPOF-1-NH_2	1535	0.48 (71)	47 (4.3)	166 (2.5)	32.1	25	10
NPOF-1-NH_2(xs)	1074	0.35 (77)	39 (3.5)	129 (1.9)	32.6	41	8

[a]BET surface areas are reported in m^2 g^{-1}. [b]Micropore volume determined by NLDFT; the values in parentheses are the percentage of micropore volume relative to total pore volume. [c]The uptakes of CO_2 at corresponding pressure in mg g^{-1} at 298 K; the values in parenthesis are the ratio of the uptake to NPOF-1 in the same column to illustrate the enhancement in uptake compared to NPOF-1. [d]Isosteric heat of adsorption of corresponding gas at zero coverage calculated from isotherms collected at 273 and 298 K using Virial equation. [d]Selectivity calculated by IAST at 298 K and 1 bar.

procedure and exhibits high surface area (SA_{BET} = 2062 m^2 g^{-1}). As expected, the surface areas of all functionalized polymers are lower compared to NPOF-1. The use of excess (125 eq./phenyl) HNO_3 and longer reaction time (6 h), NPOF-1-NO_2(xs) shows the lowest surface area (749 m^2 g^{-1}). On the other hand, when NPOF-1-NO_2 was synthesized from only 2 eq. of HNO_3 per phenyl ring and the reaction was quenched after 90 minutes, the surface area was enhanced by 73% (1295 m^2 g^{-1}). The combination of high surface area and chemical functionality is crucial for improving CO_2 uptake. Subsequent reduction of nitro functionalized NPOFs yielded NPOF-1-NH_2 and NPOF-1-NH_2(xs) with surface areas of 1535 m^2 g^{-1} and 1074 m^2 g^{-1}, respectively. Pore size distribution was estimated by

المنارة للاستشارات
www.manaraa.com

fitting the nitrogen uptake branch of the isotherms using the NLDFT (cylindrical/spherical pore geometry with zeolites/silica) model and was found to be in a broad range of micropore/mesopore region for NPOF-1. After the nitration of NPOF-1, all of the mesopores (centered around 42.5 Å) were successfully converted to micropores (9-13 Å). It was expected to observe a slight shift in the pore width maxima after reduction of NO_2 to NH_2 groups due to size difference, however this change was almost negligible. The use of CO_2 adsorption at 273 K has been often employed to calculate

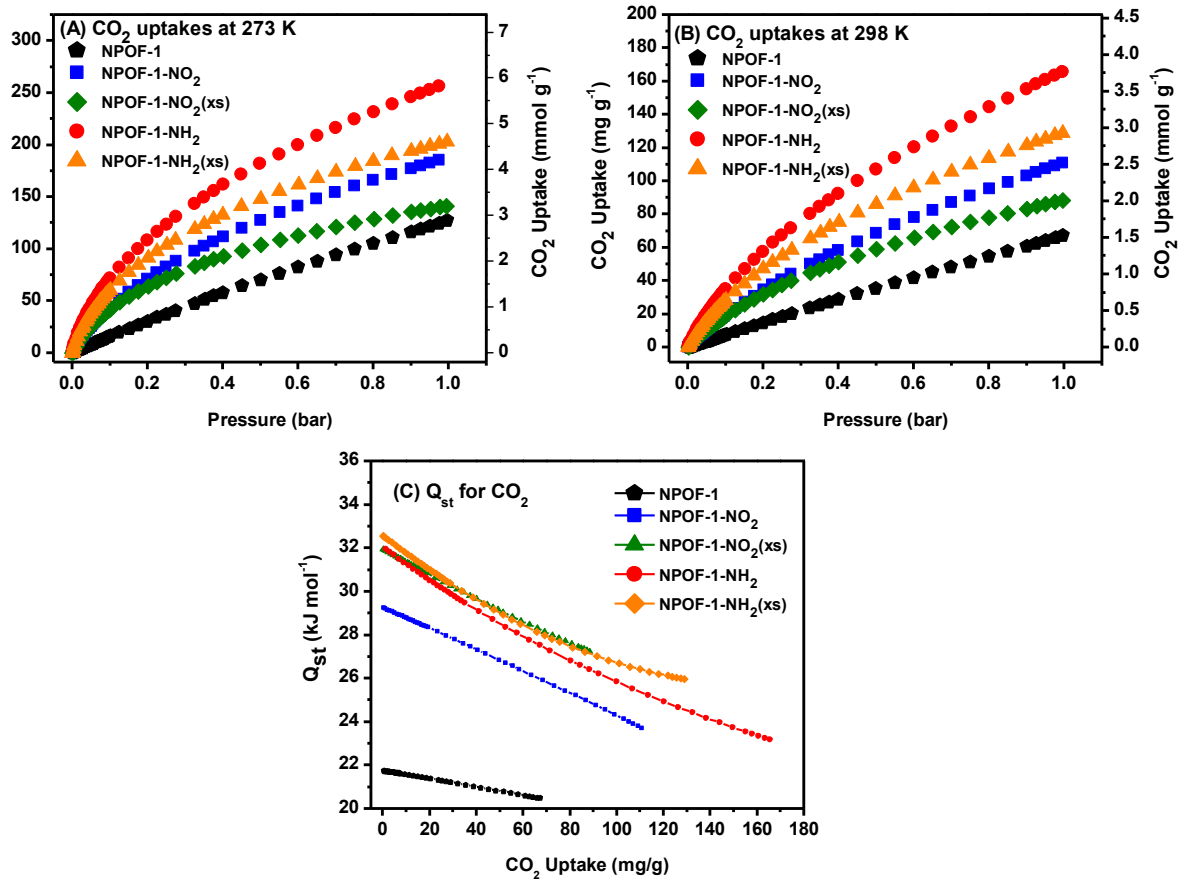

Figure 3.8. CO_2 uptakes at 273 (A) and 298 K (B), and corresponding *Qst* plot (C) of NPOFs.

المنارة للاستشارات
www.manaraa.com

ultramicoporosity (pores less than 0.7 nm) for microporous materials instead of N_2 adsorption at 77 K. This is due to the much slower diffusion of N_2 at 77 K which could prevent N_2 adsorption in ultramicropores and lead to very long data collection time.[100] Therefore, we have also employed CO_2 as a probe molecule in order to obtain more information about pore sizes and this revealed that ultramicropores (<4 Å) were created after postsynthetic-modification of NPOF-1 (**Figure 3.7**). Pore volumes of NPOF-1 and its derivatives are calculated from N_2 isotherms collected at 77 K using NLDFT under the same settings used for PSD calculation. Since the scope of the current study is to maintain/and or generate microporosity in the frameworks, we have calculated micropore percentage rather than reporting total pore volume from a single point calculation. Micropore and total pore volumes are calculated by considering the pores up to 2 nm and 10 nm, respectively. For total pore volume calculation, 10 nm thresholds were selected as PSD analysis did not show any pores beyond 10 nm. As shown in **Table 3.1**, micropore volume percentage increased dramatically up to 77% of total pore volume for NPOF-1-NH_2(xs). Moreover, a closer look at the data reveals that NPOF-1-NH_2 might be more beneficial for CO_2 capture since it possesses 0.48 cm^3 g^{-1} micropore volume which corresponds to 71% of its total pore volume and is 37% higher compared to NPOF-1-NH_2(xs). This new synthetic strategy enables controlled functional group loading while maintaining high porosity making the functionalized networks very promising for selective CO_2 capture from gas mixtures as detailed below.

3.3.3 Gas uptake and selectivity studies

To assess the potential of functionalized NPOFs in CO_2 capture from flue gas and landfill gas, adsorption isotherms on activated samples for carbon dioxide, methane and nitrogen

المنارة للاستشارات
www.manaraa.com

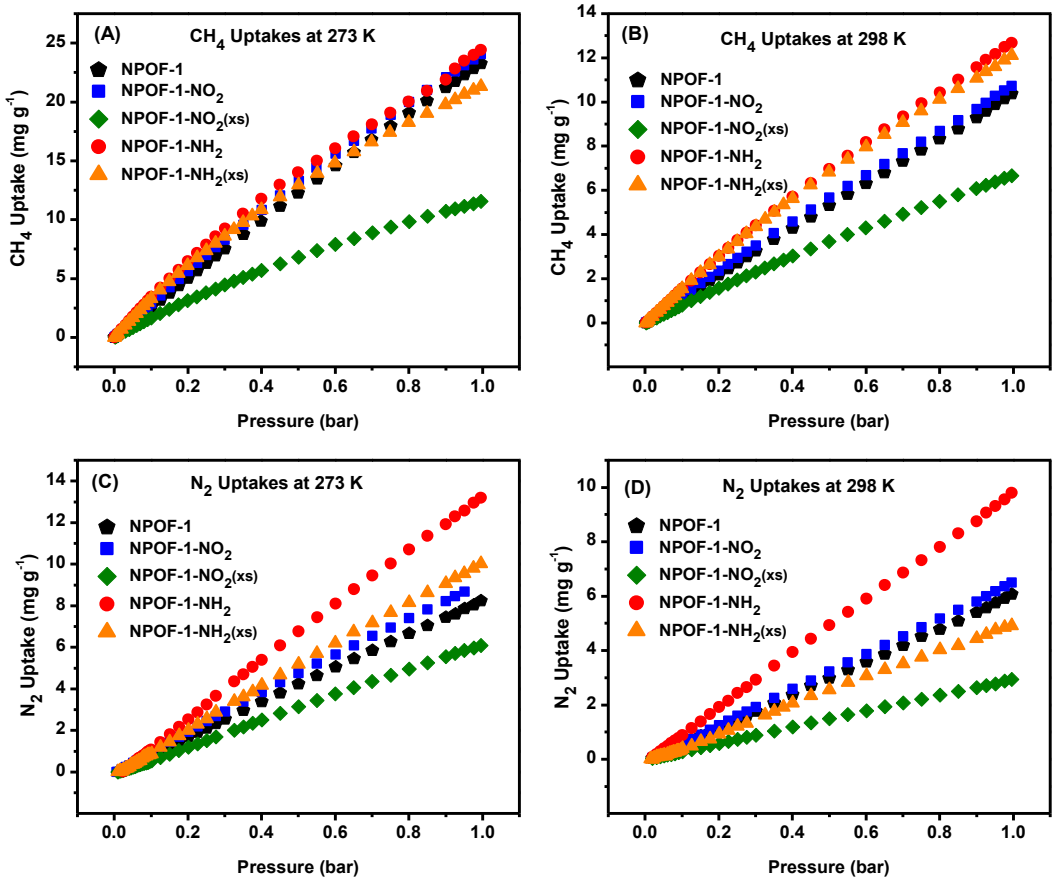

Figure 3.9. CH_4 uptakes at 273 K (A) and 298 K (B), N_2 uptakes at 273 K (C) and 298 K (D) of polymers.

were collected at 273 and 298 K (**Figure 3.8** and **Figure 3.9**). All isotherms are fully reversible illustrating the facile uptake and release of gases, which makes them energetically attractive for gas separation applications. It is well documented that microporosity is essential for CO_2 capture from gas mixtures that possess low CO_2 content. We have recently shown that high percentage of microporosity in addition to functionality can be achieved for NPOFs by PSM. Despite an increase in CO_2 uptake upon PSM, the use of excess amounts of HNO_3 and longer reaction time allowed nitration

المنارة للاستشارات
www.manaraa.com

Table 3.2. CH_4 and N_2 uptakes of polymers at 273 and 298 K.

	CH_4 Uptake (mg g^{-1})				N_2 Uptake (mg g^{-1})			
	273 K		298 K		273 K		298 K	
	0.5 bar	1 bar	0.5 bar	1 bar	0.1 bar	1 bar	0.1 bar	1 bar
NPOF-1	12.24	23.27	5.31	10.36	0.84	8.24	0.51	6.08
NPOF-1-NO2	13.27	24.04	5.67	10.73	0.97	8.68	0.59	6.51
NPOF-1-NO2(xs)	6.82	11.54	3.68	6.67	0.53	6.08	0.27	2.94
NPOF-1-NH2	14.00	24.40	6.97	12.66	1.08	13.18	0.88	9.79
NPOF-1-NH2(xs)	12.94	21.33	6.83	12.11	0.88	10.02	0.40	4.92

to take place in narrow micropores which limits their accessibility by gas molecules as evidenced by dramatic decrease in surface area values. However controlled functionalization by reducing the reaction time and limiting the acid amount allowed us to synthesize NPOF-1-NH_2 which uniquely combines high surface area, ultramicroporosity, and amine functionality. Integrating these properties into porous adsorbents is needed in order to enable high and selective CO_2 uptake at low pressures (0.15 bar) which is desirable for post-combustion carbon capture where the flue gas usually consists of ~15 % CO_2, ~75 % N_2 and ~10 % other gases.[8] Figure 3 illustrates the advantages associated with controlled post functionalization on CO_2 uptake. The observed CO_2 isotherms suggest that using stoichiometric amount of HNO_3 with shortened reaction time results in high CO_2 uptake at low pressures. For instance, NPOF-1-NH_2 takes 2.07 mmol g^{-1} (91.2 mg g^{-1}) CO_2 at 273 K and 0.15 bar whereas NPOF-1-NH_2(xs) takes 1.76 mmol g^{-1} CO_2 (77.6 mg g^{-1}) under the same conditions. Notably, both amine functionalized NPOFs take more CO_2 then nitro functionalized NPOFs and non-functionalized NPOF-1. These observations originate from the polarizable nature of the CO_2 molecule and its large

المنارة للاستشارات
www.manaraa.com

quadrupole moment. The relatively large dipole moment of NO_2 and NH_2 results in dipole-quadrupole interactions with CO_2, and remarkable increases the initial CO_2 uptake at low pressure range. At 1.0 bar and 273 K NPOF-1-NH_2(xs) adsorbs 4.61 mmol g^{-1} (203.1 mg g^{-1}) of CO_2 whereas NPOF-1-NH_2 adsorbs 5.88 mmol g^{-1} of CO_2 (258.9 mg g^{-1}). It is worth noting that the uptake by NPOF-1-NH_2 exceeds top performing adsorbents such as cage frameworks,[101] functionalized CMPs,[102] ALPs,[32, 91] BILPs,[30, 103] metal containing organic polymers,[104, 105] and amine appended POPs.[44, 53, 106-109]

Comparison of methane uptake reveals that in contrast to CO_2, functionalization with polar groups does not enhance methane uptake as a result of the low CH_4-framework interactions (~22 kJ mol^{-1}). These findings suggest that pore functionality along with microporosity are central parameters for enhanced CO_2 uptake at low pressures (up to 1 bar) while high accessible surface area improves CH_4 uptake. (**Figure 3.10** and **Table 3.2**). The Q_{st} values show all functionalized NPOFs to have higher heats of adsorption for CO_2 over non-functionalized NPOF-1 over the entire loading range. The enhanced Q_{st} values are expected due to both chemical and physical pore modification. In addition to the electronic nature of -NH_2 and -NO_2, upon framework functionalization, the pore size of NPOF-1 is also reduced and this provides higher adsorption potentials for CO_2 via possible multi-pore wall interactions. Pore modification increases CO_2 binding affinity from 21.7 kJ mol^{-1} to 32.6 kJ mol^{-1} for NPOF-1-NH_2. These observations again can be ascribed to the polarizable nature of the CO_2 molecule and its large quadrupole moment in addition to Lewis acid-base interactions between CO_2 and primary amines. The Q_{st} drops with higher CO_2 loadings for functionalized NPOFs as functional sites become saturated; however, non-functionalized NPOF-1 did not follow this trend due to lack of

المنارة للاستشارات
www.manaraa.com

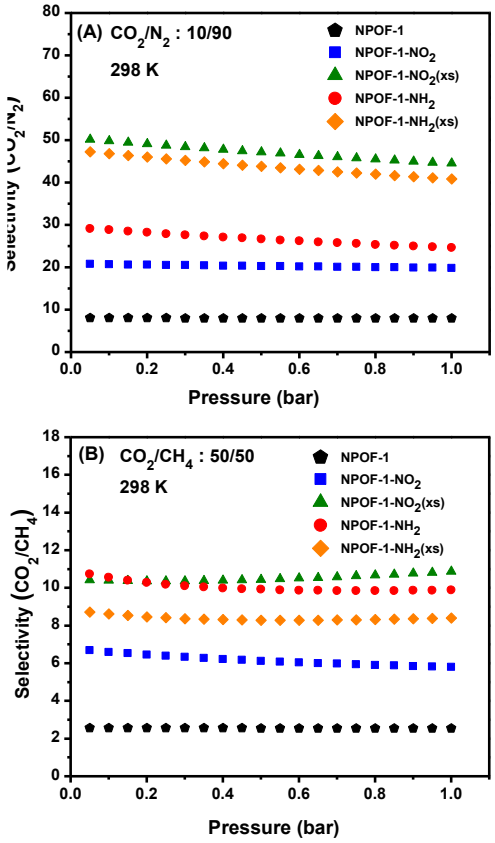

Figure 3.10. Selectivity calculated by IAST for CO_2/N_2 (A) and CO_2/CH_4 (B) at 298 K.

chemical heterogeneity. It is worth mentioning that the interaction between aniline like primary amines and CO_2 resulted in a moderate Q_{st} value which is desired for cost effective CO_2 adsorbents. On the other hand, alkyl amine appended MOFs[110] and POPs[50] resulted in much higher (>50 kJ mol^{-1}) binding affinities which require higher energy input for regeneration of the adsorbents. The high binding affinity of alkylamines towards CO_2 originates from high electron density localized on nitrogen sites in addition to multiple amine (inter and/or intra molecular)-CO_2 interactions favored by the flexible nature of the tethered amines. On the other hand, the electron density of aniline-like amines are

المنارة للاستشارات
www.manaraa.com

Table 3.3. Adsorbents for VSA in flue gas (CO_2/N_2: 10/90) separation at 298 K, P_{ads} = 1 bar and P_{des} = 0.1 bar.

Adsorbent	N_1^{ads}	ΔN_1	**% R**	α_{12}^{ads}	***S***
NPOF-1	0.17	0.15	89.7	8	7
NPOF-1-NO_2	0.42	0.37	88.5	20	42
NPOF-1-NO_2(xs)	0.41	0.36	87.6	**45**	194
NPOF-1-NH_2	**0.76**	**0.66**	87.1	25	57
NPOF-1-NH_2(xs)	0.63	0.55	87.1	41	159
TBILP-2 (Ref. 89)	0.67	0.59	88.3	42	192
BILP-12 (Ref. 39)	0.55	0.49	88.7	27	73
ZIF-78 (Ref. 54)	0.60	0.58	**96.3**	35	**396**
SNU-Cl-va (Ref. 54)	0.47	0.41	87.3	38	262

Table 3.4. Adsorbents for VSA in landfill gas (CO_2/CH_4: 50/50) separation at 298 K, P_{ads} = 1 bar and P_{des} = 0.1 bar.

Adsorbent	N_1^{ads}	ΔN_1	**% R**	α_{12}^{ads}	***S***
NPOF-1	0.79	0.71	**89.2**	2.5	6
NPOF-1-NO_2	1.52	1.30	85.2	5.8	29
NPOF-1-NO_2(xs)	1.39	1.16	83.2	**10.9**	**125**
NPOF-1-NH_2	**2.53**	**2.10**	82.9	9.9	91
NPOF-1-NH_2(xs)	2.01	1.65	82.1	8.4	68
TBILP-2 (Ref. 89)	2.20	1.84	83.7	7.6	63
BILP-12(Ref. 39)	2.01	1.71	85.3	6.0	34
SNU-Cl-va (Ref. 54)	1.51	1.21	80.6	9.7	84
Diimide-POP (Ref. 54)	1.39	1.05	76.0	5.8	16

المنارة للاستشارات
www.manaraa.com

delocalized through the pi-electrons of benzene rings directly linked to the amine. In this case, the amine basicity is much lower and therefore only physical interactions between the amine sites and CO_2 molecules take place. Nevertheless, the Q_{st} values for functionalized NPOFs are strong enough to accommodate high CO_2 at low pressures and exceed most of the best performing materials such as BILPs[39] and bio-MOF-11.[111]

Selectivity of an adsorbent towards CO_2 is also as important as the uptake since CO_2 is not the main component in the gas mixtures to be purified. Therefore, great efforts have been directed towards the design of porous materials that have high CO_2/N_2 and CO_2/CH_4 selectivity for CO_2 removal from flue gas and landfill gas, respectively. Ideal Adsorbed Solution Theory (IAST) is a widely accepted method for investigating the selectivity of porous adsorbents using only pure gas isotherms to calculate gas mixture adsorption.[80] As depicted in **Figure 3.10.**, the IAST results indicate that NPOF-1-NO_2(xs) has the highest selectivity among the NPOFs studied here for CO_2/N_2 as it has the lowest surface area and therefore lowest N_2 uptake at 298 K. NPOF-1-NH_2 has a CO_2/N_2 selectivity of 25 at 298 K and 1 bar. However, for CO_2/CH_4 selectivity, NPOF-1-NH_2 performed very similar to that of NPOF-1-NO_2(xs) due to much higher CO_2 uptake of the former at 0.5 bar. The high surface area along with amine functionality allows NPOF-1-NH_2 to perform better at higher CO_2 concentrations.

3.3.4 Working Capacity Study

Although numerous porous organic and organic–inorganic hybrid materials have been evaluated for CO_2 capture and separation, a careful analysis of the trade-off between selectivity and uptake capacity was not evaluated until recently.[54] The general observation made by Bae and Snurr was that high surface area favours CO_2 separation

المنارة للاستشارات
www.manaraa.com

from landfill gas in pressure swing adsorption (PSA), whereas narrow pore size and high enthalpies of adsorption lead to optimal CO_2 removal from flue gas using vacuum swing adsorption (VSA). Furthermore, five evaluation criteria (*vide infra*) were adopted from the chemical engineering field to investigate the effectiveness of porous adsorbents: CO_2 uptake, working capacity for CO_2, adsorbent regenerability, selectivity under adsorption conditions, and sorbent selection parameter. These criteria, although not perfect, provide

a comprehensive approach for assessing the suitability of porous adsorbents in CCS processes.

Because 87% of the world's total energy production comes from burning fossil fuels, there is an urgent need for selective capture of CO_2 from flue gas. A careful analysis of the performance of NPOFs for this task (CO_2/N_2 : 10/90) using VSA at 298 K is presented in **Table 3.3.** Adsorbents for VSA in flue gas (CO_2/N_2: 10/90) separation at 298 K, P_{ads} = 1 bar and P_{des} = 0.1 bar. The working capacities (ΔN_1) were determined by calculating the CO_2 adsorption difference between 1.0 and 0.1 bar using IAST derived uptakes. According to **Table 3.3**, NPOF-1-NH_2 showed great CO_2 uptake enhancement at low pressures (4.3 folds higher compared to NPOF-1) due to the unique combination of high micropore volume and chemical functionality in addition to optimum isosteric heats of adsorption for CO_2, as a consequence, NPOF-1-NH_2 revealed the highest working capacity (0.66 kg mol^{-1}) compared to other NPOFs evaluated here. On the other hand, the lower micropore volume and surface area of NPOF-1-NH_2(xs) resulted in ~17% less working capacity although both materials have primary amine functionalized frameworks and very similar Q_{st} for CO_2. It is worth noting that the high surface area of NPOF-1-NH_2

المنارة للاستشارات
www.manaraa.com

and low partial pressure (10%) of CO_2 resulted in low CO_2/N_2 selectivity and therefore low S value compared to NPOF-1-NH_2(xs) with the latter displaying much lower working capacity.

Switching from coal-fired power plants to natural gas-fired power plants presents an alternative strategy to mitigate CO_2 emissions before renewable energy sources become widely available since natural gas has a lower carbon footprint. For the same reason, the use of natural gas in automotive applications is highly desired; however, natural gas found in reservoirs has tangible amounts of CO_2, N_2, and H_2S that need to be minimized before transport and use.[112] Natural gas as well as landfill gas purification processes involve CO_2 removal to prevent pipeline corrosion and to increase the energy density of this methane rich gas making on-board storage and use more efficient. Therefore, we assessed NPOFs performance in landfill gas purification from CO_2 under VSA conditions at 298 K (**Table 3.4**). NPOF-1-NH_2 outperformed all other NPOFs reported in Table 4 in terms of working capacity (2.10 kg mol^{-1}). Since the concentration (partial pressure) of CO_2 is higher in landfill gas (50%), the outcome of high surface area adsorbents along with chemical functionality becomes more pronounced. For instance, NPOF-1-NH_2 gives a ~20% enhancement in working capacity compared to NPOF-1-NH_2(xs) in the case of flue gas; however, this difference becomes ~27% in the case of landfill gas separation due to higher partial pressure of CO_2. Although the high CO_2/CH_4 selectivity of NPOF-1-NO_2(xs) due to low surface area results in a higher S parameter, the much lower working capacity compared to NPOF-1-NH_2 makes it a less promising candidate for CO_2 separation from landfill gas. On the other hand, the ideal combination of high surface area, binding affinity and microporous nature of NPOF-1-NH_2 gives rise to high CO_2/CH_4 selectivity and

المنارة للاستشارات
www.manaraa.com

working capacity which results in very high S value. This suggests that NPOF-1-NH_2 can be more suitable for CO_2 separation from mixtures where CO_2 concentration is at or above 50%.

3.4 Conclusions

In conclusion, we have synthesized NPOF-1 and presented its post-synthetic modification of the material to functionalize the framework with –NO_2 and –NH_2 functionalities. Using stoichiometric amounts of nitric acid and shortening the reaction time allowed us to maintain and/or generate ultramicropores and to incorporate polar functional groups which are essential properties for CO_2 capture at low pressures (<1 bar). We have shown that coupling the high surface area and aniline-like amine functionality in NPOF-1-NH_2 yields very high CO_2 working capacity and selectivity which result in high sorbent selection parameter for CO_2 capture from landfill gas under VSA settings.

المنارة للاستشارات
www.manaraa.com

Chapter 4

Enhanced Carbon Dioxide Capture from Landfill Gas using Bifunctinalized Benzimidazole-Linked Polymers[3]

4.1 Introduction

Leveraging natural gas and landfill gas instead of coal and petroleum to meet energy demands is one of the promising approaches for reducing greenhouse gas emissions.[113] This has been suggested as an alternative strategy since the combustion of methane produces the smallest amount of CO_2 for each unit of heat produced as CH_4 has the highest hydrogen to carbon ratio among all hydrocarbons.[114] Landfill gas, a by-product of the decomposition of municipal solid waste, is composed of ~50% CH_4 and ~50% CO_2 and the CO_2 needs to be separated prior to usage as a fuel to increase the energy density and to prevent corrosion.[115] Considerable efforts have been made to develop efficient solid sorbent materials for CO_2 capture from gas mixtures via adsorption-based

---

[3] Islamoglu, T.; Behara, S.; Kahveci, Z.; Tessema, T.D.; Jena, P. and El-Kaderi, H.M. Enhanced Carbon Dioxide Capture from Landfill Gas using Bifunctinalized Benzimidazole-Linked Polymers **2016** (under review)

المنارة للاستشارات
www.manaraa.com

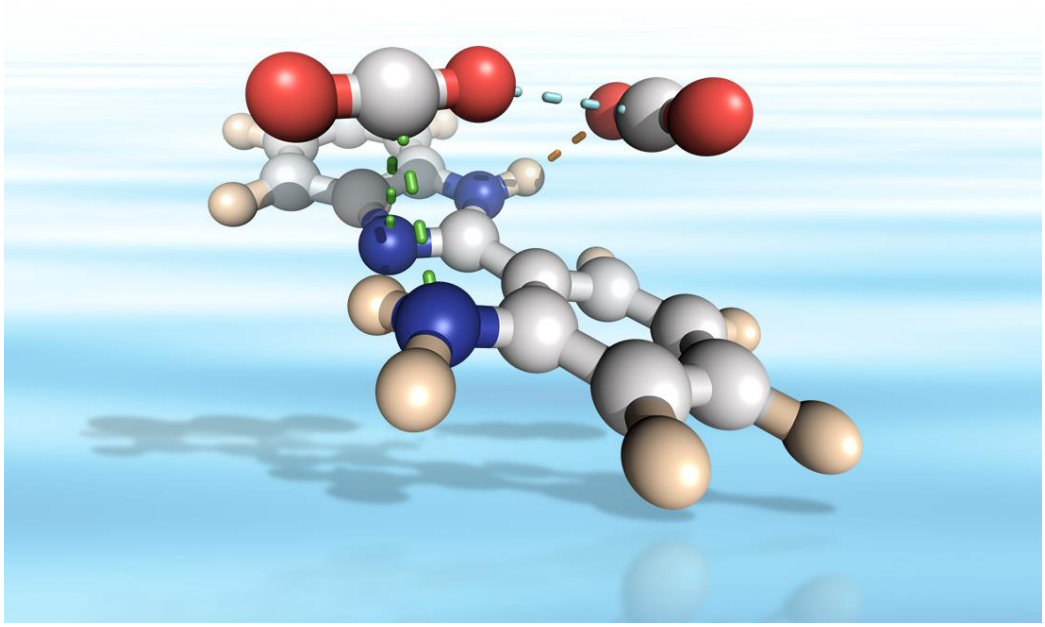

Figure 4.1. Interactions of CO_2 and BILP-6-NH_2.

separation.[12, 37, 116, 117] Among the investigated solid adsorbents, porous organic polymers (POPs) have received considerable attention because of their physical and chemical stability in addition to structural tunability.[20] Incorporating functional groups in POPs such as benzimidazole,[40] triazine,[118, 119] azo,[32, 120] sulfonate[121], nitro,[21, 90] amine,[51, 52] imide,[78, 122] imine,[45, 93, 123] Troger's base[124], porphyrin,[125] benzoin,[126] isocyanurate,[127] benzoxaole[128] and hydroxy groups[129, 130] can help to polarize CO_2 which enhance CO_2-POP interactions (**Figure 4.1**). The interactions of CO_2 with adsorbing materials are especially important for CO_2 capture at pressures below 1 bar.[37] Among the well-investigated functional groups is benzimidazole which attracted a great deal of attention because of its chemical stability and optimal pKa that favors physisorptive interactions with CO_2.[71, 131] Aniline-like amine functionalities are also of interest because of the ideal

المنارة للاستشارات
www.manaraa.com

pKa of aniline as opposed to alkyl amines where localized electron density on the nitrogen results in chemisorption of CO_2 instead of physisorption.[53, 132] Chemisorption of CO_2 is not ideal because high temperatures are then required to regenerate the sorbent.[11] It was shown recently that POPs containing multiple functional groups exhibit combined effects of each functional group that improve selective binding of CO_2.[133-136] For example, we have shown that the incorporation of triazine groups in benzimidazole linked polymers (BILPs) results in improved selective CO_2 capture capabilities.[89] Because the amine functionality is known for improved CO_2 capture and separation by porous adsorbents, we hypothesized that placing amine groups adjacent to benzimidazole units in BILPs would increase CO_2 binding capabilities through multiple interactions and/or providing extra adsorption sites.

Here, we use pre- and postsynthetic modification methods to synthesize BILP-6-NH_2 that combines both benzimidazole and amine functionalities for use in gas separation applications. We have performed DFT calculations to gain insight into the intermolecular interactions between CO_2 and BILP-6-NH_2. DFT calculations reveal that there is an intramolecular hydrogen bonding in BILP-6-NH_2 involving the N-H (amine) group (hydrogen atom donor) and N(sp^2) of the benzimidazole ring (hydrogen atom acceptor). As a result of this hydrogen bonding, the first adsorbed CO_2 molecule prefers to stay out of the plane and interacts with both the imidazole and amine nitrogen atoms. Moreover, the second CO_2 molecule interacts more strongly in the case of BILP-6-NH_2 because of the CO_2···H-N (imidazole) interaction in addition to CO_2···CO_2 interactions, which are absent in BILP-6. Experimental CO_2 isotherms show enhanced CO_2 adsorption capacity of BILP-6-NH_2 compared to BILP-6.

المنارة للاستشارات
www.manaraa.com

4.2 Experimental Section

4.2.1 General Techniques, Materials and Methods

All starting materials and solvents, unless otherwise noted, were obtained from Acros Organics and used without further purification. 2-nitroterephthaldehyde (TPAL-NO_2) was synthesized according to literature procedure and ^{1}H NMR is shown in **Figure 4.2**.[137, 138] Data for BILP-6 was used from our previous report.[139] Solvents were dried by distillation. Air-sensitive samples and reactions were handled under an inert atmosphere of nitrogen using either glovebox or Schlenk line techniques. Elemental microanalyses were performed at the Midwest Microlab, LLC. Liquid ^{1}H and ^{13}C NMR spectra were obtained using a Varian Mercury-300 MHz NMR spectrometer (75 MHz carbon frequency). Solid-state ^{13}C cross-polarization magic angle spinning (CP-MAS) NMR spectra for solid samples were taken at Spectral Data Services, Inc. Spectra were obtained using a Tecmag-based NMR spectrometer operating at a H-1 frequency of 363 MHz, using a contact time of 1 ms and a delay of three seconds for CP-MAS experiments. All samples were spun at 7.0 kHz. Thermogravimetric analysis (TGA) was carried out using a TA Instruments Q-5000IR series thermal gravimetric analyser with samples held in 50 µL platinum pans under an atmosphere of air (heating rate 5 °C /min). For scanning electron microscopy imaging (SEM), samples were prepared by dispersing the material onto a sticky carbon surface attached to a flat aluminium sample holder. The samples were then coated with platinum at a pressure of 1 x 10^{-5} mbar under a nitrogen atmosphere for 70 seconds before imaging. Images were taken on a Hitachi SU-70 Scanning Electron Microscope. Powder X-ray diffraction data were collected on a Panalytical X'pert pro

المنارة للاستشارات
www.manaraa.com

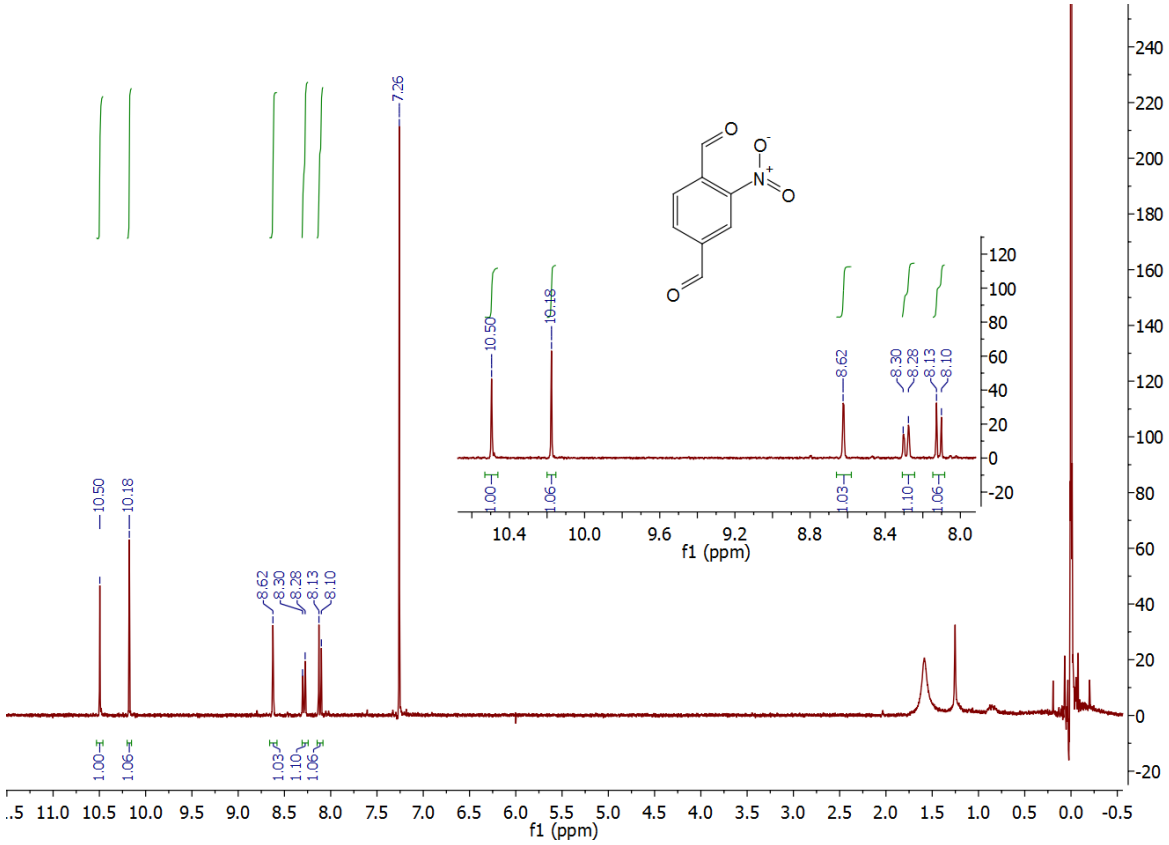

Figure 4.2. ^{1}H NMR spectra of TPAL-NO_2 in $CDCl_3$.

multipurpose diffractometer. Samples were mounted on a sample holder and measured using Cu Kα radiation with a 2θ range of 1.5-35. FT-IR spectra were obtained on a Nicolet-Nexus 670 spectrometer furnished with an attenuated total reflectance accessory. Porosity and gas sorption experiments were collected using a Quantachrome Autosorb iQ volumetric analyser using adsorbate of UHP grade. In a typical experiment, a sample of polymer (~50 mg) was loaded into a 9 mm large bulb cell (Quantachrome) of known weight which was then hooked up to a gas analyser and degassed at 130 °C / 1.0 x 10^{-5} bar for 12 hours. The degassed sample was refilled, weighed precisely and then transferred back to the analyser. The temperatures for adsorption measurements were

المنارة للاستشارات
www.manaraa.com

Scheme 4.1. Schematic representation of synthesis of BILP-6 and BILP-6-NH_2.

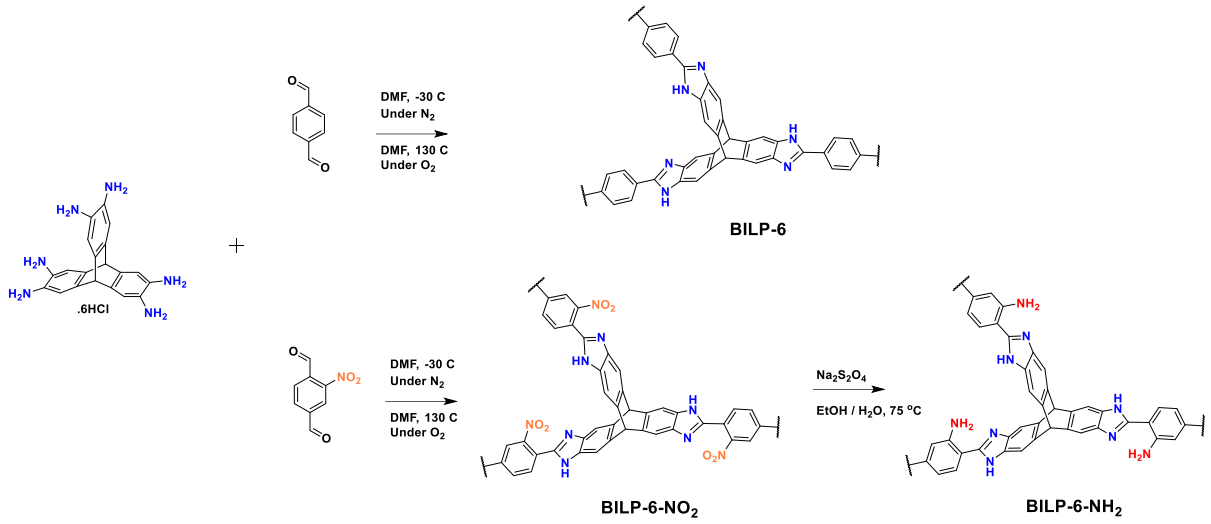

controlled by using a refrigerated bath of liquid nitrogen (77 K), and a temperature controlled water bath (273 K and 298 K).

Synthesis of BILP-6-NO_2: A 200 mL Schlenk flask was charged with 2,3,6,7,14,15-hexaaminotriptycene hexahydrochloride (110 mg, 0.195 mmol), 75 mL of anhydrous DMF, and a stir-bar. The resultant solution was cooled to ca. -30 ºC then treated drop-wise with a solution of 2-nitroterephthaldehyde (52.5 mg, 0.293 mmol) in anhydrous DMF (25 mL). The temperature was maintained around -30 ºC for 3 hours and the resultant slurry solution was left to warm to room temperature overnight. The flask containing the reaction mixture was flushed with air for 15 minutes and capped tightly. The reaction mixture was then transferred to a static oven and heated gradually to 130 °C (0.5 °C/min) and kept for 3 days to afford a fluffy brownish polymer which was isolated by filtration over a medium glass frit and subsequently washed with DMF, acetone, water, 2 M HCl, 2 M

المنارة للاستشارات
www.manaraa.com

NaOH, water, and acetone. The resultant polymer was dried under reduced pressure to afford BILP-6-NO_2 (83 mg) as a brownish powder.

Synthesis of BILP-6-NH_2: A slightly modified literature report was followed for reduction of nitro groups.[140] A 50 mL round bottom flask equipped with a stir bar was charged with 75 mg BILP-6-NO_2, 10 mL methanol, and 10 mL distilled water under nitrogen. The resultant suspension was degassed with N_2 for 20 min before adding sodium dithionite (1 g, 5.75 mmol) which was then was heated to 75 °C for 18 hours. The resultant material was filtered and suspended in warm water (25 mL) for 30 min. The suspension was filtered and washed with warm water twice. The resultant polymer was suspended in 25 mL 4 M HCl in order to ensure complete reduction to amine then was washed with water followed by 2 M NaOH in order to neutralize the amine. The isolated product was suspended in warm water (30 mL) for 60 minutes. After filtration the polymer was suspended in warm ethanol and THF twice for 30 min cycles. The polymer lastly was filtered and washed with methanol and dried overnight under vacuum at 120 ºC to yield a dark brownish BILP-6-NH_2 (55 mg). Anal. Calcd. for $C_{64}H_{37}N_{15}$: C, 75.65%; H, 3.67%; N, 20.68%. Found: C, 67.91%; H, 4.42%; N, 16.45%.

4.3 Results and Discussion

4.3.1 Synthesis and Characterization

The synthesis of BILP-6-NO_2 was performed according to a method we reported previously, where an acid-catalyzed condensation reaction between aryl-o-amine and aryl-aldehyde forms the imidazole ring as depicted in **Scheme 4.1**.[30] It is worth noting that

المنارة للاستشارات
www.manaraa.com

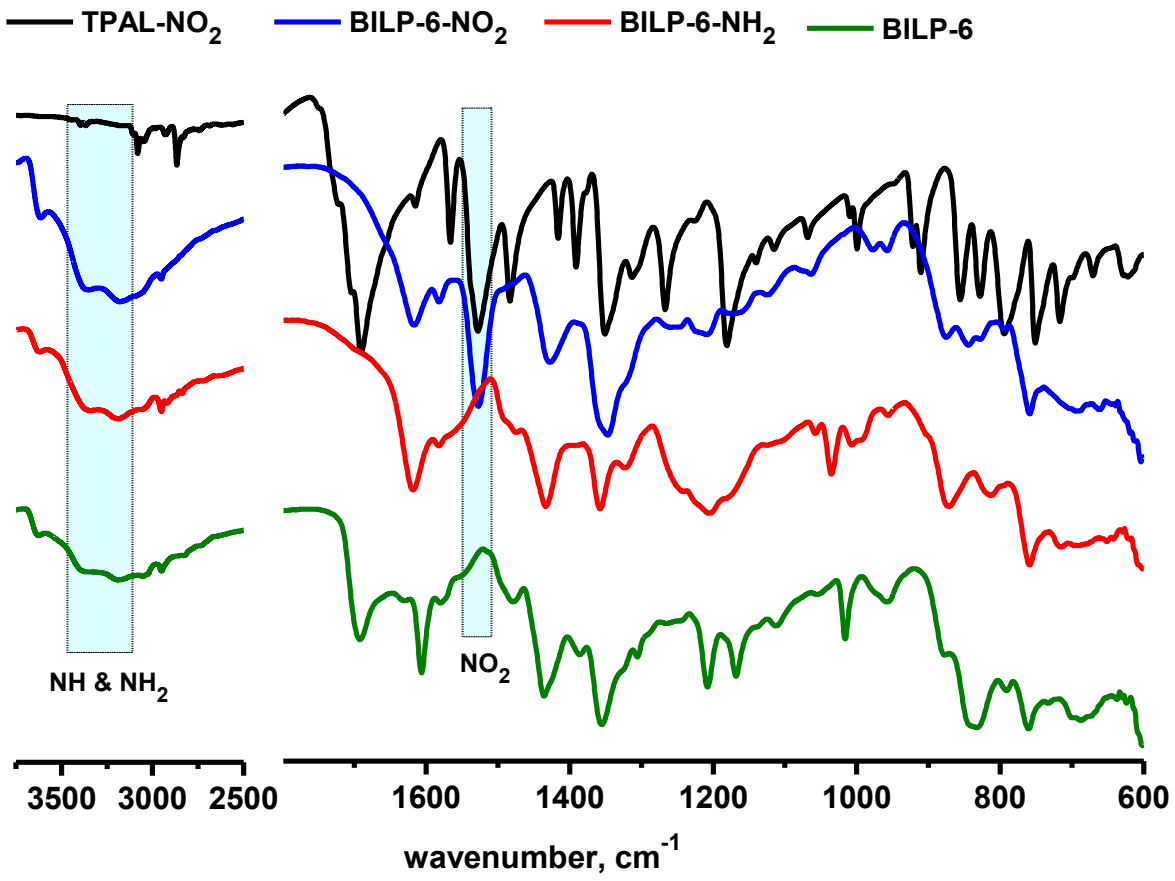

Figure 4.3. FT-IR spectra of TPAL-NO_2 and polymers.

BILP-6-NH_2 cannot be synthesized *de novo* because of a side reaction that could possibly lead to homopolymerization of amine functionalized aldehyde linker. Therefore, we first synthesized the –NO_2 functionalized network (BILP-6-NO_2) followed by reduction of the nitro groups to amines to give BILP-6-NH_2. Although postsynthetic modification (PSM) has been instrumental for introducing targeted functionality into POPs, complete functionalization of all possible sites is nearly impossible even when excess equivalents of reagents are used (~0.6 functional group/benzene achieved).[51] Most likely this is due to a lack of accessibility of all sites that can be functionalized in these amorphous

المنارة للاستشارات
www.manaraa.com

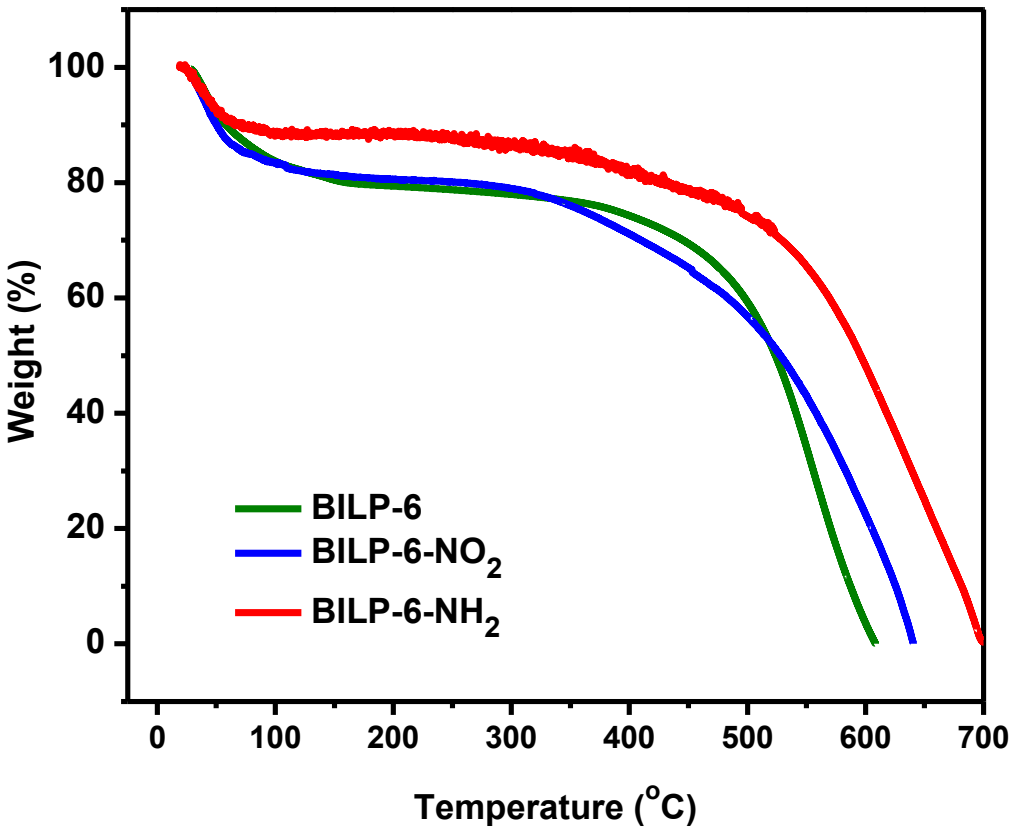

Figure 4.4. TGA traces of polymers.

materials. Very recently we developed controlled PSM of NPOFs to prevent micropore blocking upon functionalization, however, controlling the loading of functional group sites remains a great challenge.[51] On the other hand, pre-synthesis functionalization ensures a loading of 1 nitro/phenyl ring which enables a more accurate prediction and visualization of the final structure. In addition, by employing pre-synthesis functionalization we have excluded the possibility of additional nitro/amine groups being loaded onto the benzene rings of the triptycene moieties. As expected, BILP-6-NH_2 was not soluble in common organic solvents such as tetrahydrofuran, dimethylformamide, dichloromethane and

المنارة للاستشارات
www.manaraa.com

BILP-6

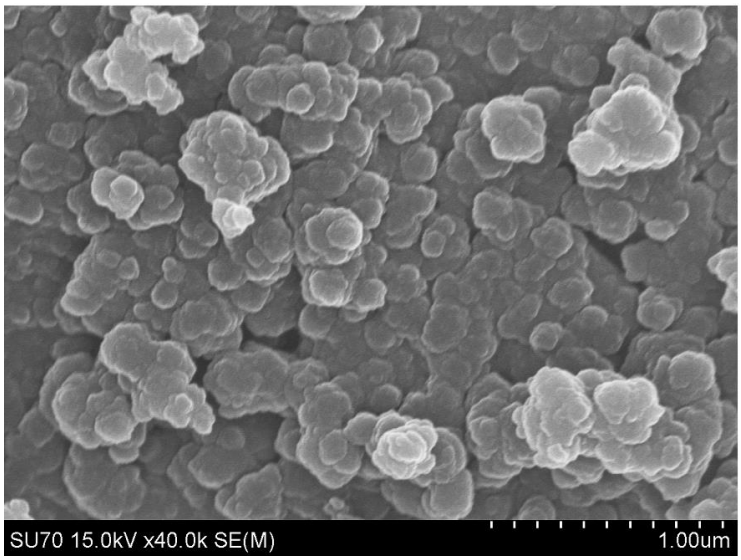

BILP-6-NH_2

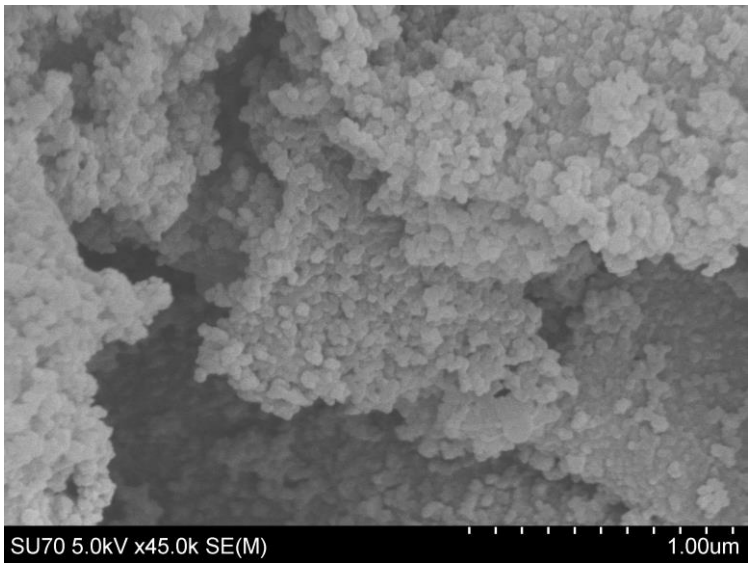

Figure 4.5. SEM images of BILP-6 and BILP-6-NH_2.

المنارة للاستشارات
www.manaraa.com

methanol. The chemical stability of BILP-6-NH_2 was confirmed by washing the polymer with 2 M NaOH and 2 M HCl and the thermal stability was confirmed by TGA where it was found that only ~8 wt% is lost up to 400 °C after the initial weight loss due to residual solvent and/or moisture (**Figure 4.4**). FT-IR studies showed that the peak at 1690 cm^{-1} (C=O from aldehyde) is almost completely diminished which confirms successful polymerization (**Figure 4.3**). Complete reduction of nitro groups is demonstrated by a significant decrease in the intensity of the band at 1528 cm^{-1} (asymmetrical and stretching of NO_2). Symmetrical stretching of NO_2 can also be seen at 1350 cm^{-1}; however, the decrease in this peak cannot be interpreted upon reduction of nitro groups due to overlapping of peaks from other groups around the same region. Peaks at 3369 and 3172 cm^{-1} can be assigned to N-H stretches from the imidazole ring and amino group. The peak around 3600 cm^{-1} can be attributed to H-bonded water molecules.[141] According to PXRD studies, all polymers are amorphous and lack long-range ordering as previously reported for BILPs. SEM images revealed aggregated plated particles of variable sizes as shown in **Figure 4.5**. Microelemental analysis results showed 16.45 wt% nitrogen for BILP-6-NH_2 which is ~28% higher compared to BILP-6 (12.87 wt%). This is expected because of incorporation of amine groups. A deviation in microelemental analysis for POPs is common due to their amorphous nature.

4.3.2 Textural Properties

The specific surface area and pore size distribution of BILP-6 and BILP-6-NH_2 were characterized by means of N_2 (77 K) adsorption-desorption measurements. The corresponding nitrogen adsorption isotherms and pore size distributions of BILPs are

المنارة للاستشارات
www.manaraa.com

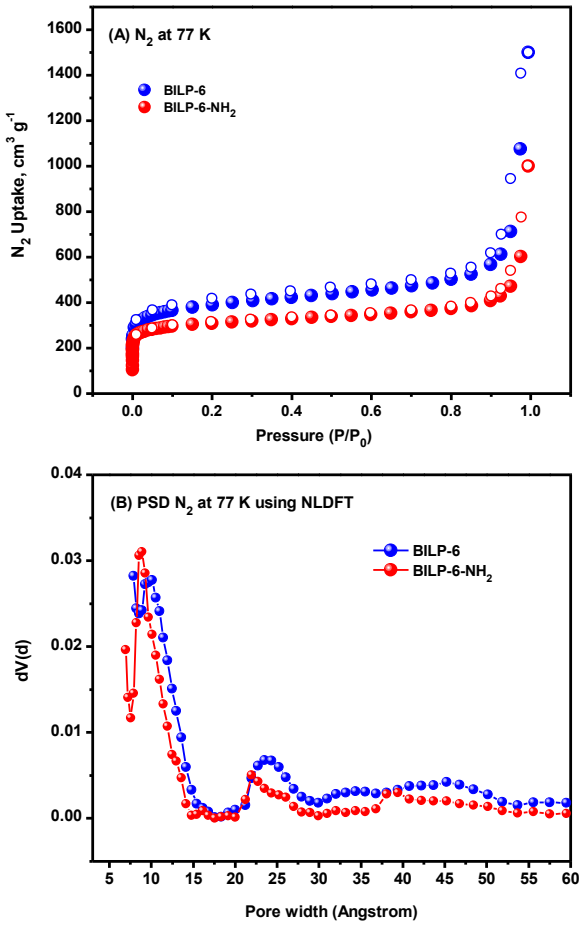

Figure 4.6. Nitrogen isotherms at 77 K (A) and pore size distribution from NLDFT using N_2 at 77 K (B).

depicted in **Figure 4.6.** Both nitrogen isotherms show a sharp uptake at very low pressure ($P/P_0 < 0.01$) followed by a plateau ($0.01<P/P_o<0.9$) which is consistent with their expected microporous nature. A sharp increase in N_2 uptake around $P/P_o > 0.9$ is observed and can be attributed to N_2 condensation in inter-particle voids which is common in POPs having small particle sizes. The textural properties of BILPs are listed in **Table 4.1.** The Brunauer-Emmett-Teller surface areas of BILP-6 and BILP-6-NH_2 were measured to be 1458 and 1185 $m^2 g^{-1}$, respectively. It is worth noting that BILP-6-NH_2 is

المنارة للاستشارات
www.manaraa.com

Table 4.2. Surface areas, CO_2 uptakes at 298 K, *Qst* and IAST selectivity results of polymers.

			CO_2 Uptake			IAST
Polymer	[a]**SA_{BET}**	[b]**$V_{Mic,DFT}$**	[c]*0.5 bar*	[c]*1 bar*	[d]Q_{st}	[e]CO_2/CH_4
BILP-6	1458	0.44 (0.64)	153.5 (90.6)	208.8 (121.3)	28.3	3
BILP-6-NH_2	1185	0.38 (0.48)	184.5 (119.3)	244.8 (164.7)	29.5	6

[a]BET surface areas are reported in m^2 g^{-1}. [b]Micropore volume determined by NLDFT in cm^{-3} g^{-1} ; the values in parentheses are the percentage of micropore volume relative to total pore volume. [c]The uptakes of CO_2 at corresponding pressure in mg g^{-1} at 273 K (298 K) [d]Isosteric heat of adsorption of corresponding gas at zero coverage calculated from isotherms collected at 273 and 298 K using Virial equation. [d]Selectivity calculated by IAST at 298 K and 1 bar.

~9.2 % heavier than BILP-6 and in addition, the amino groups are occupying some space in the pores. Thus the 18% drop in surface area from BILP-6-NH_2 to BILP-6 is expected. This further confirms the efficiency of the pre-synthesis functionalization method for construction of functionalized POPs where a noninvasive pore functionalization can be achieved. A pore size distribution (PSD) analysis of the polymers was determined by fitting the N_2 adsorption isotherm (77 K) using NLDFT with the carbon model (slit/cylindr. pores, QSDFT adsorption branch). The analysis shows that the pores in BILP-6-NH_2 and BILP-6 are 8.8 and 10 Å, respectively. The mesopore peaks observed at ~23 Å are most likely due to N_2 condensation at inter-particle voids which are acting as mesopores. Pore volumes from single point adsorption at $P/P_o = 0.9$ are measured to be 0.64 and 0.48 cm^{-3} g^{-1} for BILP-6 and BILP-6-NH_2, respectively.

المنارة للاستشارات
www.manaraa.com

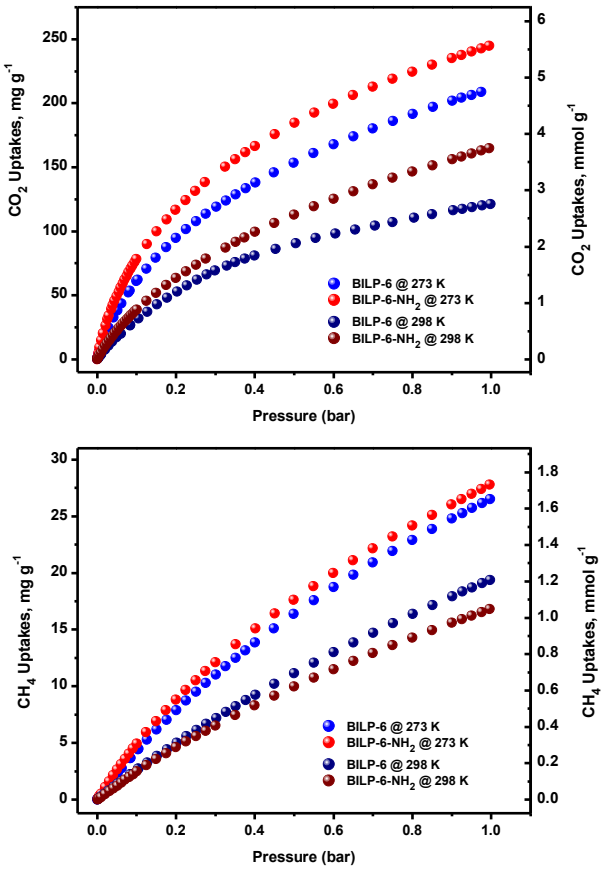

Figure 4.7. CO_2 (A) and CH_4 (B) uptakes of BILP-6 and BILP-6-NH_2 at 273 and 298 K.

4.3.3 Gas uptake and selectivity studies

To reveal the effect of amine functionalized BILP on CO_2 capture from landfill gas settings we have collected carbon dioxide and methane adsorption isotherms at 273 and 298 K. The hysteresis-free isotherms confirm the reversibility of gas uptake/release in the polymers which is essential fo r identifying cost efficient CO_2 capture (**Figure 4.7**). The superior CO_2 uptake of BILP-NH_2 relative to BILP-6 is also demonstrated by CO_2 adsorption isotherms at both temperatures. At 298 K, the difference in uptake becomes more pronounced after ~0.4 bar where BILP-6 starts to plateau but BILP-6-NH_2 continues

المنارة للاستشارات
www.manaraa.com

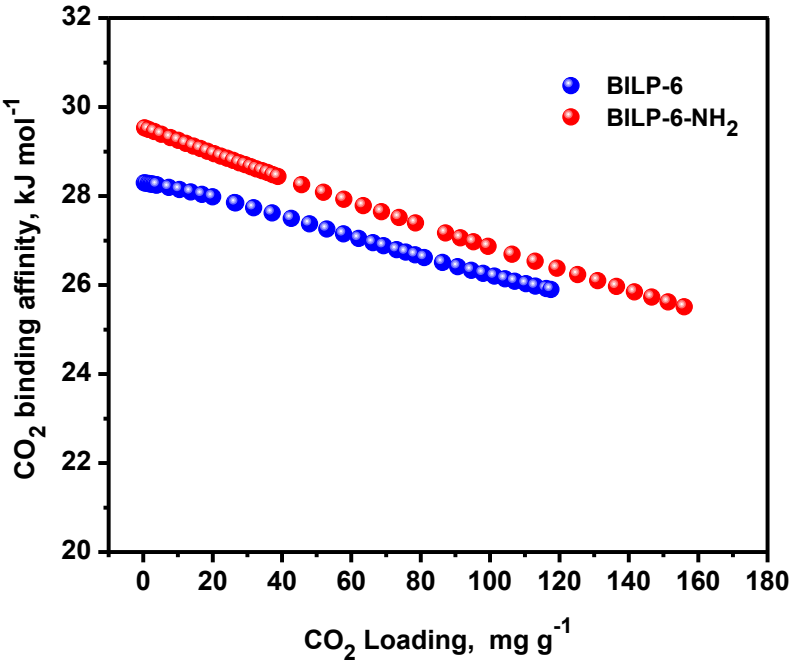

Figure 4.8. Isosteric heat of adsorption of CO_2 for BILP-6 and BILP-6-NH_2.

to show a rise in uptake. At 0.4 bar and 298 K, BILP-6-NH_2 shows 22% (81 vs 99 mg g^{-1}) enhancement in CO_2 uptake while it increases to 36% (121 vs 165 mg g^{-1}) at 1 bar. This is most likely because of the amine functionalities in BILP-6-NH_2 which provide extra/cooperative adsorption sites for CO_2. On the other hand, CH_4 uptake for BILP-6-NH_2 at 298 K is lower than BILP-6 due to the higher surface area of the latter. These findings are in agreement with recent findings in the literature where CO_2 uptake correlates with pore functionality while the surface area plays a dominant role for CH_4 uptake.[21] It is worth noting that a high CO_2 uptake at 0.5 bar is desirable for landfill gas separation under vacuum swing adsorption (VSA) settings as the CO_2 content in landfill gas is generally ~50%. BILP-6 adsorbs 2.05 mmol g^{-1} of CO_2 at 298 K and 0.5 bar while BILP-6-NH_2 adsorbs 2.57 mmol g^{-1} under the same conditions which corresponds to a

المنارة للاستشارات
www.manaraa.com

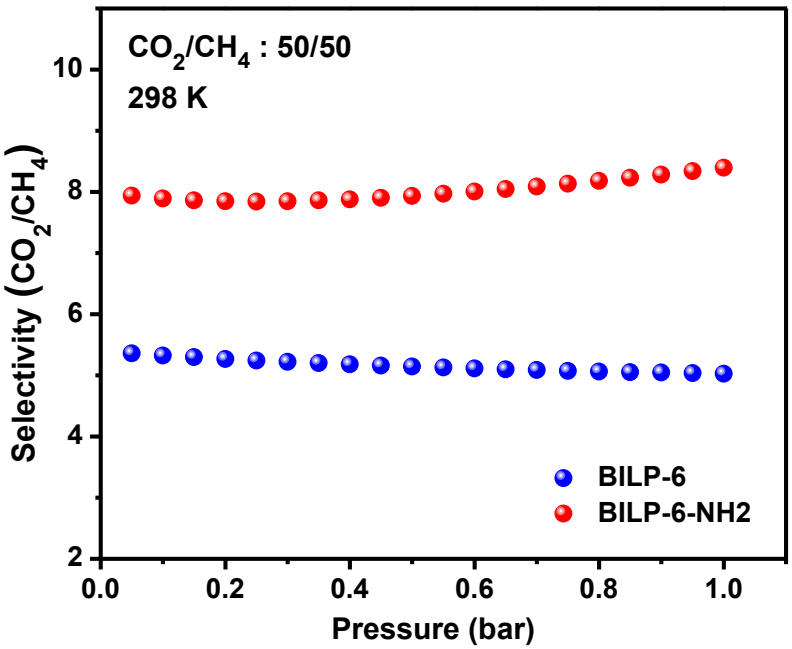

Figure 4.9. CO_2/CH_4 selectivity calculated by IAST for BILPs at 298 K.

25% enhancement in the uptake. At 1 bar, BILP-6-NH_2 stores of 5.56 and 3.74 mmol g^{-1} of CO_2 at 273 and 298 K, respectively, which exceeds top performing POP adsorbents such as cage frameworks,[101] functionalized conjugated miroporous polymers (CMPs),[68] azo-linked polymers (ALPs),[32, 92] BILPs,[103] and amine appended POPs.[53]

The virial equation was fitted to CO_2 and CH_4 isotherms collected at 273 and 298 K to calculate isosteric heats of adsorption of the guest molecules. At zero coverage, the interaction of CO_2 with the most energetically favored sites are calculated to be 28.3 and 29.5 kJ mol^{-1} for BILP-6 and BILP-6-NH_2, respectively (**Figure 4.8**). The strength of this interaction drops to ~26 kJ mol^{-1} with increasing CO_2 loading due to saturation of the active binding sites. The higher Q_{st} for BILP-6-NH_2 is most likely due to a combination of CO_2–benzimidazole/amine interactions and the small pores of BILP-6-NH_2 that allow for

المنارة للاستشارات
www.manaraa.com

multiple pore wall interactions with CO_2. The reported Q_{st} for BILP-6-NH_2 is consistent with fully reversible CO_2 isotherm where CO_2 release is achieved by pressure drop without heating. Although the CH_4 uptake by BILP-6-NH_2 is lower than that of BILP-6 at 298 K and 1 bar, the binding affinity of CH_4 increased significantly upon incorporation of amino groups which can be attributed to slightly smaller pores of BILP-6-NH_2.

Given the high CO_2 uptake and desirable binding affinity, we studied the use of BILP-6-NH_2 in selective CO_2 capture from landfill gas. Ideal Adsorbed Solution Theory (IAST) is a widely accepted method for investigating the selectivity of porous adsorbents using only pure gas isotherms to calculate gas mixture adsorption.[80] As depicted in **Figure 4.9**, BILP-6-NH_2 shows enhanced CO_2/CH_4 selectivity (5.0 vs 8.4 at 1 bar) compared to BILP-6 at all pressure ranges (0-1 bar) at 298 K. A slight increase in selectivity observed with increasing pressure for BILP-6-NH_2 can be attributed to the effect of the amino groups which provide additional adsorption sites for CO_2.

4.3.4 DFT Study

In order to have a better understanding of the effect of incorporating amino groups adjacent to an imidazole moiety on CO_2 binding modes, we carried out DFT calculations with local density approximation (LDA) functional consisting of the Slater exchange and Volk–Wilk–Nusair correlation functional (SVWN)[142]. It is worth noting that since the interaction of CO_2 molecules with BILPs are calculated using only active sites of the structure, it is expected to have a deviation between calculated and experimental binding affinity since the effect of pore size and multi-pore wall interactions are ignored in DFT calculations for the sake of computational expense. We have used the Gaussian 09 package[143] and the 6-311+G*[144] basis set for all our computations. The convergence in

المنارة للاستشارات
www.manaraa.com

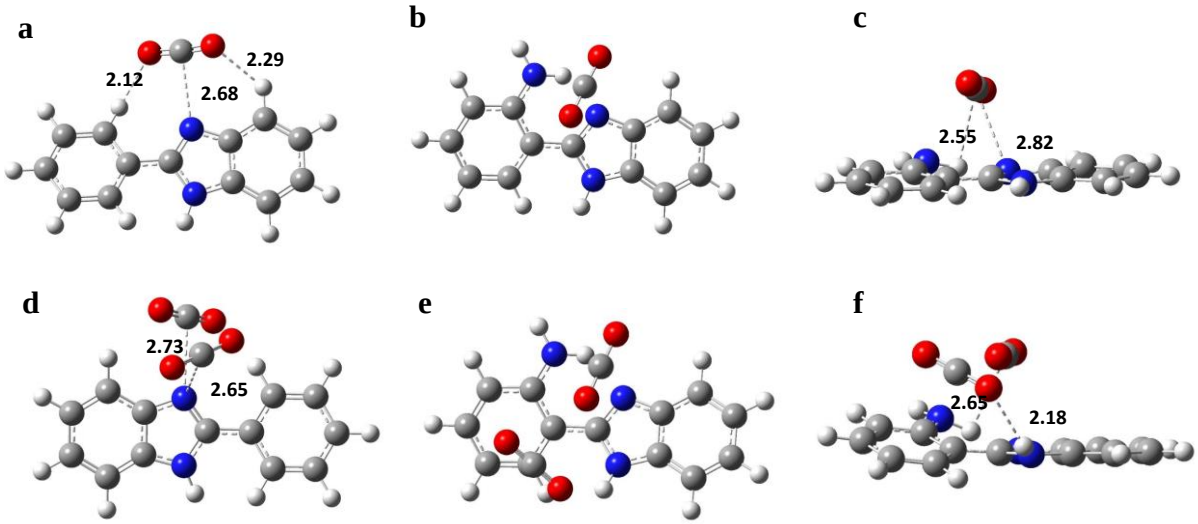

Figure 4.10. Fully optimized geometries of BILPs–CO_2 interactions calculated at the M06/6-311+G* level of theory. (a) BILP-6@CO_2 top view; (b) and (c) BILP-6-NH_2@CO_2 top and side view, respectively; (d) BILP-6@2CO_2 top view; (e) and (f) BILP-6-NH_2@2CO_2 top and side view, respectively; The bond lengths are in Å. The blue, grey, white and red colours stand for N, C, H and O atoms, respectively.

the total energy and force was set at 1×10^{-6} eV and 1×10^{-2} eV Å^{-1}, respectively. Initially different geometries were considered where the CO_2 molecules were allowed to approach different binding sites of the benzimidazole/amine-containing units (**Figure 4.10**). The electrostatic potential (ESP) maps of structures are shown in (**Figure 4.11**). We recently reported on BILP-CO_2 interactions sites which were identified using two different levels of theory, LDA and MO6.[145] Our findings showed that the interaction of CO_2 with benzimidazole was mainly through N(sp^2) in imidazole and C in CO_2 in addition to complementary interactions involving aryl C–H and CO_2 (C–H···O=C=O) with variable bond distances in the range of 2.79–2.94 Å.[145] The other nitrogen, N(sp^3), was not preferred by CO_2 presumably because of delocalization of the lone pairs on that nitrogen

المنارة للاستشارات
www.manaraa.com

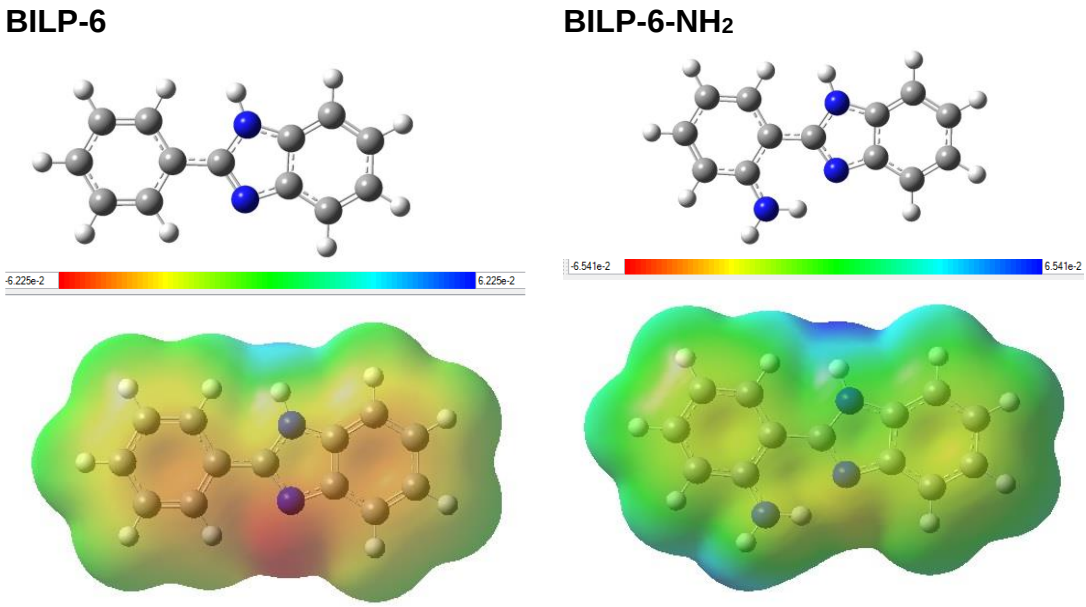

Figure 4.11. Electrostatic potential map for BILP-6- and BILP-6-NH2.

with the aromatic system. The same calculations were performed for BILP-6 for comparison purposes and we have found very similar CO_2–framework interaction modes. We postulated that incorporation of amino groups in BILP-6-NH_2 would facilitate an increase in binding affinity for the first CO_2 molecule; however, due to intramolecular hydrogen bonds in the BILP-6-NH_2 involving the N(sp^2) of the heterocyclic five-membered ring and N-H group, the binding affinity was slightly lower compared to BILP-6 (31.78 vs 28.77 kJ mol^{-1}). However, the average binding affinity of the second CO_2 molecule in BILP-6 and BILP-6-NH_2 follows a different trend. In the case of BILP-6, the second CO_2 molecule prefers to stay out of the plane and interacts with the same nitrogen atom resulting in an average binding affinity of 29.34 kJ mol^{-1}. In the case of BILP-6-NH_2, the second CO_2 also prefers to stay out of the plane; however it can interact with the first CO_2 in a T-shaped orientation to minimize its energy since the first CO_2 is also out of the plane.

المنارة للاستشارات
www.manaraa.com

In addition, the second CO_2 is aligned to form a hydrogen bond with the H atom in N-H (imidazole) which shows a distance of 2.18 Å. Therefore, the average binding affinity of the second CO_2 molecules is calculated to be 36.57 kJ mol^{-1}. It is clear from the DFT calculations that amino groups are responsible for enhanced CO_2 uptake in BILP-6-NH_2 compared to BILP-6 in which the imidazole is the only active site as preferred adsorption sites. The bond lengths between the C and O atoms of the CO_2 molecule does not change (*i.e*. 1.16 Å) compared to neutral CO_2, whereas the shape is slightly bended (bond angle reduces to 176°) which is consistent with previous reports.[146]

4.3.5 Sorbent Evaluation Criteria

Although CO_2 uptake is important at the partial pressure of interest, selectivity under the same condition is of similar significance. A recent report by Bae and Snurr has been instrumental for evaluating porous solid adsorbents for a given application.[54] We have applied the sorbent evaluation criteria to BILP-6 and BILP-6-NH_2 and compared them to some of the best performing materials in the literature.[39, 51, 54, 89, 91, 135] We postulate that the narrow pore size and higher enthalpy of adsorption for BILP-6-NH_2 for CO_2 would make it superior under vacuum swing adsorption (VSA). Briefly, sorbent evaluation criteria show CO_2 uptake under adsorption conditions (N_1^{ads}), working capacity for CO_2 (ΔN_1), adsorbent regenerability (R), selectivity under adsorption conditions (α_{12}^{ads}) and sorbent selection parameter (S), which combines the selectivity and working capacity in one parameter. We assessed the performance of BILP-6-NH_2 in landfill gas purification from CO_2 (CO_2/CH_4 : 50/50) under VSA conditions at 298 K and an adsorption pressure of 1 bar and desorption pressure of 0.1 bar (**Table 4.2**). BILP-6-NH_2 presents a working capacity of 2.14 kg mol^{-1} which corresponds to a 43% increase compared to

المنارة للاستشارات
www.manaraa.com

Table 4.3. VSA Evaluation Criteria for CO_2 Separation from Landfill Gas[a]

Adsorbents	$^{b}N_1^{ads}$	$^{b}\Delta N_1$	*R*	α_{12}^{ads}	*S*	*Ref*
BILP-6	1.89	1.50	79.2	5.0	23.5	*This work*
BILP-6-NH_2	2.63	2.14	81.3	8.4	76.0	*This work*
BILP-10	1.70	1.44	84.3	7.6	59.3	*39*
BILP-12	2.01	1.71	85.3	6.0	33.7	*39*
NPOF-1-NH_2	2.53	2.10	82.9	9.9	91.0	*51*
ALP-1	2.04	1.73	85.1	5.8	35.1	*91*
ALP-5	2.07	1.67	80.9	8.3	75.0	*91*
TBILP-2	2.20	1.84	83.7	7.6	62.5	*89*
SNU-Cl-sca	1.99	1.60	80.4	7.5	38	*135*
Dimide-POP	1.39	1.05	76.0	5.8	16	*54*
ZIF-82	1.42	1.20	84.9	5.6	20.5	*54*
HKUST-1	2.81	1.90	67.5	5.5	19.8	*54*

[a]CO_2:CH_4= 50:50, T= 298K, P^{ads}= 1 bar, and P^{des} = 0.1 bar. [b] In mol kg^{-1}.

BILP-6 and it is higher than all other sorbents listed in **Table 4.2**. The combination of higher CO_2/CH_4 selectivity (α_{12}^{ads}) for BILP-6-NH_2 in addition to higher working capacity translates into more than 3 fold enhancement in *S* factor compared to BILP-6. It is worth nothing that NPOF-1-NH_2 has higher selectivity of CO_2/CH_4 compared to BILP-6-NH_2 and therefore presents higher *S* value despite the higher working capacity of the latter.

4.4 Conclusions

We have successfully synthesized a high surface area bifunctionalized (benzimidazole and amine) BILP. DFT calculations revealed that BILP-6-NH_2 shows

المنارة للاستشارات
www.manaraa.com

different interaction modes with CO_2 compared to its counterpart BILP-6. Amine groups provide co-adsorption sites and hence facilitate CO_2-CO_2 interactions. Enhanced CO_2 uptake in BILP-6-NH_2 was also shown with experimental isotherms. The high CO_2 uptake and selectivity in BILP-6-NH_2 give rise to a very promising working capacity and sorbent selection parameter for landfill gas purification from CO_2 under VSA settings. Overall, this work demonstrates the effect of functionalized nanoporous organic polymers design on CO_2 separation from methane-rich gases.

المنارة للاستشارات
www.manaraa.com

Chapter 5

Concluding Remarks

The research presented in this dissertation entails the design and synthesis of nanoporous organic polymers and their postsynthetic modification for gas separation applications. Novel heteroatom free porous organic polymers (POPs) were synthesized then functionalized with nitro and amine groups to investigate the effect of nitro and amine functionality on selective carbon dioxide capture. In addition, a novel amine functionalized Benzimidazole-Linked Polymer (BILP) was designed and the synergetic effect of the functional groups on CO_2 uptake was studied. The important aspects of this dissertation are summarized below.

First, we have target the synthesis of a novel POP using metal free synthesis approach. To do that we have synthesized a novel building block, 1,3,5,7-tetrakis(4-acetylphenyl)adamantane and acid catalyzed cyclotrimerization of that molecule in ethanol/xylenes yields a Nanoporous Organic Framework (NPOF-4) with a BET surface area of 1249 m^2 g^{-1}. High physicochemical stability of NPOF-4 allowed us to perform post-synthetic modification on NPOF-4 which afforded NPOF-4-NO_2 after nitration in sulfuric acid/nitric acid mixture and its subsequent reduction resulted in an amine-functionalized framework NPOF-4-NH_2. Surface modification resulted in a significant enhancement in CO_2 binding affinity: 32.5 and 30.1 kJ mol^{-1} and selective binding over nitrogen and methane: CO_2/N_2 (139) and CO_2/CH_4 (15) at 273 K. These results confirmed that surface functionality overweigh the high surface area with regards to high CO_2 uptake and binding affinity. Therefore, we concluded that having polar groups (-NO_2 and -NH_2)

المنارة للاستشارات
www.manaraa.com

on pore walls notably enhance the initial CO_2 uptake and overall selectivity. These results highlight the potential use of functionalized NPOFs in post-combustion CO_2 separation and in natural gas purification processes. The functionalized NPOFs are also capable of storing up to 1.15 wt% H_2 at 77 K and 1 bar with high isosteric hydrogen heats of adsorption (8.1 and 8.3 kJ mol^{-1}). The relatively high initial uptake of H_2 by functionalized NPOFs also indicates the significance of the physical and electronic nature of the pores in the design of future hydrogen storage sorbents.

Our first work showed that nitro and amine functionalities can significantly enhance the CO_2 selectivity of POPs; however, because of the drastic decrease in surface area upon functionalization, the effect of functionalization on final gas uptake was much less pronounced. As it was explained in Chapter 1, CO_2 uptake at relevant pressures and temperatures is also as important as selectivity. Therefore we developed controlled postsynthetic modification of NPOF-1 to achieve non-invasive modification. NPOF-1, first reported by our group in 2011, is a nanoporous organic framework constructed by nickel(0)-catalyzed Yamamoto coupling of 1,3,5-tris(4-bromophenyl)benzene shows a BET surface area of 2062 m^2 g^{-1}. Controlled nitration is proven to be a promising route to introduce nitro groups and to convert mesopores to micropores without compromising surface area. Reduction of the nitro groups yields aniline-like amine-functionalized NPOF-1-NH_2 that has a micropore volume of 0.48 cm^3 g^{-1}, which corresponds to 71% of the total pore volume and a Brunauer–Emmett–Teller surface area of 1535 m^2 g^{-1}. Adequate basicity of the amine functionalities leads to modest isosteric heats of adsorption for CO_2, which allow for high regenerability. The unique combination of high surface area, microporous structure, and amine-functionalized pore walls enables NPOF-1-NH_2 to have

المنارة للاستشارات
www.manaraa.com

remarkable CO_2 working capacity values for removal from landfill gas and flue gas. The performance of NPOF-1-NH_2 in CO_2 removal ranks among the best by porous organic materials.

Lastly, we have synthesized a novel amine functionalized BILP named BILP-6-NH_2 to investigate the synergetic CO_2 adsorption effect of amine and benzimidazole groups. We hypothesized that placing the amine groups adjacent to benzimidazole would increase CO_2 binding capabilities via facilitating a co-adsorption and/or providing an extra adsorption site. We have performed DFT calculations to gain insight into the intermolecular interactions between CO_2 and BILP-6-NH_2. DFT calculations reveal that the second CO_2 molecule interacts more strongly in the case of BILP-6-NH_2 because of the CO_2···HN (imidazole) interaction in addition to CO_2···CO_2 interactions which were absent in BILP-6. Enhanced CO_2 adsorption capacity as well as higher CO_2/CH_4 selectivity in BILP-6-NH_2 compared to BILP-6 was also confirmed experimentally from the collection of CO_2 isotherms showing that this material has a very promising working capacity and sorbent selection parameter for landfill gas separation under VSA settings.

المنارة للاستشارات
www.manaraa.com

List of References

1. Inventory of U.S. Greenhouse Gas: Emissions and Sinks. *U.S. Environmental Protection Agency* **2016**, (https://www3.epa.gov/climatechange/Downloads/ghgemissions/US-GHG-Inventory-2016-Main-Text.pdf), Accessed 3/19/2016.
2. Tollefson, J.; Monastersky, R., The global energy challenge: Awash with carbon. *Nature* **2012,** *491*, 654-655.
3. D'Alessandro, D. M.; Smit, B.; Long, J. R., Carbon Dioxide Capture: Prospects for New Materials. *Angew Chem Int Edit* **2010,** *49*, (35), 6058-6082.
4. de Coninck, H.; Benson, S. M., Carbon Dioxide Capture and Storage: Issues and Prospects. *Annu. Rev. Environ. Resour.* **2014,** *39*, (1), 243-270.
5. Landfill Gas Energy: A Guide to Developing and Implementing Greenhouse Gas Reduction Programs. *U.S. Environmental Protection Agency* **2012**, (https://www3.epa.gov/statelocalclimate/documents/pdf/landfill_methane_utilization.pdf), Accessed 3/17/2016.
6. Boot-Handford, M. E.; Abanades, J. C.; Anthony, E. J.; Blunt, M. J.; Brandani, S.; Mac Dowell, N.; Fernandez, J. R.; Ferrari, M.-C.; Gross, R.; Hallett, J. P.; Haszeldine, R. S.; Heptonstall, P.; Lyngfelt, A.; Makuch, Z.; Mangano, E.; Porter, R. T. J.; Pourkashanian, M.; Rochelle, G. T.; Shah, N.; Yao, J. G.; Fennell, P. S., Carbon capture and storage update. *Energ Environ Sci* **2014,** *7*, (1), 130-189.
7. Li, J.-R.; Ma, Y.; McCarthy, M. C.; Sculley, J.; Yu, J.; Jeong, H.-K.; Balbuena, P. B.; Zhou, H.-C., Carbon dioxide capture-related gas adsorption and separation in metal-organic frameworks. *Coord. Chem. Rev.* **2011,** *255*, (15-16), 1791-1823.
8. Sumida, K.; Rogow, D. L.; Mason, J. A.; McDonald, T. M.; Bloch, E. D.; Herm, Z. R.; Bae, T. H.; Long, J. R., Carbon Dioxide Capture in Metal-Organic Frameworks. *Chem. Rev.* **2012,** *112*, (2), 724-781.
9. Rochelle, G. T., Amine Scrubbing for CO2 Capture. *Science* **2009,** *325*, (5948), 1652-1654.
10. Lu, A.-H.; Hao, G.-P., Porous materials for carbon dioxide capture. *Annu. Rep. Prog. Chem., Sect. A: Inorg. Chem.* **2013,** *109*, (0), 484-503.
11. Mason, J. A.; Sumida, K.; Herm, Z. R.; Krishna, R.; Long, J. R., Evaluating metal-organic frameworks for post-combustion carbon dioxide capture via temperature swing adsorption. *Energ Environ Sci* **2011,** *4*, (8), 3030-3040.
12. Li, J. R.; Ma, Y. G.; McCarthy, M. C.; Sculley, J.; Yu, J. M.; Jeong, H. K.; Balbuena, P. B.; Zhou, H. C., Carbon dioxide capture-related gas adsorption and separation in metal-organic frameworks. *Coord. Chem. Rev.* **2011,** *255*, (15-16), 1791-1823.
13. Zhou, H. C.; Long, J. R.; Yaghi, O. M., Introduction to Metal-Organic Frameworks. *Chem. Rev.* **2012,** *112*, (2), 673-674.
14. Li, J.-R.; Kuppler, R. J.; Zhou, H.-C., Selective gas adsorption and separation in metal-organic frameworks. *Chem. Soc. Rev.* **2009,** *38*, (5), 1477-1504.

المنارة للاستشارات
www.manaraa.com

15. Liu, J.; Chen, L.; Cui, H.; Zhang, J.; Zhang, L.; Su, C.-Y., Applications of metal-organic frameworks in heterogeneous supramolecular catalysis. *Chem. Soc. Rev.* **2014,** *43*, (16), 6011-6061.
16. Zhao, M.; Ou, S.; Wu, C.-D., Porous Metal–Organic Frameworks for Heterogeneous Biomimetic Catalysis. *Acc. Chem. Res.* **2014,** *47*, (4), 1199-1207.
17. Lee, J.; Farha, O. K.; Roberts, J.; Scheidt, K. A.; Nguyen, S. T.; Hupp, J. T., Metal-organic framework materials as catalysts. *Chem. Soc. Rev.* **2009,** *38*, (5), 1450-1459.
18. Kreno, L. E.; Leong, K.; Farha, O. K.; Allendorf, M.; Van Duyne, R. P.; Hupp, J. T., Metal–Organic Framework Materials as Chemical Sensors. *Chem. Rev.* **2012,** *112*, (2), 1105-1125.
19. Howarth, A. J.; Liu, Y.; Li, P.; Li, Z.; Wang, T. C.; Hupp, J. T.; Farha, O. K., Chemical, thermal and mechanical stabilities of metal–organic frameworks. *Nature Reviews Materials* **2016,** *1*, 15018.
20. Wu, D.; Xu, F.; Sun, B.; Fu, R.; He, H.; Matyjaszewski, K., Design and Preparation of Porous Polymers. *Chem. Rev.* **2012,** *112*, (7), 3959-4015.
21. Islamoglu, T.; Rabbani, M. G.; El-Kaderi, H. M., Impact of post-synthesis modification of nanoporous organic frameworks on small gas uptake and selective CO2 capture. *J. Mater. Chem. A* **2013,** *1*, (35), 10259-10266.
22. Jiang, J.; Zhao, Y.; Yaghi, O. M., Covalent Chemistry beyond Molecules. *J. Am. Chem. Soc.* **2016,** *138*, (10), 3255-3265.
23. Dawson, R.; Cooper, A. I.; Adams, D. J., Chemical functionalization strategies for carbon dioxide capture in microporous organic polymers. *Polym. Int.* **2013,** *62*, (3), 345-352.
24. Li, J. R.; Kuppler, R. J.; Zhou, H. C., Selective gas adsorption and separation in metal-organic frameworks. *Chem. Soc. Rev.* **2009,** *38*, (5), 1477-1504.
25. Rouquerol, J.; Avnir, D.; Fairbridge, C. W.; Everett, D. H.; Haynes, J. M.; Pernicone, N.; Ramsay, J. D. F.; Sing, K. S. W.; Unger, K. K., Recommendations for the characterization of porous solids (Technical Report). In *Pure Appl. Chem.*, 1994; Vol. 66, p 1739.
26. Dawson, R.; Cooper, A. I.; Adams, D. J., Nanoporous organic polymer networks. *Prog. Polym. Sci.* **2012,** *37*, (4), 530-563.
27. Trewin, A.; Cooper, A. I., Porous Organic Polymers: Distinction from Disorder? *Angew. Chem. Int. Ed.* **2010,** *49*, (9), 1533-1535.
28. Ben, T.; Ren, H.; Ma, S.; Cao, D.; Lan, J.; Jing, X.; Wang, W.; Xu, J.; Deng, F.; Simmons, J. M.; Qiu, S.; Zhu, G., Targeted synthesis of a porous aromatic framework with high stability and exceptionally high surface area. *Angew Chem Int Ed Engl* **2009,** *48*, (50), 9457-60.
29. Xu, Y.; Jin, S.; Xu, H.; Nagai, A.; Jiang, D., Conjugated microporous polymers: design, synthesis and application. *Chem. Soc. Rev.* **2013,** *42*, (20), 8012-31.
30. Rabbani, M. G.; El-Kaderi, H. M., Synthesis and Characterization of Porous Benzimidazole-Linked Polymers and Their Performance in Small Gas Storage and Selective Uptake. *Chem. Mater.* **2012,** *24*, (8), 1511-1517.

المنارة للاستشارات
www.manaraa.com

31. Rabbani, M. G.; Sekizkardes, A. K.; Kahveci, Z.; Reich, T. E.; Ding, R. S.; El-Kaderi, H. M., A 2D Mesoporous Imine-Linked Covalent Organic Framework for High Pressure Gas Storage Applications. *Chem-Eur J* **2013,** *19*, (10), 3324-3328.
32. Arab, P.; Rabbani, M. G.; Sekizkardes, A. K.; Islamoglu, T.; El-Kaderi, H. M., Copper(I)-Catalyzed Synthesis of Nanoporous Azo-Linked Polymers: Impact of Textural Properties on Gas Storage and Selective Carbon Dioxide Capture. *Chem. Mater.* **2014,** *26*, (3), 1385-1392.
33. Kuhn, P.; Antonietti, M.; Thomas, A., Porous, Covalent Triazine-Based Frameworks Prepared by Ionothermal Synthesis. *Angew. Chem. Int. Ed.* **2008,** *47*, (18), 3450-3453.
34. Rose, M.; Klein, N.; Senkovska, I.; Schrage, C.; Wollmann, P.; Bohlmann, W.; Bohringer, B.; Fichtner, S.; Kaskel, S., A new route to porous monolithic organic frameworks via cyclotrimerization. *J. Mater. Chem.* **2011,** *21*, (3), 711-716.
35. Yuan, D. Q.; Lu, W. G.; Zhao, D.; Zhou, H. C., Highly Stable Porous Polymer Networks with Exceptionally High Gas-Uptake Capacities. *Adv. Mater.* **2011,** *23*, (32), 3723-+.
36. Lu, W. G.; Yuan, D. Q.; Zhao, D.; Schilling, C. I.; Plietzsch, O.; Muller, T.; Brase, S.; Guenther, J.; Blumel, J.; Krishna, R.; Li, Z.; Zhou, H. C., Porous Polymer Networks: Synthesis, Porosity, and Applications in Gas Storage/Separation. *Chem. Mater.* **2010,** *22*, (21), 5964-5972.
37. Wilmer, C. E.; Farha, O. K.; Bae, Y. S.; Hupp, J. T.; Snurr, R. Q., Structure-property relationships of porous materials for carbon dioxide separation and capture. *Energ Environ Sci* **2012,** *5*, (12), 9849-9856.
38. Xiang, Z.; Mercado, R.; Huck, J. M.; Wang, H.; Guo, Z.; Wang, W.; Cao, D.; Haranczyk, M.; Smit, B., Systematic Tuning and Multifunctionalization of Covalent Organic Polymers for Enhanced Carbon Capture. *J. Am. Chem. Soc.* **2015,** *137*, (41), 13301-13307.
39. Sekizkardes, A. K.; Islamoglu, T.; Kahveci, Z.; El-Kaderi, H. M., Application of pyrene-derived benzimidazole-linked polymers to CO2 separation under pressure and vacuum swing adsorption settings. *J. Mater. Chem. A* **2014,** *2*, (31), 12492-12500.
40. Rabbani, M. G.; El-Kaderi, H. M., Template-Free Synthesis of a Highly Porous Benzimidazole-Linked Polymer for CO2 Capture and H-2 Storage. *Chem. Mater.* **2011,** *23*, (7), 1650-1653.
41. Jackson, K. T.; Rabbani, M. G.; Reich, T. E.; El-Kaderi, H. M., Synthesis of highly porous borazine-linked polymers and their application to H-2, CO2, and CH4 storage. *Polym Chem-Uk* **2011,** *2*, (12), 2775-2777.
42. Budd, P. M.; Ghanem, B. S.; Makhseed, S.; McKeown, N. B.; Msayib, K. J.; Tattershall, C. E., Polymers of intrinsic microporosity (PIMs): robust, solution-processable, organic nanoporous materials. *Chem. Commun.* **2004**, (2), 230-231.
43. Dawson, R.; Laybourn, A.; Clowes, R.; Khimyak, Y. Z.; Adams, D. J.; Cooper, A. I., Functionalized Conjugated Microporous Polymers. *Macromolecules* **2009,** *42*, (22), 8809-8816.
44. Patel, H. A.; Karadas, F.; Canlier, A.; Park, J.; Deniz, E.; Jung, Y.; Atilhan, M.; Yavuz, C. T., High capacity carbon dioxide adsorption by inexpensive covalent organic polymers. *J. Mater. Chem.* **2012,** *22*, (17), 8431-8437.

المنارة للاستشارات
www.manaraa.com

45. Pandey, P.; Katsoulidis, A. P.; Eryazici, I.; Wu, Y.; Kanatzidis, M. G.; Nguyen, S. T., Imine-Linked Microporous Polymer Organic Frameworks. *Chem. Mater.* **2010,** *22*, (17), 4974-4979.
46. Shen, C. J.; Bao, Y. J.; Wang, Z. G., Tetraphenyladamantane-based microporous polyimide for adsorption of carbon dioxide, hydrogen, organic and water vapors. *Chem. Commun.* **2013,** *49*, (32), 3321-3323.
47. Lu, W. G.; Yuan, D. Q.; Sculley, J. L.; Zhao, D.; Krishna, R.; Zhou, H. C., Sulfonate-Grafted Porous Polymer Networks for Preferential CO2 Adsorption at Low Pressure. *J. Am. Chem. Soc.* **2011,** *133*, (45), 18126-18129.
48. Ratvijitvech, T.; Dawson, R.; Laybourn, A.; Khimyak, Y. Z.; Adams, D. J.; Cooper, A. I., Post-synthetic modification of conjugated microporous polymers. *Polymer* **2014,** *55*, (1), 321-325.
49. Wang, Z.; Cohen, S. M., Postsynthetic modification of metal-organic frameworks. *Chem. Soc. Rev.* **2009,** *38*, (5), 1315-1329.
50. Lu, W. G.; Sculley, J. P.; Yuan, D. Q.; Krishna, R.; Wei, Z. W.; Zhou, H. C., Polyamine-Tethered Porous Polymer Networks for Carbon Dioxide Capture from Flue Gas. *Angew Chem Int Edit* **2012,** *51*, (30), 7480-7484.
51. Islamoglu, T.; Kim, T.; Kahveci, Z.; El-Kadri, O. M.; El-Kaderi, H. M., Systematic Postsynthetic Modification of Nanoporous Organic Frameworks for Enhanced CO2 Capture from Flue Gas and Landfill Gas. *J. Phys. Chem. C* **2016,** *120*, (5), 2592-2599.
52. Guillerm, V.; Weselinski, L. J.; Alkordi, M.; Mohideen, M. I. H.; Belmabkhout, Y.; Cairns, A. J.; Eddaoudi, M., Porous organic polymers with anchored aldehydes: a new platform for post-synthetic amine functionalization en route for enhanced CO2 adsorption properties. *Chem. Commun.* **2014,** *50*, (16), 1937-1940.
53. Garibay, S. J.; Weston, M. H.; Mondloch, J. E.; Colon, Y. J.; Farha, O. K.; Hupp, J. T.; Nguyen, S. T., Accessing functionalized porous aromatic frameworks (PAFs) through a de novo approach. *CrystEngComm* **2013,** *15*, (8), 1515-1519.
54. Bae, Y. S.; Snurr, R. Q., Development and Evaluation of Porous Materials for Carbon Dioxide Separation and Capture. *Angew Chem Int Edit* **2011,** *50*, (49), 11586-11596.
55. Dawson, R.; Stoeckel, E.; Holst, J. R.; Adams, D. J.; Cooper, A. I., Microporous organic polymers for carbon dioxide capture. *Energ Environ Sci* **2011,** *4*, (10), 4239-4245.
56. Drage, T. C.; Snape, C. E.; Stevens, L. A.; Wood, J.; Wang, J.; Cooper, A. I.; Dawson, R.; Guo, X.; Satterley, C.; Irons, R., Materials challenges for the development of solid sorbents for post-combustion carbon capture. *J. Mater. Chem.* **2012,** *22*, (7), 2815-2823.
57. Jiang, J.-X.; Trewin, A.; Adams, D. J.; Cooper, A. I., Band gap engineering in fluorescent conjugated microporous polymers. *Chem Sci* **2011,** *2*, (9), 1777-1781.
58. Kaur, P.; Hupp, J. T.; Nguyen, S. T., Porous Organic Polymers in Catalysis: Opportunities and Challenges. *Acs Catal* **2011,** *1*, (7), 819-835.
59. Liu, X.; Xu, Y.; Jiang, D., Conjugated Microporous Polymers as Molecular Sensing Devices: Microporous Architecture Enables Rapid Response and Enhances Sensitivity in Fluorescence-On and Fluorescence-Off Sensing. *J. Am. Chem. Soc.* **2012,** *134*, (21), 8738-8741.

المنارة للاستشارات
www.manaraa.com

60. Rakow, N. A.; Wendland, M. S.; Trend, J. E.; Poirier, R. J.; Paolucci, D. M.; Maki, S. P.; Lyons, C. S.; Swierczek, M. J., Visual Indicator for Trace Organic Volatiles. *Langmuir* **2010,** *26*, (6), 3767-3770.
61. Zhang, Y.; Riduan, S. N., Functional porous organic polymers for heterogeneous catalysis. *Chem. Soc. Rev.* **2012,** *41*, (6), 2083-2094.
62. Ma, H.; Ren, H.; Zou, X.; Sun, F.; Yan, Z.; Cai, K.; Wang, D.; Zhu, G., Novel lithium-loaded porous aromatic framework for efficient CO2 and H-2 uptake. *J. Mater. Chem. A* **2013,** *1*, (3), 752-758.
63. Patel, H. A.; Yavuz, C. T., Noninvasive functionalization of polymers of intrinsic microporosity for enhanced CO2 capture. *Chem. Commun.* **2012,** *48*, (80), 9989-9991.
64. McDonald, T. M.; Lee, W. R.; Mason, J. A.; Wiers, B. M.; Hong, C. S.; Long, J. R., Capture of Carbon Dioxide from Air and Flue Gas in the Alkylamine-Appended Metal-Organic Framework mmen-Mg-2(dobpdc). *J. Am. Chem. Soc.* **2012,** *134*, (16), 7056-7065.
65. Tollefson, J.; Monastersky, R., AWASH IN CARBON. *Nature* **2012,** *491*, (7426), 654-655.
66. Reichert, V. R.; Mathias, L. J., Expanded Tetrahedral Molecules From 1,3,5,7-Tetraphenyladamantane. *Macromolecules* **1994,** *27*, (24), 7015-7023.
67. Bernt, S.; Guillerm, V.; Serre, C.; Stock, N., Direct covalent post-synthetic chemical modification of Cr-MIL-101 using nitrating acid. *Chem. Commun.* **2011,** *47*, (10), 2838-2840.
68. Dawson, R.; Adams, D. J.; Cooper, A. I., Chemical tuning of CO2 sorption in robust nanoporous organic polymers. *Chem Sci* **2011,** *2*, (6), 1173-1177.
69. Wood, C. D.; Tan, B.; Trewin, A.; Niu, H.; Bradshaw, D.; Rosseinsky, M. J.; Khimyak, Y. Z.; Campbell, N. L.; Kirk, R.; Stoeckel, E.; Cooper, A. I., Hydrogen storage in microporous hypercrosslinked organic polymer networks. *Chem. Mater.* **2007,** *19*, (8), 2034-2048.
70. Makal, T. A.; Li, J.-R.; Lu, W.; Zhou, H.-C., Methane storage in advanced porous materials. *Chem. Soc. Rev.* **2012,** *41*, (23), 7761-7779.
71. Rabbani, M. G.; Sekizkardes, A. K.; El-Kadri, O. M.; Kaafarani, B. R.; El-Kaderi, H. M., Pyrene-directed growth of nanoporous benzimidazole-linked nanofibers and their application to selective CO2 capture and separation. *J. Mater. Chem.* **2012,** *22*, (48), 25409-25417.
72. Mohanty, P.; Kull, L. D.; Landskron, K., Porous covalent electron-rich organonitridic frameworks as highly selective sorbents for methane and carbon dioxide. *Nat Commun* **2011,** *2*, 401.
73. Phan, A.; Doonan, C. J.; Uribe-Romo, F. J.; Knobler, C. B.; O'Keeffe, M.; Yaghi, O. M., Synthesis, Structure, and Carbon Dioxide Capture Properties of Zeolitic Imidazolate Frameworks. *Acc. Chem. Res.* **2010,** *43*, (1), 58-67.
74. Banerjee, R.; Furukawa, H.; Britt, D.; Knobler, C.; O'Keeffe, M.; Yaghi, O. M., Control of Pore Size and Functionality in Isoreticular Zeolitic Imidazolate Frameworks and their Carbon Dioxide Selective Capture Properties. *J. Am. Chem. Soc.* **2009,** *131*, (11), 3875-+.

المنارة للاستشارات
www.manaraa.com

75. An, J.; Geib, S. J.; Rosi, N. L., High and Selective CO2 Uptake in a Cobalt Adeninate Metal-Organic Framework Exhibiting Pyrimidine- and Amino-Decorated Pores. *J. Am. Chem. Soc.* **2010,** *132*, (1), 38-+.
76. Lewinski, J.; Kaczorowski, T.; Prochowicz, D.; Lipinska, T.; Justyniak, I.; Kaszkur, Z.; Lipkowski, J., Cinchona Alkaloid-Metal Complexes: Noncovalent Porous Materials with Unique Gas Separation Properties. *Angew Chem Int Edit* **2010,** *49*, (39), 7035-7039.
77. Farha, O. K.; Bae, Y.-S.; Hauser, B. G.; Spokoyny, A. M.; Snurr, R. Q.; Mirkin, C. A.; Hupp, J. T., Chemical reduction of a diimide based porous polymer for selective uptake of carbon dioxide versus methane. *Chem. Commun.* **2010,** *46*, (7), 1056-1058.
78. Farha, O. K.; Spokoyny, A. M.; Hauser, B. G.; Bae, Y.-S.; Brown, S. E.; Snurr, R. Q.; Mirkin, C. A.; Hupp, J. T., Synthesis, Properties, and Gas Separation Studies of a Robust Diimide-Based Microporous Organic Polymer. *Chem. Mater.* **2009,** *21*, (14), 3033-3035.
79. Li, J. R.; Sculley, J.; Zhou, H. C., Metal-Organic Frameworks for Separations. *Chem. Rev.* **2012,** *112*, (2), 869-932.
80. Myers, A. L.; Prausnitz, J. M., Thermodynamics of mixed-gas adsorption. *AIChE J.* **1965,** *11*, (1), 121-127.
81. Reich, T. E.; Behera, S.; Jackson, K. T.; Jena, P.; El-Kaderi, H. M., Highly selective CO2/CH4 gas uptake by a halogen-decorated borazine-linked polymer. *J. Mater. Chem.* **2012,** *22*, (27), 13524-13528.
82. Yang, R. T., *Adsorbents: fundamentals and applications*. John Wiley & Sons: 2003.
83. Dawson, R.; Stevens, L. A.; Drage, T. C.; Snape, C. E.; Smith, M. W.; Adams, D. J.; Cooper, A. I., Impact of water coadsorption for carbon dioxide capture in microporous polymer sorbents. *J. Am. Chem. Soc.* **2012,** *134*, (26), 10741-4.
84. Pachfule, P.; Chen, Y.; Jiang, J.; Banerjee, R., Fluorinated Metal-Organic Frameworks: Advantageous for Higher H-2 and CO2 Adsorption or Not? *Chem-Eur J* **2012,** *18*, (2), 688-694.
85. Colombo, V.; Montoro, C.; Maspero, A.; Palmisano, G.; Masciocchi, N.; Galli, S.; Barea, E.; Navarro, J. A. R., Tuning the Adsorption Properties of Isoreticular Pyrazolate-Based Metal-Organic Frameworks through Ligand Modification. *J. Am. Chem. Soc.* **2012,** *134*, (30), 12830-12843.
86. Slater, A. G.; Cooper, A. I., Function-led design of new porous materials. *Science* **2015,** *348*, (6238).
87. Woodward, R. T.; Stevens, L. A.; Dawson, R.; Vijayaraghavan, M.; Hasell, T.; Silverwood, I. P.; Ewing, A. V.; Ratvijitvech, T.; Exley, J. D.; Chong, S. Y.; Blanc, F.; Adams, D. J.; Kazarian, S. G.; Snape, C. E.; Drage, T. C.; Cooper, A. I., Swellable, water- and acid-tolerant polymer sponges for chemoselective carbon dioxide capture. *J. Am. Chem. Soc.* **2014,** *136*, (25), 9028-35.
88. Holst, J. R.; Stöckel, E.; Adams, D. J.; Cooper, A. I., High Surface Area Networks from Tetrahedral Monomers: Metal-Catalyzed Coupling, Thermal Polymerization, and "Click" Chemistry. *Macromolecules* **2010,** *43*, (20), 8531-8538.

المنارة للاستشارات
www.manaraa.com

89. Sekizkardes, A. K.; Altarawneh, S.; Kahveci, Z.; Islamoglu, T.; El-Kaderi, H. M., Highly Selective CO2 Capture by Triazine-Based Benzimidazole-Linked Polymers. *Macromolecules* **2014,** *47*, (23), 8328-8334.
90. Shen, C.; Wang, Z., Tetraphenyladamantane-Based Microporous Polyimide and Its Nitro-Functionalization for Highly Efficient CO2 Capture. *J. Phys. Chem. C* **2014,** *118*, (31), 17585-17593.
91. Arab, P.; Parrish, E.; Islamoglu, T.; El-Kaderi, H. M., Synthesis and evaluation of porous azo-linked polymers for carbon dioxide capture and separation. *J. Mater. Chem. A* **2015,** *3*, (41), 20586-20594.
92. Patel, H. A.; Je, S. H.; Park, J.; Jung, Y.; Coskun, A.; Yavuz, C. T., Directing the Structural Features of N-2-Phobic Nanoporous Covalent Organic Polymers for CO2 Capture and Separation. *Chem-Eur J* **2014,** *20*, (3), 772-780.
93. Popp, N.; Homburg, T.; Stock, N.; Senker, J., Porous imine-based networks with protonated imine linkages for carbon dioxide separation from mixtures with nitrogen and methane. *J. Mater. Chem. A* **2015,** *3*, (36), 18492-18504.
94. Merino, E.; Verde-Sesto, E.; Maya, E. M.; Iglesias, M.; Sanchez, F.; Corma, A., Synthesis of Structured Porous Polymers with Acid and Basic Sites and Their Catalytic Application in Cascade-Type Reactions. *Chem. Mater.* **2013,** *25*, (6), 981-988.
95. Tanabe, K. K.; Cohen, S. M., Postsynthetic modification of metal-organic frameworks-a progress report. *Chem. Soc. Rev.* **2011,** *40*, (2), 498-519.
96. Shen, C. J.; Wang, Z. G., Tetraphenyladamantane-Based Microporous Polyimide and Its Nitro-Functionalization for Highly Efficient CO2 Capture. *J. Phys. Chem. C* **2014,** *118*, (31), 17585-17593.
97. Kassab, R. M.; Jackson, K. T.; El-Kadri, O. M.; El-Kaderi, H. M., Nickel-catalyzed synthesis of nanoporous organic frameworks and their potential use in gas storage applications. *Res. Chem. Intermed.* **2011,** *37*, (7), 747-757.
98. Jiang, J.-X.; Trewin, A.; Su, F.; Wood, C. D.; Niu, H.; Jones, J. T. A.; Khimyak, Y. Z.; Cooper, A. I., Microporous Poly(tri(4-ethynylphenyl)amine) Networks: Synthesis, Properties, and Atomistic Simulation. *Macromolecules* **2009,** *42*, (7), 2658-2666.
99. Liu, Y.; Wu, S.; Wang, G.; Yu, G.; Guan, J.; Pan, C.; Wang, Z., Control of porosity of novel carbazole-modified polytriazine frameworks for highly selective separation of CO2-N-2. *J. Mater. Chem. A* **2014,** *2*, (21), 7795-7801.
100. Lozano-Castello, D.; Cazorla-Amoros, D.; Linares-Solano, A., Usefulness of CO2 adsorption at 273 K for the characterization of porous carbons. *Carbon* **2004,** *42*, (7), 1233-1242.
101. Buyukcakir, O.; Seo, Y.; Coskun, A., Thinking Outside the Cage: Controlling the Extrinsic Porosity and Gas Uptake Properties of Shape-Persistent Molecular Cages in Nanoporous Polymers. *Chem. Mater.* **2015,** *27*, (11), 4149-4155.
102. Dawson, R.; Stöckel, E.; Holst, J. R.; Adams, D. J.; Cooper, A. I., Microporous organic polymers for carbon dioxide capture. *Energ Environ Sci* **2011,** *4*, (10), 4239.

المنارة للاستشارات
www.manaraa.com

103. Altarawneh, S.; Islamoglu, T.; Sekizkardes, A. K.; El-Kaderi, H. M., Effect of acid-catalyzed formation rates of benzimidazole-linked polymers on porosity and selective CO2 capture from gas mixtures. *Environ. Sci. Technol.* **2015,** *49*, (7), 4715-23.
104. Fu, X.; Zhang, Y.; Gu, S.; Zhu, Y.; Yu, G.; Pan, C.; Wang, Z.; Hu, Y., Metal Microporous Aromatic Polymers with Improved Performance for Small Gas Storage. *Chem-Eur J* **2015,** *21*, (38), 13357-13363.
105. Arab, P.; Verlander, A.; El-Kaderi, H. M., Synthesis of a Highly Porous Bis(imino)pyridine-Linked Polymer and Its Postsynthetic Modification with Inorganic Fluorinated Ions for Selective CO2 Capture. *J. Phys. Chem. C* **2015,** *119*, (15), 8174-8182.
106. Lu, W.; Sculley, J. P.; Yuan, D.; Krishna, R.; Wei, Z.; Zhou, H.-C., Polyamine-Tethered Porous Polymer Networks for Carbon Dioxide Capture from Flue Gas. *Angew Chem Int Edit* **2012,** *51*, (30), 7480-7484.
107. Sung, S.; Suh, M. P., Highly efficient carbon dioxide capture with a porous organic polymer impregnated with polyethylenimine. *J. Mater. Chem. A* **2014,** *2*, (33), 13245-13249.
108. Wang, X.; Zhao, Y.; Wei, L.; Zhang, C.; Jiang, J.-X., Nitrogen-rich conjugated microporous polymers: impact of building blocks on porosity and gas adsorption. *J. Mater. Chem. A* **2015,** *3*, (42), 21185-21193.
109. Satilmis, B.; Alnajrani, M. N.; Budd, P. M., Hydroxyalkylaminoalkylamide PIMs: Selective Adsorption by Ethanolamine- and Diethanolamine-Modified PIM-1. *Macromolecules* **2015,** *48*, (16), 5663-5669.
110. McDonald, T. M.; D'Alessandro, D. M.; Krishna, R.; Long, J. R., Enhanced carbon dioxide capture upon incorporation of N,N '-dimethylethylenediamine in the metal-organic framework CuBTTri. *Chem Sci* **2011,** *2*, (10), 2022-2028.
111. Li, T.; Chen, D.-L.; Sullivan, J. E.; Kozlowski, M. T.; Johnson, J. K.; Rosi, N. L., Systematic modulation and enhancement of CO2 : N-2 selectivity and water stability in an isoreticular series of bio-MOF-11 analogues. *Chem Sci* **2013,** *4*, (4), 1746-1755.
112. Cavenati, S.; Grande, C. A.; Rodrigues, A. E., Removal of carbon dioxide from natural gas by vacuum pressure swing adsorption. *Energy Fuels* **2006,** *20*, (6), 2648-2659.
113. Leveraging Natural Gas to Reduce Greenhouse Gas Emissions. *Center for Climate and Energy Solutions* **2013**, (http://www.c2es.org/publications/leveraging-natural-gas-reduce-greenhouse-gas-emissions), Accessed 3/19/2016.
114. He, Y.; Zhou, W.; Qian, G.; Chen, B., Methane storage in metal-organic frameworks. *Chem. Soc. Rev.* **2014,** *43*, (16), 5657-5678.
115. Available And Emerging Technologies for Reducing Greenhouse Gas Emissions from Municipal Solid Waste Landfills. *U.S. Environmental Protection Agency* **2011**, (https://www.epa.gov/sites/production/files/2015-12/documents/landfills.pdf), Accessed 03/19/2016.
116. Xu, C.; Hedin, N., Microporous adsorbents for CO2 capture – a case for microporous polymers? *Mater. Today* **2014,** *17*, (8), 397-403.

المنارة للاستشارات
www.manaraa.com

117. Nugent, P.; Belmabkhout, Y.; Burd, S. D.; Cairns, A. J.; Luebke, R.; Forrest, K.; Pham, T.; Ma, S.; Space, B.; Wojtas, L.; Eddaoudi, M.; Zaworotko, M. J., Porous materials with optimal adsorption thermodynamics and kinetics for CO2 separation. *Nature* **2013,** *495*, (7439), 80-84.
118. Wu, S.; Liu, Y.; Yu, G.; Guan, J.; Pan, C.; Du, Y.; Xiong, X.; Wang, Z., Facile Preparation of Dibenzoheterocycle-Functional Nanoporous Polymeric Networks with High Gas Uptake Capacities. *Macromolecules* **2014,** *47*, (9), 2875-2882.
119. Bojdys, M. J.; Jeromenok, J.; Thomas, A.; Antonietti, M., Rational Extension of the Family of Layered, Covalent, Triazine-Based Frameworks with Regular Porosity. *Adv. Mater.* **2010,** *22*, (19), 2202-2205.
120. Patel, H. A.; Je, S. H.; Park, J.; Chen, D. P.; Jung, Y.; Yavuz, C. T.; Coskun, A., Unprecedented high-temperature CO2 selectivity in N-2-phobic nanoporous covalent organic polymers. *Nat Commun* **2013,** *4*.
121. Lu, W.; Yuan, D.; Sculley, J.; Zhao, D.; Krishna, R.; Zhou, H.-C., Sulfonate-Grafted Porous Polymer Networks for Preferential CO2 Adsorption at Low Pressure. *J. Am. Chem. Soc.* **2011,** *133*, (45), 18126-18129.
122. Li, G. Y.; Wang, Z. G., Microporous Polyimides with Uniform Pores for Adsorption and Separation of CO2 Gas and Organic Vapors. *Macromolecules* **2013,** *46*, (8), 3058-3066.
123. Wang, J.; Senkovska, I.; Oschatz, M.; Lohe, M. R.; Borchardt, L.; Heerwig, A.; Liu, Q.; Kaskel, S., Imine-Linked Polymer-Derived Nitrogen-Doped Microporous Carbons with Excellent CO2 Capture Properties. *ACS Appl. Mater. Interfaces* **2013,** *5*, (8), 3160-3167.
124. Byun, J.; Je, S.-H.; Patel, H. A.; Coskun, A.; Yavuz, C. T., Nanoporous covalent organic polymers incorporating Troger's base functionalities for enhanced CO2 capture. *J. Mater. Chem. A* **2014,** *2*, (31), 12507-12512.
125. Modak, A.; Nandi, M.; Mondal, J.; Bhaumik, A., Porphyrin based porous organic polymers: novel synthetic strategy and exceptionally high CO2 adsorption capacity. *Chem. Commun.* **2012,** *48*, (2), 248-250.
126. Zhao, Y.-C.; Wang, T.; Zhang, L.-M.; Cui, Y.; Han, B.-H., Facile Approach to Preparing Microporous Organic Polymers through Benzoin Condensation. *ACS Appl. Mater. Interfaces* **2012,** *4*, (12), 6975-6981.
127. Preis, E.; Schindler, N.; Adrian, S.; Scherf, U., Microporous Polymer Networks Made by Cyclotrimerization of Commercial, Aromatic Diisocyanates. *ACS Macro Letters* **2015,** *4*, (11), 1268-1272.
128. Patel, H. A.; Ko, D.; Yavuz, C. T., Nanoporous Benzoxazole Networks by Silylated Monomers, Their Exceptional Thermal Stability, and Carbon Dioxide Capture Capacity. *Chem. Mater.* **2014,** *26*, (23), 6729-6733.
129. Jia, S.-H.; Ding, X.; Yu, H.-T.; Han, B.-H., Multi-hydroxyl-containing porous organic polymers based on phenol formaldehyde resin chemistry with high carbon dioxide capture capacity. *Rsc Adv* **2015,** *5*, (87), 71095-71101.

المنارة للاستشارات
www.manaraa.com

130. Li, H.; Meng, B.; Mahurin, S. M.; Chai, S.-H.; Nelson, K. M.; Baker, D. C.; Liu, H.; Dai, S., Carbohydrate based hyper-crosslinked organic polymers with -OH functional groups for CO2 separation. *J. Mater. Chem. A* **2015,** *3*, (42), 20913-20918.
131. Sekizkardes, A. K.; Culp, J. T.; Islamoglu, T.; Marti, A.; Hopkinson, D.; Myers, C.; El-Kaderi, H. M.; Nulwala, H. B., An ultra-microporous organic polymer for high performance carbon dioxide capture and separation. *Chem. Commun.* **2015,** *51*, (69), 13393-13396.
132. McDonald, T. M.; Mason, J. A.; Kong, X.; Bloch, E. D.; Gygi, D.; Dani, A.; Crocella, V.; Giordanino, F.; Odoh, S. O.; Drisdell, W. S.; Vlaisavljevich, B.; Dzubak, A. L.; Poloni, R.; Schnell, S. K.; Planas, N.; Lee, K.; Pascal, T.; Wan, L. F.; Prendergast, D.; Neaton, J. B.; Smit, B.; Kortright, J. B.; Gagliardi, L.; Bordiga, S.; Reimer, J. A.; Long, J. R., Cooperative insertion of CO2 in diamine-appended metal-organic frameworks. *Nature* **2015,** *519*, (7543), 303-8.
133. Zhu, X.; Mahurin, S. M.; An, S.-H.; Do-Thanh, C.-L.; Tian, C.; Li, Y.; Gill, L. W.; Hagaman, E. W.; Bian, Z.; Zhou, J.-H.; Hu, J.; Liu, H.; Dai, S., Efficient CO2 capture by a task-specific porous organic polymer bifunctionalized with carbazole and triazine groups. *Chem. Commun.* **2014,** *50*, (59), 7933-7936.
134. Jiang, X.; Liu, Y.; Liu, J.; Luo, Y.; Lyu, Y., Facile synthesis of porous organic polymers bifunctionalized with azo and porphyrin groups. *Rsc Adv* **2015,** *5*, (119), 98508-98513.
135. Xie, L.-H.; Suh, M. P., High CO2-Capture Ability of a Porous Organic Polymer Bifunctionalized with Carboxy and Triazole Groups. *Chem-Eur J* **2013,** *19*, (35), 11590-11597.
136. Muhammad, R.; Rekha, P.; Mohanty, P., Facile synthesis of a thermally stable imine and benzimidazole functionalized nanoporous polymer (IBFNP) for CO2 capture application. *Greenhouse Gases Sci. Technol.* **2016,** *6*, (1), 150-157.
137. Sainz-Díaz, I. C., A New Approach to the Synthesis of 2-Nitrobenzaldehyde. Reactivity and Molecular Structure Studies. *Monatshefte für Chemie / Chemical Monthly 133*, (1), 9-22.
138. Moth-Poulsen, K.; Patrone, L.; Stuhr-Hansen, N.; Christensen, J. B.; Bourgoin, J.-P.; Bjørnholm, T., Probing the Effects of Conjugation Path on the Electronic Transmission through Single Molecules Using Scanning Tunneling Microscopy. *Nano Lett.* **2005,** *5*, (4), 783-785.
139. Rabbani, M. G.; Reich, T. E.; Kassab, R. M.; Jackson, K. T.; El-Kaderi, H. M., High CO2 uptake and selectivity by triptycene-derived benzimidazole-linked polymers. *Chem. Commun.* **2012,** *48*, (8), 1141-1143.
140. Van Humbeck, J. F.; McDonald, T. M.; Jing, X. F.; Wiers, B. M.; Zhu, G. S.; Long, J. R., Ammonia Capture in Porous Organic Polymers Densely Functionalized with Bronsted Acid Groups. *J. Am. Chem. Soc.* **2014,** *136*, (6), 2432-2440.
141. Deria, P.; Chung, Y. G.; Snurr, R. Q.; Hupp, J. T.; Farha, O. K., Water stabilization of Zr6-based metal-organic frameworks via solvent-assisted ligand incorporation. *Chem Sci* **2015,** *6*, (9), 5172-5176.
142. Vosko, S. H.; Wilk, L.; Nusair, M., Accurate spin-dependent electron liquid correlation energies for local spin density calculations: a critical analysis. *Can. J. Phys.* **1980,** *58*, (8), 1200-1211.

المنارة للاستشارات
www.manaraa.com

143. Frisch, M. J.; Trucks, G. W.; Schlegel, H. B.; Scuseria, G. E.; Robb, M. A.; Cheeseman, J. R.; Scalmani, G.; Barone, V.; Mennucci, B.; Petersson, G. A.; Nakatsuji, H.; Caricato, M.; Li, X.; Hratchian, H. P.; Izmaylov, A. F.; Bloino, J.; Zheng, G.; Sonnenberg, J. L.; Hada, M.; Ehara, M.; Toyota, K.; Fukuda, R.; Hasegawa, J.; Ishida, M.; Nakajima, T.; Honda, Y.; Kitao, O.; Nakai, H.; Vreven, T.; Montgomery Jr., J. A.; Peralta, J. E.; Ogliaro, F.; Bearpark, M. J.; Heyd, J.; Brothers, E. N.; Kudin, K. N.; Staroverov, V. N.; Kobayashi, R.; Normand, J.; Raghavachari, K.; Rendell, A. P.; Burant, J. C.; Iyengar, S. S.; Tomasi, J.; Cossi, M.; Rega, N.; Millam, N. J.; Klene, M.; Knox, J. E.; Cross, J. B.; Bakken, V.; Adamo, C.; Jaramillo, J.; Gomperts, R.; Stratmann, R. E.; Yazyev, O.; Austin, A. J.; Cammi, R.; Pomelli, C.; Ochterski, J. W.; Martin, R. L.; Morokuma, K.; Zakrzewski, V. G.; Voth, G. A.; Salvador, P.; Dannenberg, J. J.; Dapprich, S.; Daniels, A. D.; Farkas, Ö.; Foresman, J. B.; Ortiz, J. V.; Cioslowski, J.; Fox, D. J. *Gaussian 09*, Gaussian, Inc.: Wallingford, CT, USA, 2009.

144. Krishnan, R.; Binkley, J. S.; Seeger, R.; Pople, J. A., Self-consistent molecular orbital methods. XX. A basis set for correlated wave functions. *J. Chem. Phys* **1980,** *72*, (1), 650-654.

145. Altarawneh, S.; Behera, S.; Jena, P.; El-Kaderi, H. M., New insights into carbon dioxide interactions with benzimidazole-linked polymers. *Chem. Commun.* **2014,** *50*, (27), 3571-3574.

146. Vogiatzis, K. D.; Mavrandonakis, A.; Klopper, W.; Froudakis, G. E., Ab initio Study of the Interactions between CO2 and N-Containing Organic Heterocycles. *ChemPhysChem* **2009,** *10*, (2), 374-383.

المنارة للاستشارات
www.manaraa.com

Vita

Timur İslamoğlu

Department of Chemistry

Virginia Commonwealth University

1001 W. Main St.

Richmond, VA 23284-2006

E-mail: islamoglut@vcu.edu

ACADEMIC PREPARATION

Northwestern University, Evanston, IL, USA Chemistry, Research Scholar, 2015-present

Virginia Commonwealth University, Richmond, VA, USA Chemistry Ph.D 2013-2016

Virginia Commonwealth University, Richmond, VA, USA Chemistry M.Sc, 2013

Master Thesis: Impact of post-synthesis modification of nanoporous organic frameworks on small gas uptake and selective CO_2 capture.

Advisor: Dr. Hani M. El-Kaderi

Dumlupinar University, Kutahya, Turkey Mathematics (Double Major) B.Sc., 2009

Dumlupinar University, Kutahya, Turkey Chemistry B.Sc., 2008

المنارة للاستشارات

www.manaraa.com

PUBLICATIONS

- **Publications in Peer Rewieved Journals**

1. **İslamoğlu, T;** Behera, S; Kahveci, Z.; Tessema, T.D.; Jena, P.; El-Kaderi, H. M., Enhanced Carbon Dioxide Capture from Landfill Gas using Bifunctinalized Benzimidazole-Linked Polymers **2016** (**under review**).

2. Demir, M.; Farghaly, A.; Nyankson, E.; Aksoy, B.; **İslamoğlu, T.;** Collinson, M.; El Kaderi,H.; Gupta, R., Lignin Biomass-derived N-doped Graphitic Carbon Electrode Material for Supercapacitors **2016** (**under review**).

3. **İslamoğlu, T.;** Kim, T.; Kahveci, Z.; El-Kadri, O. M.; El-Kaderi, H. M., Systematic Postsynthetic Modification of Nanoporous Organic Frameworks for Enhanced CO_2 Capture from Flue Gas and Landfill Gas. *J Phys Chem C* **2016**, *120*, 2592-2599.

4. Xu, Y.; Howarth, A.J.; **İslamoğlu, T.;** Silva, C.T.; Hupp, J.T.; Farha, O.K; Combining solvent-assisted linker exchange and transmetallation strategies to obtain a new non-catenated nickel (II) pillared-paddlewheel MOF. *Inorg. Chem. Commun.*, **2016,** 67, 60-63.

5. Altarawneh, S.; **İslamoğlu, T**.; Sekizkardes, A. K.; El-Kaderi, H. M., Effect of Acid-Catalyzed Formation Rates of Benzimidazole-Linked Polymers on Porosity and Selective CO2 Capture from Gas Mixtures. *Environ. Sci. Technol.*, **2015**, *49* (7), 4715–4723.

6. Arab, P.; Parrish, E.; **İslamoğlu, T**.; El-Kaderi, H. M., Synthesis and Evaluation of Porous Azo-Linked Polymers for Carbon Dioxide Capture and Separation, *J. Mater. Chem. A* **2015,** 3 (41), 20586-20594.

7. Sekizkardes, A. K.; Culp, J. T.; **İslamoğlu, T.;** Marti, A.; Hopkinson, D.; Myers, C.; El-Kaderi, H. M.; Nulwala, H. B., An Ultra-Microporous Organic Polymer for High

المنارة للاستشارات
www.manaraa.com

Performance Carbon Dioxide Capture and Separation. *Chem. Commun.* **2015**, *51*, 13393-13396.

8. Sekizkardes, A. K.; **İslamoğlu, T.**; Kahveci, Z.; El-Kaderi, H. M., Application of pyrene-derived benzimidazole-linked polymers to CO2 separation under pressure and vacuum swing adsorption settings. *J. Mater. Chem. A* **2014**, *2*, (31), 12492-12500.

9. Sekizkardes, A. K.; Altarawneh, S.; Kahveci, Z.; **İslamoğlu, T.**; El-Kaderi, H. M., Highly Selective CO2 Capture by Triazine-Based Benzimidazole-Linked Polymers. *Macromolecules* **2014**, *47*, (23), 8328-8334.

10. Arab, P.; Rabbani, M. G.; Sekizkardes, A. K.; **İslamoğlu, T**.; El-Kaderi, H. M., Copper(I)-Catalyzed Synthesis of Nanoporous Azo-Linked Polymers: Impact of Textural Properties on Gas Storage and Selective Carbon Dioxide Capture. *Chem. Mater.* **2014**, *26*, (3), 1385-1392. (**Highlighted as front cover and cover is designed by Timur İslamoğlu**)

11. **İslamoğlu, T**.; Rabbani, M. G.; El-Kaderi, H. M., Impact of post-synthesis modification of nanoporous organic frameworks on small gas uptake and selective CO2 capture. *J. Mater. Chem. A* **2013**, *1*, (35), 10259-10266.

12. Kahveci, Z.; **İslamoğlu, T**.; Shar, G. A.; Ding, R.; El-Kaderi, H. M., Targeted synthesis of a mesoporous triptycene-derived covalent organic framework. *CrystEngComm* **2013,** *15*, (8), 1524-1527.

- **Book Chapters**

1. Arab, P.; **İslamoğlu, T**.; El-Kadri, O.; El-Kaderi, H. M., "Porous Polymers" Materials for Carbon Capture, John Wiley & Sons, **2016,** (submitted)

المنارة للاستشارات
www.manaraa.com

SERVED AS REVIEWER

Journal Title	Impact Factor	Publisher
Chemical Society Reviews	33.383	Royal Society of Chemistry
Chemical Communications	6.834	Royal Society of Chemistry
ACS Applied Materials & Interfaces	6.723	American Chemical Society
Crystal Engineering and Communications	4.034	Royal Society of Chemistry
RSC Advances	3.840	Royal Society of Chemistry
Greenhouse Gases: Science and Technology	2.147	John Wiley & Sons

SELECTED PRESENTATIONS

- **İslamoğlu, T;** Behera, S; Kahveci, Z.; Jena, P.; El-Kaderi, H. M., "Landfill Gas Purification by Nanoporous Benzimidazole-Linked Polymers." Porous and Powder Materials Symposium and Exhibition, Cesme, Izmir, 15-18 September **2015**. (Oral)
- **İslamoğlu, T**.;Kim, T.; El-Kaderi H. M. "Post-synthesis modification of nanoporous organic frameworks for enhanced CO_2 capture" 249th ACS National Meeting, Denver, CO, March 22, **2015**. (Oral)
- **Timur İslamoğlu** "Catalytic Incorporation of Carbon Dioxide into Biodegradable Polymers", Virginia Commonwealth University (Richmond, VA), November 1, **2012**. (Oral)
- **İslamoğlu, T.;** Rabbani, M. G.; El-Kaderi, H. M. "Post-Synthesis Modification of Nanoporous Organic Framework for Highly Selective CO_2 Capture." Virginia Commonwealth University (Richmond, VA), October 12, **2012**. (Poster)

AWARDS, SCHOLARSHIPS, AND HONORS

2008 Undergraduate Honor Degree in Chemistry, Dumlupinar University, Turkey

2008 Full - scholarship granted by Republic of Turkey Prime Minister for graduate education at Dumlupinar University

01/10-06/10 Full - scholarship granted by Turkish Ministry of National Education for English Learning Program in the Marmara University, Istanbul, Turkey

المنارة للاستشارات
www.manaraa.com

08/10-current Full - scholarship granted by Turkish Ministry of National Education for graduate education at Virginia Commonwealth University

2015 Kapp Award, Department of Chemistry, Virginia Commonwealth University.

EXPERIENCE

Synthesis and characterization of Porous Organic Polymers (POPs)

Synthesis and characterization of Metal-Organic Frameworks (MOFs)

Synthesis of organic ligands

Post-synthesis modification of POPs and MOFs

Air-free synthesis technique (Schlenk line, Glove box)

Data processing for gas separation and storage applications (IAST, Qst, sorbent selection parameters)

Low-pressure gas analyzer collecting data for N_2, Ar, CO_2, CH_4, H_2 at cryogenic and non-cryogenic temperatures

5 years experience with Quantachrome 1C and IQ2, Nova 4200e, Master Prep and

1 year experience with Micromeritics ASAP 2020, Tristars, Smart Vacuum Prep

High-pressure volumetric analysis (HPVA)

Hitachi SU-70 Field Emission Scanning Electron Microscope (FE-SEM)

Panalytical X'pert Pro, Powder X-Ray Diffractometer (PXRD)

Nuclear Magnetic Resonance (NMR), Varian Inova-400 MHz and Varian Mercury-300 MHz

Thermo/Nicolet 670 Nexus, Fourier Transform Infrared Spectroscopy (FTIR) with pallet, ATR and DRIFT aperatus

X-ray photoelectron microscopy (XPS) (Thermofisher Escalab 250)

Materials Studio (Forcite, Adsorption Locator, Sorption Modules) and building porous structures

Structure visualization softwares, (Crystal Maker, Diamond, Pymol)

ACADEMIC AFFILIATIONS

2011-present American Chemical Society

المنارة للاستشارات
www.manaraa.com